EQUILIBRIUM OF STRESSED SOLIDS WITH RESPECT TO PHASE CHANGES, AND ITS GEOLOGICAL APPLICATIONS

by

PIERRE-YVES FRANCOIS ROBIN

Ingenieur Civil des Mines, Nancy
(1965)

M.Sc., Toronto
(1968)

SUBMITTED IN PARTIAL FULFILLMENT
OF THE REQUIREMENTS FOR THE
DEGREE OF DOCTOR OF
PHILOSOPHY

at the

MASSACHUSETTS INSTITUTE OF TECHNOLOGY

July, 1974

Signature of Author . . . . . .
Department of Earth and Planetary Sciences
July 5, 1974

Certified by . . . . . .
Thesis Supervisor

Accepted by . . . . . .
Chairman,
Department Committee on Graduate Students

ABSTRACT : Equilibrium of stressed solids with respect to phase changes, and its geological applications

by Pierre-Yves François ROBIN, Ingénieur Civil des Mines, M. Sc.

A general condition of equilibrium of coherent interfaces with respect to migration is established, which does not assume that the transformation strain is infinitesimal, nor that the two coherent phases have the same compositions. Fundamental in this context are (i) Gibbs' distinction between fluid and solid components of a solid, and (ii) the distinction, familiar to petrologists and also clearly made by Gibbs, between chemical components and actual chemical species. The equilibrium condition obtained is applied to the coherent cryptoperthite exsolution lamellae in alkali feldspars; by inserting the Helmholtz elastic strain energy in the lamellae, it permits an exact calculation of the coherent solvus which is in good agreement with hitherto unexplained experimental data. The same equilibrium condition is also used to show how a shear stress applied on a coherent boundary such as that between Fe, Mg orthopyroxene and clinopyroxene ($P2_1/c$) leads to a definite shift in temperature of the binary two-phase field. Although the result appears to justify Harker's concept of stress- and anti-stress-minerals, it is emphasized that no stressed solid is ever in equilibrium if the equilibrium criterion taken is that of the chemist or the petrologist. Accordingly the concept of 'thermodynamic pressure' for stressed mineral assemblages has theoretically no absolute validity, although such a 'pressure' can be defined for specific, and rather restricted conditions.

Kamb's thermodynamic theory of preferred orientation under stress is also examined, and several of its assumptions are found unjustified; its basic mechanism, that is, interface migration driven by differences in molar strain energy and volume between adjacent grains may nevertheless be important in rocks. Experiments designed to measure the kinetics of such a migration in quartz crystals were not conclusive.

Thesis supervisor: William F. BRACE
Professor of Geology

Table of content

BIOGRAPHY

Pierre-Yves Francois ROBIN was born on May 31, 1942 in NIMES(France). His family moved back to Paris in 1944, and, in 1952, moved to DAKAR(Senegal). In 1959, Pierre-Yves came back to France to attend the so-called 'Classes préparatoires aux Grandes Ecoles' at the Ecole Sainte-Geneviève in VERSAILLES. He entered the Ecole Nationale Supeřieure de la Métallurgie et de l'Industrie des Mines (ENSMIM) in NANCY in September 1962, and graduated as Ingénieur Civil des Mines in June 1965. Subsequent to an operation on his vertebral column, Pierre-Yves was exempted from the French military service, and came instead to the University of TORONTO with the support of a Canada Council scholarship. After obtaining an M.Sc. in Geology, he came to the Massachusetts Institute of Technology in September 1968. Since September 1973, Pierre-Yves is teaching at Erindale College, University of TORONTO.

Pierre-Yves married Barbara J. CASSON in 1970, and they have one child, Catherine.

His professional experience in France were of temporary employments in a coal mine, in a locomotive repair yard, on the construction site of the tide-powered Barrage de la RANCE, and in a lead-zinc mine. In Canada, he worked for one summer with the Ontario Department of Mines as a senior assistant geologist. He has held several research and teaching assistantships at the University of Toronto and the Massachusetts Institute of Technology.

Publications:

Robin, P.-Y., and J.B. Currie (1971) Analysis of fracturing in PreCambrian volcanics north of Madox, Ontario. Can.J.Earth Sci. 8(10) 1302-1312.

Robin, P.-Y.F. (1973) Note on effective pressures. J. Geophys. Res. 78, 2434-2437.

Robin, P.-Y.F. (1974) Thermodynamic equilibrium across a coherent interface in a stressed crystal. Amer. Mineral. (in press)

Robin, P.-Y.F. (1974) Stress and strain in cryptoperthite lamellae and the coherent solvus of alkali feldspars. Amer. Mineral. (in press)

Stesky, R.M., W.F. Brace, D.K. Riley and P.-Y.F. Robin (1974) Friction in faulted rocks at high temperature and pressure. Tectonophysics (in press)

Robin, P.-Y.F. (1974) Angular relationships between host and exsolution lamellae and the use of the Mohr circle. (submitted to Amer. Mineral.)

ACKNOWLEDGMENTS

My years at the Massachusetts Institute of Technology have been most rewarding ones. This I owe to a general 'atmosphere' of the Institute, a certain spirit of all its faculty, staff and student body which makes Science look like such an exciting adventure. All the teachers, colleagues and co-workers with whom I have been in contact thus deserve my gratitude.

However, I wish to thank more specifically:

Professor William F. Brace for the financial support he provided me throughout, for his guidance and encouragements, for his careful editing of several chapters of the present thesis, and, last but not least, for his trust and patience;

Dr. David L. Kohlstedt for performing the transmission electron microscopy of the larvikite reported in Chapter 3; the results of his work were not only extremely important for Chapter 3 itself, but also indirectly influenced the course of the rest of the thesis, and, to some extent, of my present research;

Professor Chris Goetze, Professor John W. Cahn , Dr. David L. Kohlstedt and Mr. Robert M. Stesky for discussions on many topics directly or indirectly related to the content of this thesis, and for their comments on one or several of its chapters;

Mr. Robert Stesky for teaching me how to use the high Argon pressure equipment, and for the (too many?) conversations we have had over the three years we shared in the same office;

Mr. Avner A. Arzi for the heat treatment of the quartz samples used in my experimental work, and for his good-humored companionship during many evenings in the laboratory;

Mr. William B. Durham for providing me with the description and the results of his experiments on single orthopyroxene crystals;

Dr. Michael M. Kimberley for his careful editing of Chapters 1 and 4;

Mr. Derrick Hirst for his patience and care in helping me design and in machining many parts of my experimental apparatus;

Mr. David Riach for help in machining parts also, but, above all, for maintaining an invariably high and friendly spirit for many years in the laboratory and machine shop of the seventh floor;

Ms. Madge Slavin for her helpfulness in many dealings with the administration, for her kindness, and for the great applecakes she so often brings.

Finally, I want to thank my wife Barbara for her support, trust and forebearance. "One-and-a-half to two years" had I told her when she came to Boston ..... She stayed three-and-a-half years!

CHAPTER 1

INTRODUCTION

"We have still to consider shearing stress as one of the factors controlling chemical reactions and determining the stability of different minerals and mineral associations. It is here that the inadequacy of our data, both on the theoretical and on the experimental side, is most severely felt. It is safe to assert that, for a crystal in a state of stress, chemical activity, no less than solubility, is very sensibly augmented. Shearing stress in a rock will then increase the rate of chemical reactions, just as a rise of temperature would do, and will sometimes make effective a reaction which would otherwise be in abeyance. But it is clear that wider possibilities are indicated. We have already remarked that, from the point of view of the Phase Rule, a stressed and an unstressed crystal of the same mineral constitute two distinct solid phases; and it is easy to believe that a state of shearing stress, by altering the atomic configuration of a crystal, changes also its chemical properties. This possibility, however, has been generally disregarded in discussing the chemistry of regional metamorphism, and finds no expression in the equations which are written down to represent supposed reactions. It would seem indeed that we have to do here with a <u>new chemistry</u>, differing - we know not how much - from that of the laboratory, and offering a new field of investigation" (Harker, 1939, pp. 145-146).

In his classic work on metamorphism, Harker repeatedly emphasized that shear stresses, which he presumed to be large, should affect the relative stability of minerals and mineral assemblages in rocks. Although admitting that the theoretical foundation for his theory was lacking, Harker believed that some minerals, which he called <u>stress-minerals</u> were favored by shear stresses, while

anti-stress minerals became less stable, or unstable, in presence of stresses. Harker based his thesis on a comparison of rocks of similar compositions and which he thought were formed under the same pressure-temperature conditions; however, some minerals (kyanite, tremolite-actinolite, anthophyllite, glaucophane, zoïzite-epidote, chloritoid-ottrelite, staurolite) appeared to be restricted to those rocks exhibiting large strains, and were thus classified as stress-minerals.

"Today," as Turner (1968, p. 61) remarks, "the concept of stress and antistress minerals has fallen into general disrepute". Most occurrences are well accounted for by our experimentally acquired knowledge of their stability fields; what Harker assigned to stresses is now generally attributed to the higher hydrostatic pressures acting during regional metamorphism.

Although the field evidence which prompted Harker's belief has thus disappeared, the theoretical question which he raised has remained unanswered; it can be stated as follows:

> What effect have nonhydrostatic stresses on the relative stability of mineral assemblages?

In geology, this petrological problem has been the major stimulus of research within the more general field described in the title of this thesis.

The deformation exhibited by many regionally metamorphosed rocks is often accompanied by preferred orientation of minerals.

> Why are some orientations of crystals with respect to a stress-field more favorable than others, causing some crystals to grow at the expense of others?

This, which could be called a petrofabrics problem, has been the second major reason for geologists to study 'nonhydrostatic thermodynamics'. This petrofabrics problem is similar to the petrological problem above in two ways. The existence

of stresses during formation of the minerals is inferred from the same evidence of large strains in the rock. Also, if several crystals of an elastically anisotropic mineral have different orientations in a given stress field, they are, in a way, different phases; the problem is to determine which of these phases is the most stable. This, in essence, is identical to the petrological problem. A renewal of interest in theories of preferred orientations has recently been prompted by the simultaneous observation of seismic velocity anisotropies within the crust and upper mantle underlying ocean basins, and of preferred orientations of olivine crystals in peridotite samples thought to have been brought up from the upper mantle. The hope is that these velocity anisotropies could be related to preferred mineral orientations and, ultimately, to stress patterns within the mantle.

More recently, geologists have also concerned themselves with 'nonhydrostatic thermodynamics' in relation with a mineralogical problem. The essential question is one with which materials scientists have been familiar for some time:

> When a change of conditions brings about a phase transformation in a mineral, how do the mechanical constraints inherent to its solid state affect the transformation?

This mineralogical problem thus differs from the petrological and petrofabrics problems in that the stresses are not externally applied; rather they are internally generated by the phase transformation itself. Such possible influence of solid constraints on exsolution and order-disorder transformations have been mentioned most often in the geological literature, albeit with little quantitative analysis or detailed description.

The literature relating to 'nonhydrostatic thermodynamics' and its geological applications has been recently reviewed by Paterson (1973). Such a review need not be duplicated, and references have therefore been purposely

omitted here. However, a short list of papers which, in my opinion, contain the essential contributions to the field is given at the end of the chapter. It should not be assumed from this selection that the present author agrees with all the analyses and results presented in these papers; some of the disagreements will appear in the course of the following chapters.

Harker, perhaps unwittingly, referred to a "new chemistry , differing from that of the laboratory ...". It is indeed remarkable how so little of the abundant literature in this field reports or incorporates any direct experimental work; most of the papers which do are in fact included in the list above. Too often, free from the constraints of experimental results, authors have not examined the mechanisms of the reactions in sufficient detail to obtain valid results.

The work presented in this thesis is also largely theoretical. However, I hope to have given enough attention to the study and description of the physical mechanisms at work to avoid the pitfalls of purely theoretical work, emulating in this the example of J.W. Gibbs, the first and foremost contributor to the field.

Chapter 1 reviews Gibbs' work and emphasizes Gibbs' distinction between solid and fluid components. The existence of a solid component is essential to any consideration of a stressed solid in equilibrium. The important distinction between chemical components and actual chemical species, familiar to petrologists, is useful in this context. As shown in Chapters 3 and 5, an appropriate definition of components yields simple solutions to problems involving substitutional chemical species in a crystal.

Gibbs (1906) had only established an equilibrium condition for a stressed solid in chemical equilibrium along its interface with a fluid. Chapter 1 shows what assumptions a boundary which supports a shear stress must satisfy to be in

equilibrium with respect to migration, and develops the corresponding equilibrium condition.

The petrological problem is dealt with in Chapter 5, which uses the equilibrium condition found in Chapter 1, and Chapter 6, which only uses Gibbs' result. The petrofabrics problem is briefly discussed in Chapter 6, and is the object of the experimental work reported in Chapter 7. Chapters 3 and 4 are contributions to the mineralogical problem for the important case of coherent lamellar exsolution.

REFERENCES

BRACE, W.F. (1960) Orientation of anisotropic minerals in a stress field: discussion. Geol. Soc. Amer. Mem. 79, 9-20.

CAHN, J.W. (1962) Coherent fluctuations and nucleation in isotropic solids. Acta Metal. 10, 907-913.

COE, R.S. (1970) The thermodynamic effect of shear stress on the ortho-clino inversion in enstatite and other coherent phase transitions characterized by a finite simple shear. Contr. Mineral. Petrol. 26, 247-264.

_____ AND M.S. PATERSON (1969) The α-β inversion in quartz: a coherent phase transition under non-hydrostatic stress. J. Geophys. Res. 74, 4921-4948.

GIBBS, J.W. (1906) The collected works of J. Willard Gibbs, Ph.D., Ll.D., Vol. I. Thermodynamics. Longmans, Green and Co., New-York, N.Y. 434 p.

HARKER, A. (1939) Metamorphism. Methuen & Co. Ltd., London, 362 p.

KAMB, W.B. (1959) Theory of preferred crystal orientation developed by crystallization under stress. J. Geology 67, 153-170.

_____ (1961) The thermodynamic theory of nonhydrostatically stressed solids. J. Geophys. Res. 66, 259-271.

LARCHÉ, F., AND J.W. CAHN (1973) A linear theory of thermochemical equilibrium of solids under stress. Acta Metal. 21, 1051-1063.

LI, J.C.M., R.A. ORIANI, AND L.S. DARKEN (1966) The thermodynamics of stressed solids. Zeitschrift f. Physik. Chemie Neue Folge 49, 271-290.

MACDONALD, G.J.F. (1960) Orientation of anisotropic minerals in a stress field. Geol. Soc. Amer. Mem. 79, 1-8.

PATEL, J.R., AND M. COHEN (1953) Criterion for the action of applied stress in the martensitic transformation. Acta Metal. 1, 531-538.

PATERSON, M.S. (1973) Non-hydrostatic thermodynamics and its geological applications. Rev. of Geophysics 11, 255-389.

TULLIS, J., AND T. TULLIS (1972) Preferred orientation of quartz produced by mechanical Dauphiné twinning: thermodynamics and axial experiments. In: Flow and fracture of rocks, Geoph. Monograph 16, Amer. Geophys. Union, Washington D.C., 67-82.

TURNER, F.J. (1968) Metamorphic petrology. McGraw-Hill Book Co., New-York, 403 p.

CHAPTER 2

THERMODYNAMIC EQUILIBRIUM ACROSS A COHERENT INTERFACE IN A STRESSED CRYSTAL[1]

Abstract

Migrating twin boundaries, boundaries in crystals undergoing displacive phase transformations, coherent precipitates and coherent exsolution lamellae, all provide examples of coherent interfaces propagating in a stressed crystalline framework. The motion of such boundaries is often reversible or characterized by a sufficiently small hysteresis, so that they can be considered at equilibrium within the stressed solid; the present paper is concerned with the conditions of such equilibrium. It is emphasized, following J.W. Gibbs, that a solid under stress is in equilibrium only if the motion of at least one chemical component (solid component) of the solid through the framework is considered an impossible process; other chemical components able to migrate are fluid components. After the additional 'constraint of coherency' for the migration of the interface is examined and expressed mathematically, the condition of equilibrium can be established, showing the exact dependence of equilibrium on normal and shear stress along the interface, temperature, and chemical potentials of the fluid components. The general condition is then applied to the following special cases: (1) coherent transformations

[1] American mineralogist, in press.

in which the 'stress-free transformation strain' is much larger than any elastic strain, (2) twinning, and (3) infinitesimal transformation strain. The migration of some low-angle tilt or kink boundaries can be analogous to that of coherent boundaries, and their equilibrium, if reached, is ruled by the same equations. However, growth across most high-angle grain boundaries of a polycrystalline aggregate is not constrained in the same manner; as a consequence it is argued that in presence of a shear stress such boundary cannot be in reversible equilibrium with respect both to growth and to shear.

INTRODUCTION

The general problem of thermodynamic equilibrium of stressed solids has concerned many authors because of its possible applications to mineralogy, petrology, geophysics and materials sciences. The topic has recently been reviewed by Paterson (1973). Gibbs (1906) originally derived the condition of external equilibrium of a stressed solid in contact with a fluid, and introduced the distinction between solid and fluid components of a solid. These concepts are essential to any study of the thermodynamic equilibrium of a stressed solid and, in particular, to the present work; because their significance is often not fully appreciated, Gibbs' results will be summarized, and the constraint of solid behavior defined.

At equilibrium a solid-fluid boundary does not and cannot support any shear stress; there have therefore been attempts to generalize Gibbs' results to boundaries which support shear stresses (see Paterson, 1973). Coherent interfaces are examples of such boundaries; an understanding of their equilibrium has important implications for such problems as twin-boundary migration, precipitation hardening, solid exsolution, and other phase transformations within crystals (or glasses at temperatures sufficiently below their glass transition).

The equilibrium conditions for coherent interfaces derived in this paper are quite general; they do not assume that the transformation strain or the elastic strain are infinitesimal, nor do they assume that the transformation is isochemical. However, the thickness of the interfacial region is neglected and the surface energy is not considered; the applicability of the results depends on the validity of these latter assumptions.

Not all coherent interfaces reach an equilibrium position; when they do not, the equilibrium conditions established here only provide a measure of the disequilibrium by the extent to which they are not satisfied.

CONSTRAINT OF SOLID BEHAVIOR

Gibbs (1906, pp. 184-218) considered a stressed elastic solid able to dissolve into or crystallize from a fluid. Let the fluid in contact with the solid at one point of its boundary be at a pressure P. External equilibrium is obtained when the solid neither dissolves nor grows spontaneously at its boundary with the fluid. If the solid is of uniform composition and if molar quantities are used, the chemical potential μ of its component in the fluid at pressure P is given by (Gibbs, Eq. 385)

$$\mu = \bar{E} - T\,\bar{S} + P\,\bar{V} \qquad (1)$$

where $\bar{E}$, $\bar{S}$ and $\bar{V}$ are respectively molar energy, entropy and volume of the solid in the equilibrium state considered, and T is the temperature. The significance of this result is better understood when considering, as does Gibbs, the following special case. Three fluid pressures P^1, P^2 and P^3 are each applied on two opposite faces of a rectangular parallelepiped of the solid, assumed homogeneous. The solid is then under homogeneous stress, of principal components $-P^1$, $-P^2$ and $-P^3$. The condition of equilibrium with respect to growth or solution becomes for each pair of faces (Gibbs' Equations 393-395)

$$\bar{E} - T\,\bar{S} + P^1\,\bar{V} = \mu^1$$
$$\bar{E} - T\,\bar{S} + P^2\,\bar{V} = \mu^2$$
$$\bar{E} - T\,\bar{S} + P^3\,\bar{V} = \mu^3$$

where μ^1, μ^2, μ^3 are the values of the chemical potential of the component of the solid in each fluid. If migration of the component of the solid were

possible, either through the solid itself or through some external channel, this component would indeed migrate from the fluids at the highest pressures to the fluid at the lowest pressure. Consequently, equilibrium of a non-hydrostatically stressed solid must always be understood to be limited by the constraint that such migration is not a possible mechanism. This constraint is called here the constraint of solid behavior. We note (Kamb, 1961) that a chemical potential for the component of the solid is not defined within the solid itself.

Gibbs went on to examine (p.215) the case of a solid which also contains fluid components α,β, etc. (Recent writers, e.g. Li et al., 1966 or Paterson, 1973, refer to these as mobile components). In Gibbs' words, fluid components are such "that there are no passive resistances to the motion of the fluid components except such as vanish with the velocity of the motion". For these components Gibbs shows that a chemical potential can be defined and is constant throughout the solid and the fluids when the system is in equilibrium. As Gibbs' definition makes clear, a chemical component α is fluid (and therefore a chemical potential μ^{α} must exist and have a constant value throughout the system at equilibrium) if α can move independently[2] through the solid, regardless of whether or not the corresponding

---

[2]Not all atomic, ionic or molecular species which can move may be able to do so independently: there may be relations of dependence between them, such as site constraints or constraints of electroneutrality (Thompson, 1969). A set of independent fluid components can nevertheless always be defined. Conversely, a solid component does not necessarily correspond to any one atomic, ionic or molecular species unable to diffuse through the lattice of the solid. For

(footnote 2 continued)

concentration or concentration variation of α in the solid can be detected.

When a solid contains fluid components, the constraint of solid behavior is that at least one chemical component of the solid is not free to move through the solid. Gibbs called such a component a solid component.[2] The very definitions of fluid and solid components imply that there exists a three-dimensional framework which is conserved and with respect to which motion of chemical species may or may not occur, independently of possible translations or deformations of the framework itself.

Recognition of the existence of a solid component and its identification are essential to any consideration of equilibrium of a non-hydrostatically stressed solid. In this work solid behavior is always assumed. In practice, for crystals, this means that mechanisms like unlimited motion of dislocations or Nabarro-Herring diffusion creep do not occur, or are so slow, compared to boundary migration or diffusion of fluid components, that they can be neglected. We shall also suppose the fluidity of the fluid components to be perfect, "leaving it to be determined by experiment how far and in what cases these suppositions are realized" (Gibbs, 1906, p. 215).

COHERENT TRANSFORMATIONS AND COHERENT INTERFACES

A coherent transformation in a solid is a phase transformation in which the three-dimensional framework is preserved without rupture. This definition does not exclude the possibility that atomic rearrangements occur,

---

[2](continued) example, two substitutional species, α and β may both be able to diffuse through the lattice but be tied by a site constraint.

allowing some chemical species to change position or migrate. A coherent transformation is therefore not necessarily displacive (Buerger, 1948) although displacive transformations are coherent. In the present paper, attention is concentrated on crystalline solids. Generalization to amorphous chain polymers is possible and may have applications to transition and exsolution phenomena in glasses at low temperatures.

Let us call the two possible states of a crystal 'phase' a and 'phase' b[3]. The transformation of a crystal from phase a to phase b can be visualized as the sweeping through the crystal of one or more boundaries separating domains of b from domains that are still a. Such a boundary is a coherent boundary, or coherent interface. In the presence of such an interface, stresses in a and b may arise from the very co-existence of the two phases and from the constraint that the two lattices be matched across the interface; stresses may also be imposed at the external boundaries of

---

[3]The term phase is often taken to designate only a state of a substance in which all thermodynamic parameters are uniform throughout. Because stresses, in particular, are not assumed uniform here, the term phase simply refers to a portion of the crystal characterized by a unique equation of state and by continuous thermodynamic properties. This broader definition is consistent with usage in the metallurgical or geological (e.g. Wang, 1968) literature. By contrast, 'crystal' designates the framework which is conserved, regardless of which state it is in; such usage is implicit in many studies of displacive or order-disorder transitions.

the crystal.

There are cases where, instead of sweeping through the whole crystal, a coherent interface reaches an equilibrium position. Let us look at a few examples.

Mechanical twinning

It is only when their state is affected by parameters such as electric field, magnetic field, or stress (first or higher-order tensors) that twins must be considered to be distinct phases, as their molar energies may then differ. Mineralogists are familiar with stress-induced twinning in calcite. Mechanical twinning is found in many other minerals (de Vore, 1970). The migration of Dauphiné twin boundaries in quartz under stress is particularly well documented by Frondel (1945), Thomas and Wooster (1951) and Tullis and Tullis (1972). When non-uniform stresses are applied to the external boundaries of a crystal in which mechanical twinning is possible, the two twins may coexist within the crystal, separated by coherent twin boundaries. As with other phase transformations the extent to which equilibrium is actually reached by the migrating twin boundary must be determined in each case and will depend on factors such as time, temperature, and what level of disequilibrium is considered significant. For Dauphiné twinning in quartz, hysteresis appears to vanish at temperatures nearing the α -β transition (Young, 1962). Stress-induced reversible migration of twin boundaries is also observed in metals. Basinsky and Christian (1954a) show how such observed migration can explain the rubber-like elasticity of low-temperature face-centered tetragonal twinned phases in Indium-Thallium and Gold-Cadmium alloys.

Isochemical coherent transitions

Displacive, semi-reconstructive and order-disorder transformations (Buerger, 1948) can all be classified as isochemical coherent transformation. A few examples are given by Coe (1970). Well known are the high-low transitions in crystalline phases of silica and in the feldspars, and the transition of calcite I to calcite II at high pressure (Bridgman, 1939). Which, and to what extent, martensitic reactions are coherent transitions is a subject of debate in the metallurgical literature. The W-L-R and B-M crystallographic theories of martensitic transformations (Weschler, Lieberman and Read, 1953; Bowles and Mackenzie, 1954) assume coherency and have successfully explained many features of these transformations. Yet electron microscopy of Fe-Ni-C alloys reveals that growth of martensite is accompanied by the formation of large numbers of dislocations and the boundaries have been described as semi-coherent (e.g. see Owen, Schoen and Srinivasan, 1970). In some systems, however, the reaction shows remarkably little hysteresis: 20°C or less in Au-Cd (Chang and Read, 1951); between 2°C and 4°C in In-Th (Burkart and Read, 1953; Baskinsky and Christian, 1954b); it seems accepted that these 'thermoelastic martensites' (Owen et al., 1970) form by truly coherent reactions. The influence of stresses on the temperature at which some of these reactions occur has been explored experimentally: for the α - β transition in quartz (Coe and Paterson, 1969); and for the martensitic reaction in In-Tl (Burkart and Read, 1953) and Fe-Ni alloys (Patel and Cohen, 1953). Wang (1968) has also qualitatively explained the observed smearing out of the calcite I - calcite II transition in limestones over a wide range of confining pressure by the inhomogeneous stresses arising in such aggregate. For Wang and Meltzer (1973) the high absorption of acoustic

waves in these limestones over the same range of pressure also indicates an extremely rapid migration of the phase boundaries in response to the alternating stress; their interpretation suggests that calcite I-II boundaries would be very close to their equilibrium positions under static conditions.

Coherent precipitates

A coherent precipitate is a domain within a crystal which differs from its host by its composition and, in general, by its stress-free lattice dimensions, but yet has retained the continuity of its lattice with the lattice of the host. A non-hydrostatic and often non-uniform stress-field is generally present. To the extent that these stresses are maintained without creep and without the corresponding destruction of the lattice framework, the equilibrium reached implies the existence of a solid component, common to both phases, and of at least one fluid component.

A fully coherent precipitate is one which has maintained coherency on all its boundaries with the host. Examples of fully coherent precipitates have been described mostly for metals. The G.P. zones (Guinier-Preston) in Al-Ag, Al-Zn and Al-Cu alloys, cobalt particles in Cu-Co alloys and γ' in nickel-base alloys are cited by Kelly and Nicholson (1963). A partially coherent precipitate is one for which coherency is maintained only along a specific crystallographic orientation. In metals, the Widmanstätten structures of aluminum alloys (Kelly and Nicholson, 1963) are well-known examples.

There is no general review of the nature of the boundaries of exsolution lamellae in oxides and silicates. Fully coherent submicroscopic exsolution lamellae of augite in pigeonite have been observed by transmission

electron microscopy in lunar and terrestrial pyroxenes (Christie et al., 1971). The angular relationships between clinopyroxene exsolution lamellae reported by Robinson et al. (1971) are also consistent with the assumption of coherency of the boundaries, as will be shown in Chapter 4. Champness and Lorimer (1973) observe calcium-rich submicroscopic coherent precipitates in an orthopyroxene from the Stillwater complex, for which they propose the term of G.P. zones, by analogy with metals. In Chapter 3 it will be shown that cryptoperthite lamellae in alkali feldspar are generally coherent; using a result of the present paper the lowering of the solvus expected from the strain energy of coherency, will be calculated and the result showed to be in good agreement with experimental data.

In summary, known examples of coherent interfaces are many, and more are likely to be found with the increasing use of transmission electron microscopes. It must be emphasized again, however, that whether or not a coherent interface is able to migrate to an equilibrium position must be justified in each case or be explicitly acknowledged as an assumption.

METHOD

Equilibrium criterion

Gibbs demonstrated Equation 1 by using the following minimum energy criterion:

> "For the equilibrium of any isolated system it is necessary and sufficient that, in all possible variations in the state of the system which do not alter its entropy, the variation of its energy shall either vanish or be positive".

As there have been arguments in the literature regarding the definition

and use of energy functions other than internal energy for solids under stress (see Paterson, 1973), we will use the same criterion as Gibbs. As a result, it will be found that one of the conditions of equilibrium is that the temperature be uniform throughout the system. This is, of course a result which could be accepted and bypassed by using the Helmholtz energy. The advantage would be minor, however, and Gibbs' treatment will be followed instead.

Let us then consider a portion of crystal which contains a coherent interface at equilibrium separating phases a and b. Isolate this volume by a "fixed envelope which is impermeable to matter and to heat, and to which the solid is firmly attached wherever they meet" (Gibbs, 1906, p. 187). We assume that stresses, compositions, energy and entropy densities, etc., although not necessarily uniform, vary continuously within each phase.

States and coordinate systems

During migration of the interface a portion of the lattice changes phase, and the corresponding strain is not necessarily infinitesimal. In order to describe such finite strain one must carefully distinguish between the identification of lattice points and their location. Identification of points is accomplished by the use of a reference state and a reference coordinate system; location of these points in the actual coherent equilibrium state or in variational departures from the equilibrium state is done by their coordinates in the equilibrium coordinate system. Both coordinate systems are assumed rectangular cartesian and of same handedness.

The coordinates of a point or of a vector in the reference state (noted by a prime) can be regarded mainly as a 'tagging' system. Therefore,

the reference state does not have to have any physical reality and can be chosen as is convenient for any particular problem; it must, however, preserve continuity with the actual state. It is sometimes convenient to choose the reference state and its coordinate system to coincide with the equilibrium state and coordinate system; the distinction between identification and position of points must be maintained however. Physical quantities like energy, entropy, chemical concentrations exist only in an actual state; their densities, however, can be defined with respect to volumes of the lattice equal to unity in the reference state, in which case these densities will also be noted by a primed lower-case letter. Force vectors also only exist in an actual state, and their components are defined in the equilibrium coordinates; in defining stresses or the stress tensor, however, the unit areas used and their orientations are the ones of the lattice in the reference state.

A point in the solid, identified by its reference state coordinates, x_i', has in the equilibrium state the coordinates x_i (i = 1, 2, 3). We can define the quantities

$$x_{i,j} = \frac{\partial x_i}{\partial x_j'} \qquad (2)$$

The set of $x_{i,j}$ is a description of the local deformation or <u>strain</u> between the reference and the equilibrium states. If the reference state and coordinates are chosen so as to coincide with the equilibrium state and coordinates, then at equilibrium, $x_{i,j} = \delta_{ij}$ (Kronecker's δ).

<u>Fundamental equation of state</u>

Let us first consider a crystal which does not contain any fluid component. Under conditions where we can neglect body forces, the energy density of the crystal is only a function of the state of strain and of the

entropy content. We thus write the fundamental equation of state of each phase as

$$e'^{\underline{a}} = e'^{\underline{a}}(x^{a}_{i,j},\ s'^{a})$$
$$e'^{\underline{b}} = e'^{\underline{b}}(x^{b}_{i,j},\ s'^{\underline{b}}) \qquad (3)$$

where e' and s' are respectively energy and entropy densities, or, more precisely, energy and entropy in the equilibrium state of a small volume of phase which is equal to unity in the reference state. All units of mass, volumes and areas are chosen small enough so that properties can be considered uniform within them.

In an actual state, the position of a point of the framework may differ from its equilibrium position by a variational amount δx_i, and, consequently, so may the local strain, $\delta x_{i,j}$ (see the virtual deformations of Murnaghan, 1951, p.44-50). The entropy density may also vary by $\delta s'$, and therefore, from (3), the internal energy variation is given by

$$\delta e' = \left(\frac{\partial e'}{\partial x_{i,j}}\right) \delta x_{i,j} + \left(\frac{\partial e'}{\partial s'}\right) \delta s'$$

(Einstein's summation convention on repeated subscripts is used in this paper) which we rewrite as

$$\delta e' = \sigma_{ij}\ \delta x_{i,j} + T\ \delta s' \qquad (4)$$

As Gibbs (1906, p. 186) pointed out, σ_{ij} is the i^{th} component, in the equilibrium coordinates, of the force acting (in the equilibrium state) on a surface element which would be equal to a unit area in the reference state and would be perpendicular to the j axis of the reference coordinate system. (If the reference state coincides with the equilibrium state, or

only differs from the equilibrium state by an infinitesimal strain, σ_{ij} is the stress as defined in infinitesimal strain elasticity).

Besides displacements and entropy density changes throughout each phase, there is another possible variation of the system from its equilibrium state: the interface may migrate through the solid, its migration corresponding to a change in phase at the interface and preserving coherency. We need to examine this last variation carefully.

GEOMETRY OF A MIGRATING COHERENT INTERFACE

Figure 1a represents portions of phases a and b and a portion of interface in the equilibrium state. These portions are chosen small enough for stresses and entropy to be and to remain uniform within each phase and for the variational migration of the interface to be uniform. Figure 1c is the configuration after such a migration. As Figure 1 shows, this migration can be decomposed into the following sequence:

1) An imaginary cut is made along the interface.
2) Points in a are moved by a distance δx_i^a, points in b are moved by a distance δx_i^b (Fig. 1b). The relative displacement of b with respect to a is
$$\delta x_i^b - \delta x_i^a = \overrightarrow{Q'P'}$$
3) A volume of one phase is transformed into a volume of the other phase having the same mass, thereby reestablishing coherency. Points which are not affected by this phase change are not moved (Fig. 1c).

We can make the following remarks:

i) The direction of $\overrightarrow{Q'P'}$ is imposed by the states of strain of the lattice in a and b and is therefore not an independent parameter subject to variations.

ii) The length of Q'P' is proportional to the mass transferred from $\underline{a}$ to $\underline{b}$. Let O be the intersection of the direction of Q'P' with the new position of the interface (Figure 1c). We must have $|\overline{OP'}| / |\overline{OQ'}| = \rho^{\underline{a}}/\rho^{\underline{b}}$, where $\rho^{\underline{a}}$ and $\rho^{\underline{b}}$ are molar densities of $\underline{a}$ and $\underline{b}$, respectively, in the equilibrium state.

We want to normalize variations to a unit variation. Figure 1 represents configurations of the actual state. Let us choose an element of area of interface in the actual state which has an area of unity in the reference state. Let us then consider a particular migration in which one mole is transformed from phase $\underline{a}$ to phase $\underline{b}$ over this chosen area element; we call v_i the corresponding particular vector $\overrightarrow{Q'P'}$. For an arbitrary variational migration we have, therefore,

$$\delta x_i^{\underline{b}} - \delta x_i^{\underline{a}} = \delta g \, v_i \qquad (5)$$

where δg is the arbitrary parameter, positive or negative; δg is in fact the number of moles transformed from $\underline{a}$ to $\underline{b}$ across one unit area of interface (in the reference state).

The position at equilibrium of the interface within the lattice can be 'mapped' in the reference state. The variational growth of $\underline{b}$ at the expense of $\underline{a}$ (or vice-versa) is mapped in the reference state as a displacement of the interface by a distance $\delta 1'$ perpendicular to it. From the definition of v_i, $\delta 1'$, for the same arbitrary migration as in (5), is given by

$$\delta 1' = \delta g / \rho' \qquad (6)$$

where ρ' is the molar density of the region swept by the interface in the reference state. The sign convention on v_i and δg is such that $\delta 1'$ is positive when $\underline{b}$ grows at the expense of $\underline{a}$.

Equations 5 and 6 express completely the constraint of coherency. They show how the growth of each phase and the relative displacements of $\underline{a}$ and $\underline{b}$ at that particular point of the interface are functions of only one independent parameter, δg.

In the rest of the paper v_i is called the characteristic vector[4] of the coherent boundary; in general, if the interface is curved and elastic strains are not uniform within each phase, v_i is a function of position on the interface.

CONDITIONS OF EQUILIBRIUM

The total change in energy of the system for an arbitrary variation from the equilibrium state is now stated to be zero or positive. Using (4) this statement is written

$$\delta E = \int_{V'\underline{a}} \left(\sigma^{\underline{a}}_{ij} \, \delta x^{\underline{a}}_{i,j} + T \, \delta s'^{\underline{a}} \right) dV' + \int_{V'^{\underline{b}}} \left(\sigma^{\underline{b}}_{ij} \, \delta x^{\underline{b}}_{i,j} + T \, \delta s'^{\underline{b}} \right) dV'$$

$$+ \int_{A'} (e'^{\underline{b}} - e'^{\underline{a}}) \, \delta 1' \, dA' \geq 0 \qquad (7)$$

where V' and A' are respectively volume and area in the reference state.

Not all variations in (7) are independent, however:

1) The total entropy is constrained to remain constant:

$$\int_{V'\underline{a}} \delta s'^{\underline{a}} \, dV' + \int_{V'^{\underline{b}}} \delta s'^{\underline{b}} \, dV' + \int_{A'} (s'^{\underline{b}} - s'^{\underline{a}}) \, \delta 1' \, dA' = 0. \qquad (8)$$

Equations 7 and 8 can be satisfied for any arbitrary transfer of entropy only if (Gibbs, p. 186, Eq. 364).

$$T = \text{constant} \qquad \text{throughout the system} \qquad (9)$$

---

[4] The transformation of the region swept by the interface is an invariant plane strain (see Wayman, 1964). In the transformation the length and orientation of any vector parallel to the interface are not affected. and $\overrightarrow{OP'}$ is transformed into $\overrightarrow{OQ'}$ (Figure 1). $\overrightarrow{OP'}$ and $\overrightarrow{OQ'}$ are colinear and their orientation is therefore that of the only nondegenerate characteristic vector (or eigenvector) of the transformation; the corresponding eigenvalue is $\rho^{\underline{a}}/\rho^{\underline{b}}$.

2) Variational displacements, δx_i, are continuous throughout the volumes of $\underline{a}$ and $\underline{b}$ and are zero whenever the crystal meets the fixed envelope. Green's divergence theorem gives therefore

$$\int_{V'\underline{a}} \sigma^{\underline{a}}_{ij} \, \delta x^{\underline{a}}_{i,j} \, dV' = \int_{A'} \sigma^{\underline{a}}_{ij} \, n'^{\underline{a}}_{j} \, \delta x^{\underline{a}}_{i} \, dA' - \int_{V'\underline{a}} \sigma^{\underline{a}}_{ij,j} \, \delta x^{\underline{a}}_{i} \, dV',$$

and similarly

$$\int_{V'\underline{b}} \sigma^{\underline{b}}_{ij} \, \delta x^{\underline{b}}_{i,j} \, dV' = \int_{A'} \sigma^{\underline{b}}_{ij} \, n'^{\underline{b}}_{j} \, \delta x^{\underline{b}}_{i} \, dA' - \int_{V'b} \sigma^{\underline{b}}_{ij,j} \, \delta x^{\underline{b}}_{i} \, dV'.$$

where $n'^{\underline{a}}_{j}$ and $n'^{\underline{b}}_{j}$ are unit vectors normal to the interface in the reference state, drawn outward from $\underline{a}$ and $\underline{b}$; clearly $n'^{\underline{a}}_{j} = -n'^{\underline{b}}_{j}$.

By using (5) the sum of the two above integrals can be rewritten as

$$\int_{V'\underline{a}} \sigma^{\underline{a}}_{ij} \, \delta x^{\underline{a}}_{i,j} \, dV' + \int_{V'\underline{b}} \sigma^{\underline{b}}_{ij} \, \delta x^{\underline{b}}_{i,j} \, dV' = -\int_{A'} \sigma^{\underline{a}}_{ij} \, n'^{\underline{a}}_{j} \, v_i \, \delta g \, dA'$$

$$+ \int_{A'} \left(\sigma^{\underline{a}}_{ij} \, n'^{\underline{a}}_{j} + \sigma^{\underline{b}}_{ij} \, n'^{\underline{b}}_{j} \right) \delta x^{\underline{b}}_{i} \, dA' - \int_{V'\underline{a}} \sigma^{\underline{a}}_{ij,j} \, \delta x^{\underline{a}}_{i} \, dV' - \int_{V'\underline{b}} \sigma^{\underline{b}}_{ij,j} \, \delta x^{\underline{b}}_{i} \, dV'. \tag{10}$$

3) From (6), $\delta l'$ is not independent but a function of δg.

Therefore, by inserting (6), (8), (9) and (10) into (7), the total variation of energy of the system writes as

$$\delta E = -\int_{V'\underline{a}} \sigma^{\underline{a}}_{ij,j} \, \delta x^{\underline{a}}_{i} \, dV' - \int_{V'\underline{b}} \sigma^{\underline{b}}_{ij,j} \, \delta x^{\underline{b}}_{i} \, dV' + \int_{A'} \left(\sigma^{\underline{a}}_{ij} \, n'^{\underline{a}}_{j} + \sigma^{\underline{b}}_{ij} \, n'^{\underline{b}}_{j} \right) \delta x^{\underline{b}}_{i} \, dA'$$

$$+ \int_{A'} \left(\frac{e'^{\underline{b}} - Ts'^{\underline{b}}}{\rho'} - \frac{e'^{\underline{a}} - Ts'^{\underline{a}}}{\rho'} - \sigma^{\underline{a}}_{ij} \, n'^{\underline{a}}_{j} \, v_i \right) \delta g \, dA' \geq 0 \tag{11}$$

The variational terms in each integral of (11) are now independent. The equilibrium conditions are therefore obtained by equating the Eulerian

of each integral to zero:

1) $\sigma_{ij,j} = 0$, throughout $\underline{a}$ and $\underline{b}$. (12)

This is the usual equation of mechanical equilibrium in the absence of body forces.

2) $\sigma_{ij}^{\underline{a}}\, n_j'^{\underline{a}} + \sigma_{ij}^{\underline{b}}\, n_j'^{\underline{b}} = 0$ on the interface. (13)

Equation (13) is the condition of mechanical equilibrium on the interface. All components of the stress tensor need not be equal. It is convenient to define T_i, the stress on the interface,

$$T_i = \sigma_{ij}^{\underline{a}}\, n_j'^{\underline{a}} = -\sigma_{ij}^{\underline{b}}\, n_j'^{\underline{b}} \,. \tag{14}$$

T_i is the i^{th} component in the equilibrium coordinates of the force on $\underline{a}$ across an element of area of interface equal to unity in the reference state.

3) The last condition of equilibrium, and the most important result of this analysis, is

$$\frac{e'^{\underline{b}} - Ts'^{\underline{b}}}{\rho'} - \frac{e'^{\underline{a}} - Ts'^{\underline{a}}}{\rho'} - T_i v_i = 0 \tag{15}$$

on the interface.

If molar energies and entropies are used, as ρ' is a molar density, (15) becomes

$$(\bar{E}^{\underline{b}} - T\bar{S}^{\underline{b}}) - (\bar{E}^{\underline{a}} - T\bar{S}^{\underline{a}}) - T_i v_i = 0 \tag{16a}$$

or

$$\bar{F}^{\underline{b}} - \bar{F}^{\underline{a}} - T_i v_i = 0 \tag{16b}$$

where $\bar{F}^{\underline{a}}$, $\bar{F}^{\underline{b}}$ are molar Helmholtz energies. T_i and v_i are vectors in the equilibrium coordinates, and can be decomposed into their normal and tangential components :

$$v_i = \varepsilon\, n_i + \gamma_i \quad ,$$

$$T_i = -P\, n_i + \tau_i \quad ,$$

where n_i is a unit vector normal to the interface outward from $\underline{a}$ in the equilibrium state. Then $T_i v_i = - P\varepsilon + \gamma_i \tau_i$.

If the reference state is chosen to coincide with the equilibrium state, the definition of v_i makes $\varepsilon = \bar{V}^{\underline{b}} - \bar{V}^{\underline{a}}$

where $\bar{V}^{\underline{a}}$, $\bar{V}^{\underline{b}}$ are molar volumes in the equilibrium state. Then the equilibrium condition becomes

$$(\bar{E}^{\underline{b}} - T\bar{S}^{\underline{b}} + P\,\bar{V}^{\underline{b}}) - (\bar{E}^{\underline{a}} - T\bar{S}^{\underline{a}} + P\,\bar{V}^{\underline{a}}) - \gamma_i \tau_i = 0 \qquad (16c)$$

where, it is recalled, -P and τ_i are respectively the normal stress and the components of the tangential stress on $\underline{a}$ across the interface.

In spite of their familiar look, the expressions in parentheses should not be confused with the expression of $\bar{G}$, or μ, defined for phases under hydrostatic pressure:

i) P is only one component of a nonhydrostatic stress tensor,

ii) Equality of the two parentheses does not ensure equilibrium, unless $\gamma_i \tau_i = 0$.

iii) In the most general case of equilibrium, when the interface is curved and stresses within each phase are not uniform (e.g., coherent boundaries within grains of a stressed polycrystalline aggregate) the terms in parentheses do not maintain a constant value along the interface.

EXISTENCE OF FLUID COMPONENTS

In the development leading to Equation 16 it was assumed that there was no fluid component in the solid. As noted earlier, Gibbs (1906, p. 215-218) points out that a chemical potential can be defined in the solid for each fluid component by (Gibbs' Equation 467)

$$\delta e' = \sigma_{ij}\, \delta x_{i,j} + T\delta s' + \sum_{\alpha} \mu^{\alpha}\, \delta \rho'^{\alpha} \qquad (17)$$

and demonstrates that μ^{α} is constant throughout the system at equilibrium; ρ'^{α} is the molar density of α, that is, the number moles of component α in the equilibrium state in a volume of solid equal to unity in the reference state. The demonstration is in fact formally identical to the demonstration that the temperature is uniform. It is sufficient to treat ρ'^{α} like s', and μ^{α} like T in Equations 4, 7, 8 and 9. The final equilibrium equation therefore becomes

$$(\bar{\underline{E}}^{b} - T\bar{\underline{S}}^{b} - \sum_{\alpha} \mu^{\alpha} \underline{X}^{b,\alpha}) - (\bar{\underline{E}}^{a} - T\bar{\underline{S}}^{a} - \sum_{\alpha} \mu^{\alpha} \underline{X}^{a,\alpha}) - T_i v_i = 0 \qquad (18a)$$

where $\underline{X}^{a,\alpha}$, $\underline{X}^{b,\alpha}$ are ratios of the molar density of fluid component α to the molar density of the solid component in $\underline{a}$ and $\underline{b}$ respectively. Only independent fluid components are included in the summation.

If the reference state is chosen to coincide with the equilibrium state (or only differ from that equilibrium state by an infinitesimal strain) and T_i and v_i are decomposed into normal and tangential components, (18a) becomes

$$(\bar{\underline{E}}^{b} - T\bar{\underline{S}}^{b} + P\,\bar{\underline{V}}^{b} - \sum_{\alpha} \mu^{\alpha} \underline{X}^{b,\alpha}) - (\bar{\underline{E}}^{a} - T\bar{\underline{S}}^{a} + P\bar{\underline{V}}^{a} - \sum_{\alpha} \mu\, \underline{X}^{a,\alpha}) - \gamma_i \tau_i = 0 \qquad (18b)$$

In the most general case, only temperature, T, and chemical potentials of the fluid components, μ^{α}, have a constant value throughout a volume at equilibrium. In the case of coherent parallel exsolution lamellae (Chapter 3) there are no shear stresses acting on the planar boundaries, stresses are uniform within each type of lamellae, and, in simple cases, there is only one fluid component. The equilibrium condition thus simplifies to

$$(\bar{\underline{F}}^{b} - \bar{\underline{F}}^{a}) + P(\bar{\underline{V}}^{b} - \bar{\underline{V}}^{a}) - \mu(\underline{X}^{b} - \underline{X}^{a}) = 0,$$

where -P is again only the stress component normal to the coherent boundaries

(P is equal to the hydrostatic pressure acting on the external boundaries of the composite crystal).

CASE OF FINITE TRANSFORMATION STRAIN

Let us consider here a situation in which the stress-free transformation strain is finite and much larger than any elastic strain of either phase. In practice such a transition is not coherent unless a composition plane exists over which the two phases can be matched with stresses which do not exceed the strength of the mineral. Let us therefore assume that we are dealing with a coherent interface along such a plane, at equilibrium at a temperature T. The characteristic vector of the transformation across this plane is chiefly determined by the stress-free transformation strain.

We first restrict our discussion to a solid with no fluid component. At the temperature T, $\underline{a}$ and $\underline{b}$ would also be in equilibrium if both were under a hydrostatic pressure P^e. If $\bar{F}^{\underline{a},e}$, $\bar{F}^{\underline{b},e}$, $\bar{V}^{\underline{a},e}$, $\bar{V}^{\underline{b},e}$ are the molar Helmholtz energies and molar volumes at P^e and T, this equilibrium is described by the equation of hydrostatic equilibrium

$$(\bar{F}^{\underline{b},e} - \bar{F}^{\underline{a},e}) + P^e\ (\bar{V}^{\underline{b},e} - \bar{V}^{\underline{a},e}) = 0 \qquad (19)$$

When $\underline{a}$ and $\underline{b}$ are at equilibrium across the coherent interface under stress, the equilibrium condition (Eq. 16c) is

$$(\bar{F}^{\underline{b},e} - \bar{F}^{\underline{a},e})+(\Delta\bar{F}^{\underline{b}} - \Delta\bar{F}^{\underline{a}}) + P(\bar{V}^{\underline{b},e} - \bar{V}^{\underline{a},e}) + P(\Delta\bar{V}^{\underline{b}} - \Delta\bar{V}^{\underline{a}}) - \gamma\,\tau = 0 \qquad (20)$$

where: $\Delta\bar{F}^{\underline{a}}$, $\Delta\bar{F}^{\underline{b}}$, $\Delta\bar{V}^{\underline{a}}$ and $\Delta\bar{V}^{\underline{b}}$ are molar strain energies and volume changes when going from hydrostatic pressure P^e to the coherent situation; γ is the absolute value of the tangential component, γ_i, of the characteristic vector, and τ is the resolved shear stress in the direction of γ_i. Because the transformation strain is much larger than the elastic strains, as soon as τ is of the same order of magnitude as the stresses required to maintain

coherency the term $\gamma\tau$ is much larger than the elastic strain energy terms $\Delta\bar{F}^{\underline{a}}$, $\Delta\bar{F}^{\underline{b}}$, and also than $P\Delta\bar{V}^{\underline{a}}$, $P\Delta\bar{V}^{\underline{b}}$; a fortiori, the differences $(\Delta\bar{F}^{\underline{b}} - \Delta\bar{F}^{\underline{a}})$ and $P(\Delta\bar{V}^{\underline{b}} - \Delta\bar{V}^{\underline{a}})$ are negligible compared to $\gamma\tau$. Consequently, subtracting (19) from (20), the equilibrium condition reduces to

$$(P - P^e)\ \Delta\bar{V} - \gamma\tau = 0, \tag{21}$$

where $\Delta\bar{V}$ is now the molar volume difference

$$\Delta\bar{V} = \bar{V}^{\underline{b},e} - \bar{V}^{\underline{a},e} \simeq \bar{V}^{\underline{b}} - \bar{V}^{\underline{a}}.$$

Equation 21 can be differentiated with respect to T and gives

$$\left(\frac{dP}{dT} - \frac{\Delta\bar{S}}{\Delta\bar{V}}\right) \Delta\bar{V} - \gamma \frac{d\tau}{dT} = 0 \tag{22}$$

(using the Clausius-Clapeyron equation for $\frac{dP^e}{dT}$, and neglecting $\frac{d\gamma}{dT}$).
Therefore the following relations must be satisfied for the maintenance of equilibrium:

at constant τ: $\left(\frac{\delta P}{\delta T}\right)_{\tau,\text{equil.}} = \frac{\Delta\bar{S}}{\Delta\bar{V}} = \frac{dP^e}{dT}$ (23)

at constant P: $\left(\frac{\delta\tau}{\delta T}\right)_{P,\text{ equil.}} = -\frac{\Delta\bar{S}}{\gamma}$ (24)

Patel and Cohen (1953) combined (23) and (24) to explain the effects of hydrostatic compression, uniaxial compression and uniaxial tension on the martensitic reaction in iron-nickel and iron-nickel-carbon alloys.

Finite strain with fluid components

Coherent transformations characterized by large finite strains may also involve fluid components. A possible case, for example, is the ortho (Pbca) - clino ($P2_1/c$) transition in the pyroxene quadrilateral; formation of shear-induced lamellae of chinopyroxene in orthopyroxene is reported by several authors (e.g., Coe and Müller, 1973), and, at temperatures where cation diffusion is sufficiently rapid, such chinopyroxene lamellae

could become richer than the host in Fe and Ca (becoming in effect shear-induced pigeonite lamellae) (Chapter 5).

An analogous argument leads to an equilibrium condition similar to (20) (see Chapter 5, Equation 7)

$$(\bar{F}^{b,e} + P\bar{V}^{b,e}) - (\bar{F}^{a,e} + P\bar{V}^{b,e}) - \gamma\tau = \sum_{\alpha} \mu^{\alpha}(X^{b,\alpha} - X^{a,\alpha}) \qquad (25)$$

In Chapter 5 Equation 25 is demonstrated and used to calculate the equilibrium under stress of the coherent orthopyroxene $\hookleftarrow$ clinopyroxene reaction.

Case of finite simple shear and no fluid component

In this case $\bar{V}^{a} = \bar{V}^{b} = \bar{V}$,

and (Fig. 2)

$$\gamma = \bar{V} \tan \psi. \qquad (26)$$

Equation 16b becomes

$$\bar{F}^{b} - \bar{F}^{a} - \bar{V}\,\tau \tan \psi = 0 \qquad (27)$$

Equation 24 becomes

$$\left(\frac{\delta T}{\delta \tau}\right)_{P,\text{equil.}} = \frac{\bar{V} \tan \psi}{\Delta \bar{S}} . \qquad (28)$$

Equations 27 and 28 are identical to the results of Coe (1970) (except for a different sign convention on $\Delta\bar{S}$).

Finite strain twinning

Twins are at equilibrium with each other under any hydrostatic pressure, and in particular when the hydrostatic pressure is equal to the normal component of stress P. If the stress-free transformation strain (a finite simple shear) satisfies the assumptions of this section, the

equilibrium condition (Eq. 21) becomes

$$\gamma\tau \simeq 0$$

or

$$\tau \simeq 0 \tag{29}$$

In its equilibrium position such a twin boundary therefore does not support any resolved shear stress. This does not mean that other shear stress components are zero. The finite shear stress which is often required to move a twin boundary is thus a measure of the disequilibrium ($\gamma\tau$ is a molar energy) that the boundary can support before migrating.

INFINITESIMAL TRANSFORMATION STRAIN

If the transformation strain is very small, the reference state can be chosen such that the strain of the lattice with respect to the reference state is infinitesimal in any actual state of the system. The characteristic vector of the transformation is (Appendix)

$$v_i = \bar{V}\left[2\left(e^{\underline{b}}_{ij} - e^{\underline{a}}_{ij}\right) n^{\underline{a}}_j - \left(e^{\underline{b}}_{kk} - e^{\underline{a}}_{kk}\right) n^{\underline{a}}_i\right]$$

$$\text{or} \quad v_i = \bar{V}\left(2\,\Delta e_{ij}\, n^{\underline{a}}_j - \Delta e_{kk}\, n^{\underline{a}}_i\right) \tag{30}$$

where $e^{\underline{a}}_{ij}$, $e^{\underline{b}}_{ij}$ are the symmetric strain tensors with respect to the reference state, and Δe_{ij} is therefore the total transformation strain across the interface.

The scalar product $T_i\, v_i$ writes

$$T_i v_i = \bar{V}\,(2\,\tau_i\,\Delta e_{ij}\, n^{\underline{a}}_j + P\,\Delta e_{kk}) \tag{31a}$$

If the coordinate system is such that its 1-axis is perpendicular to the

interface at the point under consideration,

$$\Delta e_{22} = \Delta e_{33} = \Delta e_{23} = 0 \quad , \quad \Delta e_{kk} = \Delta e_{11} \quad ,$$

$$v_1 = \bar{V}\, \Delta e_{11} \quad , \quad v_2 = 2\bar{V}\, \Delta e_{12} \quad , \quad v_3 = 2\bar{V}\, \Delta e_{13}$$

$$T_1 = \sigma^{\underline{a}}_{11} = \sigma^{\underline{b}}_{11} = \sigma_{11} \quad , \quad T_2 = \sigma^{\underline{a}}_{12} = \sigma^{\underline{b}}_{12} = \sigma_{12} \quad , \quad T_3 = \sigma^{\underline{a}}_{13} = \sigma^{\underline{b}}_{13} = \sigma_{13}$$

and therefore

$$T_i v_i = \bar{V}\, (\sigma_{11}\, \Delta e_{11} + 2\, \sigma_{12}\, \Delta e_{12} + 2\, \sigma_{13}\, \Delta_{13}), \tag{31b}$$

or, in matrix notation,

$$T_i v_i = \bar{V}\, (\sigma_1\, \Delta e_1 + \sigma_5\, \Delta e_5 + \sigma_6\, \Delta e_6) \tag{31c}$$

We recognize the decomposition $-p\varepsilon + \gamma_i \tau_i$ obtained previously. The equilibrium condition follows immediately by inserting (31) into (16) or (18).

PREVIOUS RESULTS AND DISCUSSION

In spite of their many possible applications, only a few attempts to obtain results analogous to the ones presented here can be found in the literature. The worksof Patel and Cohen (1953) and of Coe (1970), for finite transformation strain and no fluid component, have already been mentioned. Oriani (1966) considered the equilibrium of a coherent spherical precipitate of an isotropic phase β in an isotropic matrix α, the stress-free transformation strain being itself infinitesimal and isotropic. Because of the symmetry of the situation, pressure is hydrostatic and uniform in β and the characteristic vector of the transformation is everywhere normal to the interface. Oriani's problem is thus not different from that of finding the equilibrium between a solid matrix α and a spherical

inclusion of fluid β which can dissolve the solid. McLellan (1970) and Paterson (1973) give the condition of equilibrium of a coherent interface, when the strain is infinitesimal and there are no fluid components, as

$$\bar{F}^{b} - \bar{F}^{a} - \bar{V}\ \sigma_{ij}\ \Delta e_{ij} = 0. \tag{32}$$

Although Equation 32 appears to ignore the fact that the stresses are in general not equal on both sides of the interface, the last term does reduce to (31) when the proper coherency conditions for Δe_{ij} are taken into account.

Kamb (1959) and Paterson (1973) give the following equilibrium equation for a 'grain boundary' supporting a shear stress:

$$(\bar{E}^{b} - T\bar{S}^{b} + P\bar{V}^{b}) - (\bar{E}^{a} - T\bar{S}^{a} + P\bar{V}^{a}) = 0 \tag{33}$$

where P is, as before, the normal component of stress on the interface.

Although Kamb (1959) does not detail his derivation, the only stated assumptions are that "there is no slippage at the interface and ... the shear stress is continuous across the interface ...", conditions which are fulfilled by a coherent interface. There is also no assumption which would exclude a coherent boundary in Paterson's derivation. The discrepancy between (33) and (16) therefore requires examination.

The very notion of <u>equilibrium with respect to a possible grain growth</u> requires that such grain growth be reversible. That is, if the state of the system is altered by a small variational growth of, say, phase <u>b</u>, at the expense of <u>a</u>, the reverse variation must bring the system to its original state. In particular, in presence of a shear stress, points of one phase must have recovered their original position with respect to points of the other phase. If this requirement were not met, the sum of the two variations would amount to a slip; slip then being a possible mechanism, equilibrium would require no shear component of stress along the interface.

On the contrary, when the above requirement of reversibility is met, it can be verified that any variational migration of the boundary must occur in a way similar to that described in Figure 1, and can therefore be described by a characteristic vector v_i.

At this point it is important to recognize that the migration of an interface as in Figures 1 or 2 is indeed not restricted to coherent interfaces. We may, for example, consider a row of parallel edge dislocations oriented as in Figure 3. When conditions are such that these dislocations cannot climb and do not move independently from one another, this boundary migrates like the coherent boundaries of Figure 1 or 2. Growth of kink bands constitutes another possible example.

Therefore, in order to reach (33), Kamb (1959) and Paterson (1973) had to implicitly assume that for a grain boundary supporting a shear stress the characteristic vector v_i was perpendicular to the interface. This is particularly clear in Paterson's derivation, in which an imaginary, inert, and permeable matrix applies the stress to the solid. To calculate the change in potential energy of the matrix for a variational growth of the crystal, Paterson assumes that points of the matrix are moved along a direction perpendicular to the interface to meet the new surface of the crystal. If contact between the solid and the matrix is assumed to be reestablished by moving points of the matrix along some different direction, a different value for the change in potential energy results; yet, there is no a priori reason to choose between these two assumptions.

Kamb (1959) and Paterson (1973) sought to apply (33) to the grain boundaries in polycrystalline aggregates. However, contrary to the subgrain or the kink boundaries envisaged above, random high-angle grain boundaries generally have no mechanism which could constrain their migration in

presence of a shear stress to be reversible in the same manner. Indeed, because of the generally complete disruption of the lattices along the boundary, the position of the a lattice has no way of influencing (or of being influenced by) the position of the b lattice. It is possible to conceive equilibrium with respect to growth while at the same time the boundary is sliding irreversibly. In reality, however, sliding along the boundary is likely to occur much faster than any phase growth across it; growth, or equilibrium with respect to it, would therefore obtain when the grain boundary no longer supports any shear stress, in which case Gibbs' equilibrium condition applies.

Except for theories of preferred orientations, Gibbs equilibrium condition has so far not been used in mineralogical problems. By contrast, equilibrium conditions for coherent interfaces have found applications in various problems of phase changes in the solid state (Patel and Cohen, 1953; Coe, 1970; Robin, 1974a,b) and are likely to find more as the microscopic study of interfaces develops.

APPENDIX

The infinitesimal strain with respect to the reference state can be characterized by the symmetric strain tensors

$$e^{\underline{b}}_{ij} = \frac{1}{2}\left(x^{\underline{b}}_{i,j} + x^{\underline{b}}_{j,i}\right) - \delta_{ij}$$

$$e^{\underline{a}}_{ij} = \frac{1}{2}\left(x^{\underline{a}}_{i,j} + x^{\underline{a}}_{j,i}\right) - \delta_{ij} \qquad \text{(A1)}$$

The characteristic vector is

$$v_i = \bar{V}\left(x^{\underline{b}}_{i,j} - x^{\underline{a}}_{i,j}\right) n^{\underline{a}}_{j}$$

or, using (A1),

$$v_i = \bar{V}\left[2\left(e^{\underline{b}}_{ij} - e^{\underline{a}}_{ij}\right) n^{\underline{a}}_{j} - \left(x^{\underline{b}}_{j,i} - x^{\underline{a}}_{j,i}\right) n^{\underline{a}}_{j}\right] \qquad \text{(A2)}$$

The fact that the transformation strain leaves the plane of the interface invariant is expressed by

$$\left(x^{\underline{b}}_{j,i} - x^{\underline{a}}_{j,i}\right) t_i = 0 \qquad \text{(A3)}$$

where t_i is any vector tangent to the interface at the point under consideration. Also, the molar volume change is

$$v_i\, n^{\underline{a}}_{i} = \bar{V}\left(e^{\underline{b}}_{ii} - e^{\underline{a}}_{ii}\right) \qquad \text{(A4)}$$

The term $\left(x^{\underline{b}}_{j,i} - x^{\underline{a}}_{j,i}\right) n^{\underline{a}}_{j} = k_i$ of (A2) can be evaluated. From (A3), $k_i t_i = 0$.

Also $k_i n^{\underline{a}}_{i} = \left(x^{\underline{b}}_{j,i} - x^{\underline{a}}_{j,i}\right) n^{\underline{a}}_{j}\, n^{\underline{a}}_{i} = \frac{1}{\bar{V}}\, v_j\, n^{\underline{a}}_{j}$, $= e^{\underline{b}}_{jj} - e^{\underline{a}}_{jj}$, from (A4).

Therefore k_i is normal to the interface and equal to

$$k_i = \left(e^{\underline{b}}_{kk} - e^{\underline{a}}_{kk}\right) n^{\underline{a}}_{i}$$

Inserting into (A2), we obtain finally

$$v_i = \bar{V} \left[2(e^{\underline{b}}_{ij} - e^{\underline{a}}_{ij})\, n^{\underline{a}}_j - (e^{\underline{b}}_{kk} - e^{\underline{a}}_{kk})\, n^{\underline{a}}_i \right] \qquad (30).$$

REFERENCES

BASINSKY, Z. S., AND J. W. CHRISTIAN (1954a) Crystallography of deformation by twin boundary movements in Indium-Thallium alloys. Acta Metal. 2, 101-106.

BASINSKY, Z. S. AND J. W. CHRISTIAN (1954b) Experiments on the martensitic transformation in single crystals of Indium-Thallium alloys. Acta Metal. 2, 148-166.

BOWLES, J. S., AND J. D. MACKENZIE (1954) The crystallography of martensite transformations. Acta Metal. 2, 129-147.

BRIDGMAN, P. W. (1939) The high pressure behavior of miscellaneous minerals. Amer. J. Sci. 37, 7-18.

BUERGER, M. J. (1948) The rôle of temperature in mineralogy. Amer. Mineral. 33, 101-121.

BURKART, M. W., AND T. A. READ (1953) Diffusionless phase change in the Indium-Thallium System. Trans. A.I.M.E. 197, 1516-1524.

CHAMPNESS, P. E., AND G. W. LORIMER (1973) Precipitation (exsolution) in an orthopyroxene. J. Mat. Sci. 8, 467-474.

CHANG, L. C., AND T. A. READ (1951) Plastic deformation and diffusionless phase changes in metals - the Gold-Cadmium beta phase. Trans. A.I.M.E. 191, 47-52.

CHRISTIE, J. M., J. S. LALLY, A. H. HEUER, R. M. FISHER, D. T. GRIGGS AND S. V. RADCLIFFE (1971) Comparative electron petrography of Apollo 11, Apollo 12, and terrestrial rocks. In: Proceedings of the second Lunar conference, Vol. 1, Massachusetts Institute of Technology Press, Cambridge, Massachusetts.

COE, R. S. (1970) The thermodynamic effect of shear stress on the ortho-clino inversion in enstatite and other coherent phase transitions characterized by a finite simple shear. Contr. Mineral. and Petrol. 26, 247-264.

COE, R. S., AND W. F. MULLER (1973) Crystallographic orientation of clinoenstatite produced by deformation of orthoenstatite. Science 180, 64-66

COE, R. S. AND M. S. PATERSON (1969) The α-β inversion in quartz: a coherent phase transition under non-hydrostatic stress. J. Geoph. Res. 74, 4921-4948.

FRONDEL, C. (1945) Secondary Dauphiné twinning in quartz. Amer. Mineral. 30, 447-460.

GIBBS, J. W. (1906) The collected works of J. Willard Gibbs, Ph.D. LL.D., Vol. I, Thermodynamics, Longmans, Green, and Company, New York, N.Y., 434 p.

KAMB, W. B. (1959) Theory of preferred crystal orientation developed by crystallization under stress. J. Geology 67, 153-170.

KAMB, W. B. (1961) The thermodynamic theory of nonhydrostatically stressed solids. J. Geophys. Res. 66(1), 259-271.

KELLY, A., AND R. B. NICHOLSON (1963) Precipitation Hardening. In B. Chalmers (ed.) Progress in Materials Science, Vol. 10. The Macmillan Company, New-York, N.Y., 452 p.

LI, J. C. M., R. A. ORIANI, AND L. S. DARKEN (1966) The thermodynamics of stressed solids. Zeitschrift f. Physik. Chemie Neue Folge 49, 271-290.

MCLELLAN, A. G. (1970) Non-hydrostatic thermodynamics of chemical systems. Proc. Roy. Soc. A314, 443-455.

MURNAGHAN, F. D. (1951) Finite deformation of an elastic solid, J. Wiley and Sons, Inc., New-York, N.Y., 140 p.

ORIANI, R. A. (1966) Comments on coherent two-phase equilibrium and Ostwald ripening. Acta Metal. 14, 84-86.

OWEN, W. S., F. J. SCHOEN AND G. R. SRINIVASAN (1970) The growth of a plate of martensite. In: Phase Transformation. American Society for metals, Metals Park, Ohio, 632 p.

PATEL, J. R., AND M. COHEN (1953) Criterion for the action of applied stress in the martensitic transformation. Acta Metal. 1, 531-538.

PATERSON, M. S. (1973) Non-hydrostatic thermodynamics and its geological applications. Rev. of Geophysics 11 (2):255-389.

ROBIN, P-Y. F. (1974a) Stress and strain in cryptoperthite lamellae and the coherent solvus of alkali feldspars. Amer. Mineral. 59 (in press).

ROBIN, P-Y. F. (1974b) Doctoral dissertation, Massachusetts Institute of Technology, Cambridge, Mass., U.S.A.

ROBINSON, P., H. W. JAFFE , M. ROSS AND C. KLEIN,JR. (1971) Orientation of exsolution lamellae in clinopyroxenes and clino amphiboles: consideration of optimal phase boundaries. Amer. Mineral. 56, 909-939.

THOMAS, L. A., AND W. A. WOOSTER (1951) Piezocrescence - the growth of Dauphiné twinning in quartz under stress, Proc. Roy. Soc. A208, 43-62.

THOMPSON, J. B., JR. (1969) Chemical reactions in crystals. Amer. Mineral. 54, 341-375.

TULLIS, J., AND T. TULLIS (1972) Preferred orientation of quartz produced by mechanical Dauphiné twinning: thermodynamics and axial experiments. In: Flow and fracture of rocks, Geophysical Monograph 16, American Geophysical Union, Washington D.C., 336 p.

deVORE, G. W. (1970) Elastic compliances of minerals related to crystallographic orientation and elastic strain energy relations in twinned crystals. Lithos 3, 193-208.

WANG, C-Y. (1968) Ultrasonic study of phase transition in calcite to 20 kilobars and 180°C. J. Geophys. Res. 73, 3937-3944.

WANG, C.-Y. AND M. MELTZER (1973) Propagation of sound waves in a rock undergoing phase transformations. J. Geophys. Res. 78(8), 1293-1298.

WAYMAN, C. M. (1964) Introduction to the crystallography of martensitic transformations. MacMillan Cy., New-York, N.Y.

WESCHLER, M. S., D. S. LIEBERMAN AND T. A. REED (1953) On the theory of the formation of martensite. Trans. A.I.M.E. 197, 1503-1515.

YOUNG, R. A. (1962) Mechanism of the phase transition in quartz. U.S.A.F. office Sci. Res. Report 2569, Washington, D.C., U.S.A.

CAPTIONS

Fig. 1. Migration of a coherent interface in the actual state. Lines have been drawn in a and b to help visualization; they can be interpreted as the traces of two sets of lattice planes preserved in the transformation.

Fig. 2. Characteristic vector, for finite simple shear. The vector $\mathbf{v}_i$ has only a tangential component, of modulus γ. The transformation is more easily characterized by its shear angle ψ. When a molar volume $\bar{V}$ changes phase across a unit area of interface, $|\overline{Q'P'}| = \gamma = \bar{V} \tan \psi$; hence (26).

Fig. 3. Wall of gliding edge dislocations. The full lines are traces of glide planes. Simultaneous gliding of the dislocations results in a shear deformation of the framework, essentially similar to the interface migrations presented in Figures 1 and 2.

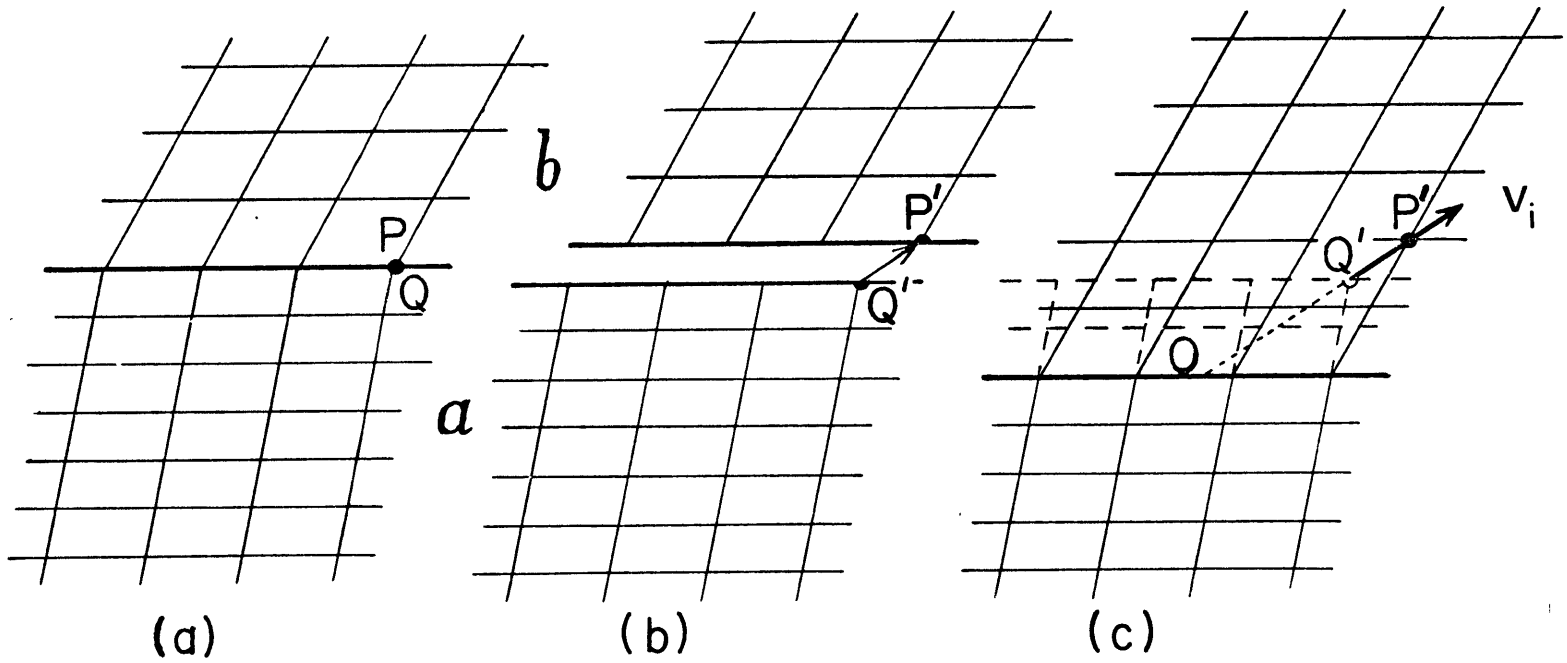

Fig.1

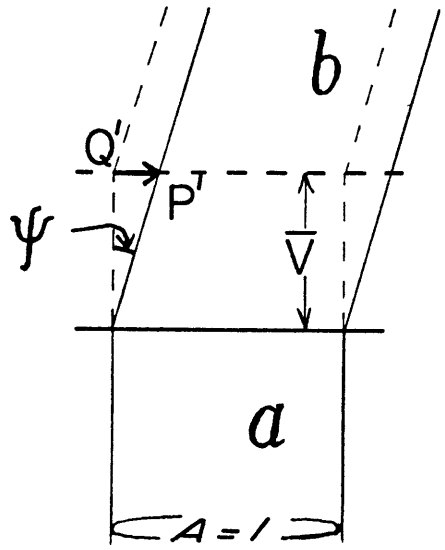

Fig. 2

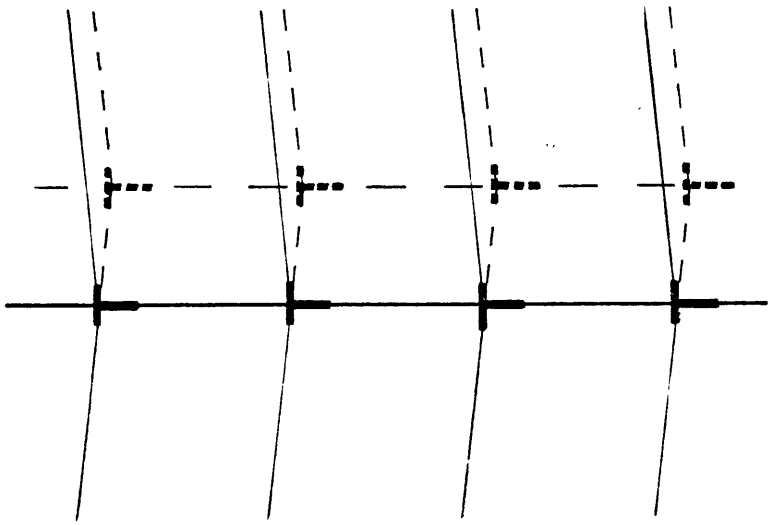

Fig. 3

CHAPTER 3

STRESS AND STRAIN IN CRYPTOPERTHITE LAMELLAE AND THE COHERENT SOLVUS OF ALKALI FELDSPARS[1]

Abstract

Transmission electron microscope observations of a cryptoperthite alkali feldspar from Larvik (Norway) show that the exsolution lamellae are fully coherent, that is, they maintain full continuity of their lattices across the lamellar interfaces; this confirms x-ray work by previous authors on other cryptoperthites.

Coherency imposes elastic strains in individual lamellae, causing the lattice parameters to differ from those of unstrained crystals of the same compositions. From known elastic constants and known compositional variation of stress-free lattice parameters, elastic strain and stress components in a lamella are calculated as linear functions of $(X-X^o)$ (where X = mole fraction $KAlSi_3O_8$; X^0 = average value for bulk crystal). The assumption that elastic strain entails no volume change and the resulting method of determining compositions of individual lamellae (Smith, 1961) can therefore be evaluated; an alternate simple method is proposed, which makes use of the fact that there are linear combinations of two (h0l) spacings which are not affected by the elastic strain.

The elastic strain energy varies as $(X-X^o)^2$. When strain energy is taken into account in the thermodynamic treatment of exsolution, a 'coherent

---

[1] American Mineralogist, in press.

solvus' can be calculated, with a critical temperature 70^{o} to 85^{o} C below the critical temperature of the solvus for unconstrained phases (e.g. Luth and Tuttle, 1966). This agrees well with the hitherto unexplained results of annealing experiments on single crystals by Tuttle and Bowen (1958) and Smith and Mackenzie (1958).

Lamellar exsolution occurs in many other mineral systems. If the lamellae have retained coherency, the relevant phase diagram is the coherent solvus, not the unconstrained one determined in hydrothermal experiments. Other transformations within crystals may also give rise to elastically strained phases coexisting along coherent interfaces. The corresponding strain energy must be taken into account in the thermodynamic analysis and the geologic interpretation of such transformations.

INTRODUCTION

Cryptoperthites are lamellar mixtures of exsolved potassium- and sodium-rich alkali feldspars in which individual lamellae are too thin to be resolved optically. Some authors (e.g. Tuttle, 1952) have restricted the use of the name to those mixtures in which lamellae have thicknesses of one μm or more. In accordance with more recent usage, however, the 'cryptoperthites' considered in this paper include Tuttle's cryptoperthites and X-ray perthites.

Lattice parametersof the two feldspars coexisting in a cryptoperthite often do not fit the description of any known homogeneous feldspar. Variations with composition of the lattice parameters of homogeneous crystals in the sanidine-high albite series have been systematically investigated (Donnay and Donnay, 1952; Orville, 1967; Wright and Stewart, 1968) and are therefore quite well known. Typically, however, in the K-rich phase of a cryptoperthite a "is too long relative to b and c ..." (Wright and Stewart, 1968). Consequently, compositions of these 'anomalous' phases, as determined by several X-ray methods using different lattice parameters, are contradictory and sometimes physically impossible (Laves, 1952; Coombs, 1954; MacKenzie and Smith, 1956; Smith and MacKenzie, 1958).

Phases coexisting in a cryptoperthite also appear to be anomalous in their exsolution behavior. The existence of a two-phase region in the high-temperature alkali feldspar solid solutions below temperatures of 650°C is well documented (e.g. Bowen and Tuttle, 1950; Orville, 1963; Luth and Tuttle, 1966; Müller, 1971). Thermodynamic equations of state have been derived by several authors (Thompson and Waldbaum, 1968, 1969; Waldbaum and Thompson, 1968, 1969; Luth et al., 1970, 1972; Delbove, 1971) and provide a basis for quantitative treatment of exsolution. However, homogenization experiments of sanidine-high albite cryptoperthites (Tuttle

and Bowen, 1958; Smith and MacKenzie, 1958) indicate a solvus very significantly lower than the ones determined in hydrothermal experiments. These authors attributed the discrepancy to the fact that they were dealing with natural feldspars, as opposed to the synthetic ones used in hydrothermal work. There has been no further discussion of Tuttle and Bowen's (1958) and Smith and MacKenzie's (1958) results. The experimental work of Müller (1971) shows in fact that for increasing degrees of Al-Si order, as expected in natural feldspars, the critical temperature becomes higher, not lower, than for the disordered high-temperature solution series synthesized in the laboratory.

Many, perhaps most, optically homogeneous high-temperature alkali feldspars of intermediate compositions occurring in nature are cryptoperthites. The present author also believes that most perthites are derived from an earlier cryptoperthitic state. The questions that cryptoperthites raise are therefore important for alkali feldspars in general. The purpose of this paper is to show that cryptoperthite lamellae are, in many cases, coherent lamellae, and that coherent lamellar exsolution quantitatively explains the lower solvus discussed above.

The anomalous cell parameters of cryptoperthite phaseswere qualitatively explained by Laves (1952) and Smith (1961). These authors observe that the repeat distances are equal in both phases along [010] and along an irrational direction between [106] and [108]. The plane which [010] and this irrational direction define corresponds to the orientation determined for the Schiller plane exhibited by many moonstones, and to the direction of microperthite lamellae observed optically. Both Laves and Smith concluded that the two phases of a cryptoperthite exsolve as lamellae oriented parallel to the $(\bar{6}01)/(\bar{8}01)$ plane but maintain continuity of their lattices along their interfaces. The anomalous parameters result from the elastic strain

necessary to satisfy this constraint. Smith (1961) further notes that, in homogeneous crystals, [106] is the direction in the ac plane along which the repeat distance is affected the least by changes in composition. Smith therefore suggests that the lamellae are oriented as observed in order to minimize the required elastic strain.

Cryptoperthite lamellae have been observed in transmission electron microscopy (TEM) (Fleet and Ribbe, 1963; Bollmann and Nissen, 1968; Brown et al., 1972; Willaime and Gandais, 1972; Willaime et al., 1973). TEM observations essentially confirm the lamellar structure postulated by Laves and by Smith, with however some complexities when the K-rich phase has partially or totally inverted to triclinic symmetry (Brown et al., 1972). Further explanations of the orientation of the lamellae are given by Bollmann and Nissen (1968), using the O-lattice theory, and by Willaime and Brown (1972) and Willaime (1973) using computer calculations of strain energy in bi-crystals made of equal amounts of both phases. Orientations predicted do not differ significantly from the one given by Smith (1961).

Coherency

A boundary between two phases across which the two lattices are in continuity is often referred to as a coherent boundary or coherent interface, and an exsolving phase which maintains coherent interfaces with its matrix is accordingly called a coherent precipitate (e.g. Kelly and Nicholson, 1963). Coherent exsolution lamellae may be considered simply as coherent precipitates with a much larger extent in two dimensions than in the third.

The requirement that two phases meet along coherent interfaces generally sets up nonhydrostatic stresses in each phase. At a given temperature the Helmholtz energy of a chosen mass of the stressed phase differs from its value under a hydrostatic pressure P by an amount called the strain energy.

The strain energy is the mechanical work performed by stresses on the mass of the phase to bring it, at constant temperature, from P to its nonhydrostatically stressed state. During coherent exsolution strain energy results in a 'penalty' against exsolution into two phases; the extent of the two-phase field is therefore reduced compared to the hydrostatic solvus[2]. Cahn (1962) first noted this fact and developed the theory of coherent phase diagrams for exsolution (coherent solvus) for the case of elastically isotropic precipitate and matrix, and isotropic stress-free transformation strain. Christie (1968), Yund and McCallister (1970) and Willaime (1973) mention the possible existence of a coherent solvus in alkali feldspars.

The derivation of the coherent solvus presented in this paper is exact under the following assumptions:

i) All phases have the same degree of Al-Si order as sanidine.

ii) All phases have monoclinic symmetry. For the part of the calculation which applies to room-temperature conditions, this assumption can only be justified by the fact that the Na-rich phase is regularly twinned in such a way as to simulate monoclinic symmetry. For the calculation of the coherent solvus the analysis can be taken to apply exactly only to that part of the solvus at temperatures above the monoclinic-triclinic transition of the Na-rich phase (a restriction similar to that of Thompson and Waldbaum, 1969). A consequence of monoclinic symmetry is that the stress and strain tensors considered have one principal axis along the b axis (diad axis), the two other principal axes being in the ac plane.

---

[2] The term hydrostatic is often used in this paper to contrast with coherent. Thus the hydrostatic solvus is the equilibrium exsolution curve for unconstrained phases, which are therefore under hydrostatic pressure. The hydrostatic equation of state is the equation of state of uniform homogeneous unconstrained phases.

iii) All relative changes of lattice parameters, whether due to changes in composition or to elastic deformation, are small enough to be considered infinitesimal. The assumptions of infinitesimal strain and of linear elasticity greatly simplify the calculations and the representation of strain.

iv) Each lamella, characterized by a definite set of stress-free lattice parameters, is bounded by two infinite parallel coherent boundaries. The thickness of the composite 'book' of lamellae is much larger than the thickness of an individual lamella, and there is no systematic variation in the bulk composition of the crystal (as averaged over many lamellae) when moving along a direction perpendicular to the lamellae. A very important property of such lamellae can be stated as follows:

> If no average stress other than hydrostatic is applied on the boundaries of the composite, stresses and strains are uniform within each lamella. There are no shear stresses on the lamellae boundaries. The stress normal to the boundaries is equal to the hydrostatic stress applied onto the composite. The other two principal components of stress are parallel to the boundaries and vary with the composition of the lamella.

This result is demonstrated in Appendix A.

In reality lamellae are not infinite in their own plane, and stresses and strains are not uniform in regions near the edges of a lamella or near the external boundaries of the crystal. Calculations of stress, elastic strain, and strain energy based on the assumption of infinite parallel lamellae are nevertheless probably applicable if thicknesses of individual lamellae are less than, say, one tenth of their planar extent.

v) Surface energy is neglected. Coherent interfacial energy (which will be a further penalty against exsolution) is generally considered low. Ardell (1968, 1970) calculated specific interfacial energies of 14 and 21 erg cm^{-2} for coherent γ' particles in Ni-Al and Ni-Ti alloys respectively. In feldspars the distance between two adjacent alkali ion sites, the only sites whose population changes across an interface, is large ($\simeq 5$ Å) compared to equivalent distances in the alloys studied by Ardell. Thus the interfacial energy in feldspars could be even lower than in alloys (Ardell and Nicholson, 1966). For an average lamellar thickness of 0.2 μm a specific interfacial energy of 20 erg cm^{-2} amounts to 2 cal mol^{-1} and can reasonably be neglected. For higher values of interfacial energy and/or smaller lamellar thicknesses the total surface energy may become important.

TRANSMISSION ELECTRON MICROSCOPY (TEM)

TEM samples were prepared from petrographic thin sections by ion bombardment thinning (Heuer et al., 1971) and examined with a 100 kV JEM (Japan Electron Microscope) and a Siemens 101 with tilting stages. The crystals studied are from a grey-blue larvikite of the M.I.T. collection, merely identified as being from Larvik, Norway. Feldspars from this general area have been studied in detail, particularly by Oftedahl (1948), Muir and Smith (1956) and Smith and Muir (1958). Some specimens have been examined in TEM by Bollmann and Nissen (1968), Willaime and Gandais (1972) and Willaime et al. (1973).

The feldspar studied here exhibits a light blue 'schiller'; its composition [mole fraction X = Or/(Ab + Or)] varies from X = 0.09 to X = 0.74 within a single polished thin section, and averages X = 0.34. This lack of homogeneity is confirmed by TEM observations. 'Large' regions (several tens

of square microns) consist entirely of albite which is twinned according to the pericline law (Figure 1). Other regions, although still mostly albite, contain irregular lamellae of K-feldspar (Figure 2). We note in Figure 2 that the periodicity of pericline twinning in albite is variable. Willaime and Gandais (1972) report a relationship between periodicity of albite twinning and thickness of albite lamellae in cryptoperthites; a similar relationship appears to be true here for pericline twinning.

Most of the crystal, however is characterized by a dense alternation of K- and Na-rich lamellae. Figure 3 is a good example of the lamellar structure to which the elastic analysis of the following section can be applied. As in Figures 1 and 2, the view is along the b axis, and the plane of the micrograph is the ac plane, Because pericline twinning corresponds to a 180° rotation of the albite lattice about the b axis, the two twin orientations give rise to only one set of diffraction spots; the other set of spots in Figure 3b belongs to the K-feldspar. Most individual lamellae are more than ten times as long as they are thick, their longest direction (IP in Figure 3) making a 107° angle with the basal cleavage.

The noticeable variation in intensity within a lamella is a result of strain contrast: inhomogeneous strain causes variations in deviation from the Bragg condition for the electron beam, and hence variations in intensity of the transmitted beam. This inhomogeneous strain may seem incompatible with the property of uniformity demonstrated in Appendix A; however, it is in fact chiefly due to the thin slicing necessary for TEM observations. Indeed, consider a slice of crystal approximately perpendicular to the plane of the lamellae and whose thickness is comparable to or smaller than the thickness of individual lamellae. The assumption of infinite extent,

acceptable for the original crystal, is no longer valid; slicing allows a non-uniform relaxation of the original stresses and gives rise to the inhomogeneous strain observed.

Stresses along some directions cannot be relaxed, however; if boundaries between lamellae are coherent, repeat distances along the lattice direction IP are still maintained equal in the two types of lamellae. In other words, the constraint of coherency is not relaxed for these lattice planes which are parallel to the axis of the microscope and give rise to the diffraction pattern of Figure 3b.

We note in Figure 3b that the line segments between two points of same index, corresponding to the K- and Na- feldspars, are all parallel to each other and perpendicular to the lamellae boundaries in real space. It is shown in Appendix B that such a relationship, exemplified in Figure B1, is a general property of the reciprocal lattices of coherent lamellae. Therefore, although the strain contrast of Figure 3a does not permit detection of possible mismatch dislocations along the boundaries, the diffraction pattern can be taken as sufficient evidence that the lamellae are coherent[3].

The absence of mismatch dislocations is confirmed by an oblique view of lamellae boundaries under high magnification (Figure 4); Moiré fringes (e.g. Hirsch et al., 1965) are visible, but no dislocations can be imaged.

TEM thus demonstrates that the cryptoperthite lamellae studied here are coherent, as were those examined by Laves and Smith. Not all cryptoperthites

---

[3] The diffraction pattern of Figure 3b satisfies the relationship of Figure B1 because the two pericline twins give rise to only one set of diffraction spots. For other orientations, or other twin laws, the situation is more complicated; in case of coherency, only mid-points between two twin spots bear the relationship to the K- feldspar spots which is shown in Figure B1. The two twin spots themselves lie on a line perpendicular to the twin boundaries in real space.

are necessarily coherent however; Aberdam and Kern (1962) and Aberdam et al. (1964) observed 0.1 to 1.1 μm thick lamellae whose boundaries were semi-coherent, that is, they exhibited regularly spaced mismatch dislocations. The analysis of elastic stresses and strains which follows only applies to those cryptoperthites which have preserved full coherency.

ELASTIC ANALYSIS

Although actual calculations are lengthy, the method of obtaining elastic stresses and strains in individual lamellae is straightforward. Known changes of the stress-free lattice parameters of high-temperature alkali feldspars are used to calculate the strain components imposed on a lamella of composition X (mole fraction $KAlSi_3O_8$) which exsolves from a crystal of average bulk composition X^o but retains coherency with it. From Hooke's law the stress and the remaining strain components can then be calculated as a function of $(X - X^o)$.

Stress-free compositional strain

Although lattice parameters do not vary exactly linearly with X, a linear approximation is sufficient here; because data will be applied to exsolution, tangential values at the anticipated critical composition are preferable. Slopes of tangents at X = 0.33 can be measured directly from Orville's (1967) curves[4] :

$$\frac{1}{\underline{b}} \frac{\partial \underline{b}}{\partial X} = 0.0162 , \qquad (1a)$$

$$\frac{1}{\underline{a}} \frac{\partial \underline{a}}{\partial X} = 0.0567, \quad \frac{1}{\underline{c}} \frac{\partial \underline{c}}{\partial X} = 0.0112, \quad \frac{\partial \beta}{\partial X} = 0.0116 . \qquad (1b)$$

---

[4] The triclinicity of the albite phase is ignored; in all rigor, when that phase is twinned according to the pericline law, $\underline{a}$ and $\underline{c}$ should be replaced by $1/\underline{a}^*$ and $1/\underline{c}^*$. Similarly, had the albite been twinned according to the albite law, $\underline{b}$ should be replaced by $1/\underline{b}^*$. The difference is insignificant here.

A change in lattice parameters is a strain. Within the approximation of monoclinic symmetry, the stress-free compositional strain coefficients in (1) are sufficient to determine the stress-free compositional strain (or, for short, compositional strain) completely. The intermediate principal axis of strain is along the b axis. Compositional strain in the ac plane is conveniently represented by its Mohr circle (see Nye, 1957) in Figure 5. The minimum principal axis of strain (point m) makes an angle of approximately 110^{o} with the a axis, and the corresponding minimum longitudinal strain coefficient is equal to 0.0105. The maximum longitudinal strain coefficient is 0.0630 (point M). The Mohr circle construction thus verifies Smith's (1961) observation that the direction of the contact plane of cryptoperthites corresponds closely to a minimum in compositional expansion. Computations of strain energy by Willaime and Brown (1972) should in principle give a more exact prediction of the orientation of the lamellae. In practice, however, longitudinal strain components enter as squared quantities in the expression of strain energy, while elastic coefficients can be verified numerically not to be very sensitive to small rotations of axes; the orientation minimizing the strain energy should therefore be close to the one containing the minimum and intermediate principal axes of compositional strain.

Choice of coordinates

Cartesian coordinate axes are chosen with the 1-axis normal to the lamellae boundaries, the 2-axis along the crystallographic b axis, and the 3-axis normal to 1 and 2 (Figure 6). Rather than take 110^{o}, predicted by Figure 5, as the angle between the contact plane and the a-axis, 107^{o} is chosen, more in line with observed values. The new coordinate axes are approximately the principal axes of compositional strain and are related

to the conventional coordinate system for monoclinic crystals by a rotation of 17^{o} about the b-axis. Let us call η_{ij} the stress-free compositional strain. In our system of coordinates the compositional strain coefficients are therefore

$$\frac{\partial \eta_{22}}{\partial X} = 0.0162 \ ,$$

$$\frac{\partial \eta_{11}}{\partial X} = 0.0630 \ , \quad \frac{\partial \eta_{33}}{\partial X} = 0.0105 \ , \quad \frac{\partial \eta_{13}}{\partial X} \simeq 0 \ .$$

Now, if we take the unstressed lattice of a homogeneous crystal of composition X^{o} (any arbitrary composition) as reference state, the compositional strain of a crystal of composition X, with respect to that reference state, is,

$$\eta_{22} = 0.0162 \ (X - X^{o}), \tag{2a}$$

$$\eta_{11} = 0.0630 \ (X - X^{o}), \ \eta_{33} = 0.0105 \ (X - X^{o}), \ \eta_{13} \simeq 0, \tag{2b}$$

$$\eta_{11} + \eta_{22} + \eta_{33} = 0.0897 \ (X - X^{o}). \tag{2c}$$

Elastic constants

The only published values of elastic constants for alkali feldspars are by Ryzhova and Aleksandrov (1965), (R and A), who measured acoustic velocities in crystals of various compositions. The reported constants do not show any systematic variation with composition and are therefore taken to be independent of the latter. The non-systematic variations of the constants are large, however, and are probably due, as Simmons (1964), R and A, and Christensen (1966) point out, to cleavages and other flaws in the crystals. Two approaches are taken to correct for these imperfections: (1) Feldspar No. 61 of R and A exhibits a relatively high absolute value

of all its stiffness constants; thus estimated to be a relatively flawless crystal, its elastic constants are taken as a first set.

(2) A second set, C, is generated by choosing for each c_{ij} the highest value calculated by R and A for all the alkali feldspars they studied (including an albite reported by Ryzhova, 1964).

The two sets, reported for the conventional coordinate system, are given in Table 1. Their values, recalculated for the new coordinate system (Voigt, 1928, p. 593), are given in Table 1. As a way to estimate the uncertainty of the results due to the uncertainty of our knowledge of the elastic constants, all calculations are carried out with the two sets of constants. Numerical results are given for each set, the ones corresponding to C being given in parentheses.

Stresses and strains

Let us now consider a cryptoperthite, of average composition X^o, made up of many coherent exsolution lamellae. The elastic strain components imposed on a lamella of composition X are

$$\left.\begin{aligned} \varepsilon_2 = \varepsilon_{22} = -\eta_{22} &= -0.0162\ (X - X^o), \\ \varepsilon_3 = \varepsilon_{33} = -\eta_{33} &= -0.0105\ (X - X^o), \\ \varepsilon_4 = 2\varepsilon_{23} &\simeq 0\ . \end{aligned}\right\} \qquad (3)$$

That is, the lamella is elastically constrained to match the lattice of the 'average crystal' across the coherent boundary plane. Equations 3 are rigorously exact only to the extent that compositional strain coefficients and elastic constants are independent of composition.

Elastic strain and stress components are related by Hooke's law, which, for our purpose, can be written (matrix notation; see Nye, 1957):

$$\sigma_1 = \sigma_4 = \sigma_5 = \sigma_6 = \varepsilon_4 = \varepsilon_6 = 0, \tag{4a}$$

$$\left.\begin{aligned} \sigma_2 - c_{12}\varepsilon_1 - c_{25}\varepsilon_5 &= c_{22}\varepsilon_2 + c_{23}\varepsilon_3 \,, \\ \sigma_3 - c_{13}\varepsilon_1 - c_{35}\varepsilon_5 &= c_{23}\varepsilon_2 + c_{33}\varepsilon_3 \,, \\ - c_{15}\varepsilon_1 - c_{55}\varepsilon_5 &= c_{25}\varepsilon_2 + c_{35}\varepsilon_3 \,, \\ - c_{11}\varepsilon_1 - c_{15}\varepsilon_5 &= c_{12}\varepsilon_2 + c_{13}\varepsilon_3 \,. \end{aligned}\right\} \tag{4b}$$

The solution of (4b), using numerical values in (3) and in Table 1, is

$$\sigma_{22} = \sigma_2 = \underset{(-\,0.0257)}{-\,0.0230}\,(X - X^o) \quad \text{Mbar}, \tag{5a}$$

$$\sigma_{33} = \sigma_3 = \underset{(-0.0140)}{-\,0.0106}\,(X - X^o) \quad \text{Mbar}, \tag{5b}$$

$$\varepsilon_{11} = \varepsilon_1 = \underset{(+\,0.0164)}{+\,0.0182}\,(X - X^o) \quad , \tag{5c}$$

$$2\varepsilon_{13} = \varepsilon_5 = \underset{(-0.0083)}{-\,0.0024}\,(X - X^o) \quad , \tag{5d}$$

where the parentheses denote values calculated for the elastic constants of C (see Table 1).

The volumetric strain is

$$\varepsilon_1 + \varepsilon_2 + \varepsilon_3 = \underset{(-\,0.0103)}{-\,0.0085}\,(X - X^o). \tag{5e}$$

If a hydrostatic pressure P is acting on the crystal, the lattice of the homogeneous crystal X^o under the pressure P may be taken as new reference

state. In that case, the elastic strain components are still given by Equations 3 and 5c, d, provided the effect of pressure on compositional strain coefficients and elastic constants can be neglected (an assumption to be justified later). The principal stress components σ_1, σ_2 and σ_3 are increased by -P over their values in (4b) and (5a,b).

Composition determinations from lattice parameters

Equations 3 and 5 determine all the components of elastic strain in a lamella of composition X coherent within a crystal of average composition X^o. The various methods of determining compositions from X-ray lattice parameters can therefore be evaluated.

Figure 7 is the Mohr circle for the elastic strain in (010). It shows that the $(\bar{2}01)$ spacing, $d(\bar{2}01)$, is elastically increased in the K-rich lamellae $[(X - X^o) > 0]$ and elastically decreased in the Na-rich lamellae $[(X - X^o) < 0]$. Consequently, if $d(\bar{2}01)$ is used without precautions to determine compositions, the K-rich lamellae will be found richer in potassium and the Na-rich lamellae poorer than either really are. If their real compositions are already close to end members the $d(\bar{2}01)$ method may thus yield physically impossible results (X>1 or X<0) such as those reported by Coombs (1954).

Figure 7 shows that, contrary to $d(\bar{2}01)$, $d(\bar{2}04)$ is elastically decreased in the K-rich lamellae and increased in the Na-rich ones. There is a linear combination of $d(\bar{2}01)$ and $d(\bar{2}04)$ which is neither increased nor decreased by the elastic strain (Appendix C); such linear combination is therefore a function of composition alone and can be used to determine the composition of the lamellae.

Smith (1961) suggested the use of the volume of the lattice cell to determine compositions of cryptoperthite lamellae, under the assumption that

this volume is unaffected by elastic strain, i.e. that $\varepsilon_1 + \varepsilon_2 + \varepsilon_3 = 0$. In fact, when the lamellae are coherently maintained within a large crystal, the variation of the cell volume with composition is no longer given by (2c) as implied by Smith; this variation must be corrected by the elastic volume change given by (5e). Comparison of (2c) and (5e) shows that Smith's assumption leads to an underestimate of X for the K-rich phase and to an overestimate for the Na-rich phase, by approximately $0.1(X-X^o)$. If X^o is known the appropriate correction can thus be made. However, such method of determining compositions is unnecessarily complicated.[5]

Wright and Stewart (1968, p.71) state that whenever they observe anomalous cell parameters "b, c or both are too low relative to a to define a consistent structural state". Considerations presented here indicate in fact that if both phases have the Al-Si order of sanidine, Wright and Stewart's statement is only true for the K-rich phase; the Na-rich phase on the contrary has its b and c cell dimensions 'stretched', and therefore too large relative to a. Wright and Stewart's statement may stem from the fact that

---

[5] Jan Tullis (1973, personal communication) has developed another method of obtaining compositions of coherent cryptoperthite lamellae by correcting the X-ray lattice parameters for the elastic strain. Her elastic analysis is more exact than the one given here as it does not assume that elastic moduli and compositional strain coefficients are independent of composition. The method J. Tullis suggests is therefore, in principle, more accurate than the one presented in Appendix C; although more complicated, it should become valuable when our knowledge of the elastic constants of alkali feldspars improves sufficiently to warrant the added accuracy.

"the character of the sodium phase is usually much more poorly known" (Wright and Stewart, 1968, p.72). Also, the average composition X^o of a cryptoperthitic feldspar is usually closer to that of the albite phase than to that of the K-feldspar; the elastic distortion of the albite should thus be less important and more likely to escape attention.

Because cryptoperthite lamellae are too thin to be resolved by standard microprobe techniques, direct chemical analysis will require a combination of micro-analysis and electron microscopy (e.g. Lorimer and Champness, 1973). In the meantime, methods which use lattice parameters and which take elastic strain into account are probably sufficient. In powders, however, the smallest grain size (say 10 μm) may not always be sufficiently larger than the thickness of the largest lamellae (up to 1 μm or more) to prevent some non-uniform stress-relaxation. One would thus expect a broadening of the diffraction peaks and a corresponding loss of accuracy. This danger is probably small for lamellar thicknesses of 0.2 μm or less.

Total strain

Equations 2 give the stress-free compositional strain η_{ij}; Equations 3, 4b and 5c,d give the elastic strain ε_{ij}. The two strains can be added to give the total strain e_{ij} of a lamella X with respect to an unstrained crystal of composition X^o. It is an invariant plane strain (see Appendix B). The total strain between coherent lamellae $X^{\underline{a}}$ and $X^{\underline{b}}$ is therefore given by

$$\left.\begin{aligned} e_{22} &= e_{33} = 0 \quad , \\ e_{11} &\underset{(0.0794)}{=} 0.0812\ (X^{\underline{a}} - X^{\underline{b}}) \quad , \\ e_{13} &\underset{(-\,0.0042)}{=} -\,0.0012\ (X^{\underline{a}} - X^{\underline{b}}) \quad . \end{aligned}\right\} \qquad (6)$$

Figure 8 is the Mohr circle (in the ac plane) for the total strain between the lamellae, constructed from (6). Point "3" corresponds to the

direction of the 3-axis, that is the direction of the contact planes. In general, other lattice directions do not have the same orientation in the two kinds of lamellae; the angular deviation of a direction [p0r] between the two latticesis given by the difference between its ordinate and the ordinate of point "3" in Figure 8. If this angular deviation is plotted versus the angle which [p0r] makes with the a axis, a sine curve is obtained, similar to the curve measured experimentally by Laves (1952). The amplitude of the sine curve is equal to the diameter of the Mohr circle of Figure 8 multiplied by $(X^a - X^b)$. In Laves' (1952) Figure 16 the amplitude is 0.068; we conclude that the composition difference in the crystal he studied was

$$X^a - X^b = 0.838 \ (0.857) \ .$$

Elastic strain energy

The Helmholtz elastic strain energy in a lamella X is the mechanical work necessary to bring the lamella from a state of hydrostatic pressure P to its nonhydrostatically stressed state at constant temperature. This elastic strain energy is given by

$$\Delta\check{F} = - P(\varepsilon_1 + \varepsilon_2 + \varepsilon_3) + (\sigma_2 \varepsilon_2 + \sigma_3 \varepsilon_3) \ , \qquad (7)$$

where $\check{F}$ is the Helmholtz energy per unit volume, ε_i are the elastic strains, and σ_2, σ_3 are the nonhydrostatic stress components which are added to the pressure P and are given by (5a,b). If we take $\bar{V} = 2.5$ cal $bar^{-1} mol^{-1}$ for the molar volume of alkali feldspars, and use (3) and (5a,b,c), the molar strain energy can be calculated:

$$\Delta\bar{F} = -P \ \Delta\bar{V}^{el} + k \ (X - X^o)^2 \ , \qquad (8)$$

where $k = 603.6 \ (704.6)$ cal mol^{-1} . $\Delta\bar{V}^{el}$ is the molar volume change due to elastic strain.

Effects of pressure and temperature

Pressure and temperature can affect our results by changing the compositional strain coefficients and by changing the elastic constants.

Strains brought about by a hydrostatic pressure of 5 kbar (for R and A's No. 61), are, in our coordinates

$$\varepsilon_2 = -0.00125 \quad \text{and} \quad \varepsilon_3 = -0.00137 \,. \tag{9}$$

Similarly, thermal expansions expected from a rise in temperature to 605°C (analbite, Stewart and von Limbach, 1967) are

$$\varepsilon_2 = +0.0033 \quad \text{and} \quad \varepsilon_3 = +0.0034 \,. \tag{10}$$

Only the variations of these quantities with composition contribute to hydrostatic compositional strain. We have already noted that elastic constants do not depend greatly on compositions; variations in the numerical values in (9) with composition will therefore be negligible compared to the corresponding compositional strain coefficients. There are no complete thermal expansion data for alkali feldspars other than pure albite. However, values of thermal expansion of a sanidine to 605°C are not likely to differ from the ones in (10) by more than 0.001 (corresponding to a 30% difference in thermal expansion coefficients); even then, corrections on $\partial\eta_{22}/\partial\mu$ and $\partial\eta_{33}/\partial\mu$ would only amount to 6 and 10 percent respectively.

The only complete study of the effect of both pressure and temperature on the elastic constants of a silicate is the one of Frisillo and Barsch (1972) on various crystals of bronzite. For a 5 kbar pressure increase, their data indicate a relative <u>increase</u> in value of the C_{ij} between 2.5 and 4% for $i=j\leq 3$, between 1.5 and 2% for $i=j\geq 4$ and 5 to 10% for $i\neq j$. For $i=j$ the stiffness coefficients <u>decrease</u> by 9 to 15% when temperature is increased

to 600°C.

Simmons (1964) measured compressional wave velocities under confining pressure in various minerals, among them a microcline, and noted a rapid increase in these velocities as confining pressure was raised from 0 to 2 kbar. Simmons attributed this increase to crack closure resulting from the pressure increase. Christensen's (1966) observation that this effect was much more pronounced for propagation directions normal to the major cleavages of a perthite and an albite reinforced Simmons' conclusion. Thus, stiffness constants measured at room pressure may be significantly lower than the intrinsic values for flawless crystals; however, the room pressure velocities measured by R and A are generally as high or higher than the 2 kbar values obtained by Christensen. The crystals used by R and A must therefore have been of higher quality than Christensen's and the correction for cracks may accordingly be much smaller.

For other minerals, only equivalent isotropic elastic properties are usually studied as a function of pressure and temperature. Temperature has the most pronounced effects and may decrease the bulk modulus (stiffness) by as much as 15% between room temperature and 600°C.

In conclusion, temperature will only affect compositional strain coefficients by 10% at most in an unknown sense. Temperature may decrease the stiffnesses by as much as 15%; on the other hand, intrinsic values of these stiffnesses may be higher than the ones used here (Tables 1 and 2) by an unknown amount and are increased further by pressure. Altogether, the net effect of pressure and temperature on our numerical results should not exceed 20%; this is less than the present uncertainty in the values of elastic constants of alkali feldspars.

COHERENT SOLVUS

Possible mechanisms during coherent exsolution

Diffusion of alkali ions through the framework structure and coherent boundary migration are mechanisms which are necessary for the development of a cryptoperthite. These mechanisms may not occur at significant rates at room temperature. When studying the coherent solvus, however, we are concerned with the equilibrium reached when the above mechanisms are possible.

It is essential to note that, of the mechanisms which are usually assumed possible in heterogeneous equilibrium studies, not all are possible during cryptoperthite formation. Anomalous parameters can only be maintained by nonhydrostatic stresses. It is clear that if all species could diffuse without constraints, the structure would behave like a fluid rather than like a solid and could support no stresses at equilibrium. In fact the thermodynamic description of a stressed solid requires making a distinction between solid components, unable to diffuse through the solid, and fluid components which describe the possible changes in composition (Gibbs, 1906, p. 215-218; see also Chapter 2).

During cryptoperthite exsolution, Na and K cations are able to diffuse through the feldspar framework. On the other hand, constraints on the other constituents of the silicate framework are such that no independent long-range diffusion of the corresponding chemical species permits the destruction of the framework itself; in fact site constraints are such that even Na and K do not migrate independently. There is therefore only one independent fluid component (assuming that no Ca is present).

The alkali feldspar formula can be chosen as solid component; that is, the number of moles of the solid component in any given volume of crystal is

equal to the sum of the number of moles (gram formula weight) of $KAlSi_3O_8$ and that of $NaAlSi_3O_8$. (That this component is solid is better understood with the remark that N lattice cells of the crystal contain 4 N moles of that component, independently of any possible strain of the lattice or of any variation in composition.) The variable composition can be described by the mole fraction X of $KAlSi_3O_8$[6].

The fundamental equation of state of the solid is then of the form (Gibbs, 1906, Eq. 468)

$$d\bar{E} = T\, d\bar{S} + \bar{V}\, \sigma_{ij}\, de_{ij} + \mu\, dX, \qquad (11a)$$

whereby

$$\mu = \left(\frac{\partial \bar{E}}{\partial X}\right)_{\bar{S},\, e_{ij}}. \qquad (11b)$$

$\bar{E}$, $\bar{S}$, and $\bar{V}$ are respectively molar energy, entropy and volume (the mole being of the solid component); e_{ij} is the total strain (which can be defined only because of the maintenance of the unbroken framework).

The constraint of coherency of the interfaces amounts to the further requirement that the framework be maintained even when a phase boundary migrates through it; the equilibrium condition of coherent interfaces is given in Chapter 2.

---

[6] In all rigor the fluid component implied by the choice of X as descriptive variable is KNa_{-1}, while the corresponding solid component is $NaAlSi_3O_8$. Indeed, when expressed in terms of these two components the $NaAlSi_3O_8$ content of an alkali feldspar is, paradoxically, constant and independent of the 'actual' composition of the feldspar:

$$K_XNa_{1-X}AlSi_3O_8 = (KNa_{-1})_X\, (NaAlSi_3O_8)_1.$$

In this section, the strain energy (Equation 8) and Thompson and Waldbaum's (1969) 'hydrostatic' equation of state are combined into the equation of thermodynamic equilibrium of coherent interfaces. The coherent solvus can then be determined exactly.

Equilibrium conditions

At equilibrium we must have (Gibbs, 1906, p.215)

$$\mu^{\underline{a}} = \mu^{\underline{b}} = \text{constant throughout the system.} \qquad (12)$$

The condition of equilibrium of the interfaces (Chapter 2, Eq. 18 and follg.) reduces to

$$(\bar{F}^{\underline{a}} + P\bar{V}^{\underline{a}}) - (\bar{F}^{\underline{b}} + P\bar{V}^{\underline{b}}) = \mu(X^{\underline{a}} - X^{\underline{b}}) \quad . \qquad (13)$$

Although Equation 13 may look familiar, it should be pointed out that -P is only one component of the stress tensor, the one acting normal to the boundaries, and that there is only one chemical potential. If $\bar{G}$ is the molar Gibbs energy of the feldspar of same composition X, at the same temperature, and under the hydrostatic pressure P alone, we have

$$\bar{F} + P\bar{V} = \bar{G} + \Delta\bar{F} + P\,\Delta\bar{V}^{el} \quad . \qquad (14)$$

We may define the function $\bar{\phi} = \bar{F} + P\bar{V}$. From Equations 8 and 14,

$$\bar{\phi} = \bar{G} + k(X - X^{o})^{2}. \qquad (15)$$

The energy function $\bar{\phi}$ can be represented on an energy-composition diagram (Figure 9). Although the applicability of $\bar{\phi}$ to coherent equilibrium had to be established quite differently, $\bar{\phi}$ is quite similar to the function defined by Cahn (1962). In fact the expression of $\bar{\phi}$ reduces to that given by Cahn when the same assumptions of isotropic elasticity and isotropic

compositional strain are made; only then, however, does the strain energy become independent of the shape of the precipitate (Crum, cited by Nabarro, 1940). The function $\bar{\phi}$ will therefore be designated here as the Cahn energy.

It is shown in Appendix D that under the present constraint of coherency

$$\left(\frac{\partial \bar{\phi}}{\partial X}\right)_{T,P} = \left(\frac{\partial \bar{E}}{\partial X}\right)_{\bar{S},\, e_{ij}} = \mu \qquad (16)$$

Conditions of equilibrium 12 and 13 are therefore equivalent to a rule of common tangent in Figure 9. Figure 9 provides in fact an intuitive explanation of the phenomenon of coherent exsolution; the strain energy term, $k(X-X^o)^2$, can be regarded as the thermodynamic cost of coherency when a lamella exsolves within a crystal of average composition X^o. The Cahn energy $\bar{\phi}$ is specific to one bulk composition X^o; as Cahn (1962) pointed out, however, the co-existing compositions are independent of X^o ($\bar{\phi} = \bar{G} + kX^2 - 2kX^oX + kX^{o2}$; the last two terms do not affect the abscissae of the points of tangency). We also see that because the parabola $k(X-X^o)^2$ is concave upward, compositions of coexisting coherent lamellae are always in the range between the compositions of co-existing feldspars in hydrostatic equilibrium under the pressure P and at the same temperature; in other words, the coherent solvus is always inside the hydrostatic solvus.

Determination of the coherent solvus

Thompson and Waldbaum (1969) and Luth et al. (1972) find that alkali feldspar solid solutions are adequately described by a Margules expansion of $\bar{G}$ of the form

$$\bar{G} = X_1 \mu_1^o + X_2 \mu_2^o + RT(X_1 \ln X_1 + X_2 \ln X_2) + (W_1X_2 + W_2X_1)X_1X_2 \qquad (17)$$

where $X_2 = X$, $X_1 = 1-X$, and W_1 and W_2 are linear functions of P and T. Thompson (1967) expresses analytically the rule of common tangent for such an equation of state. When the same algebraic treatment is performed on $\bar{\phi}$ (Appendix E), we find that the system of two equations yielding the coexisting compositions at a given P and T is formally identical to Thompson's (1967) Equations 81, with the difference that W_1 and W_2 must be replaced by $(W_1 - k)$ and $W_2 - k)$.

Thompson and Waldbaum's (1969) expressions of W_1 and W_2 (in cal mol $^{-1}$) become, for an arbitrarily chosen pressure of 1 kbar,

$$W_1 = 6420 - 4.632\ T,$$

$$W_2 = 7784 - 3.857\ T.$$

To obtain the coherent solvus at 1 kbar we must use

$$W_1 - k = \underset{(5715)}{5816} - 4.632\ T,$$

$$W_2 - k = \underset{(7079)}{7180} - 3.857\ T.$$

The corresponding binodal curves are shown in Figure 10. For the hydrostatic solvus, at a pressure of 1 kbar, the critical conditions are

$$X_c = 0.3334 \quad ,$$

$$T_c = 934.64\ K = 661.5^{\circ}C \quad .$$

For the coherent solvus under the same P, on the other hand,

$$X_c = \underset{(0.3264)}{0.3274} \quad ,$$

$$T_c = \underset{(850.14\ K = 577.0^{\circ}C)}{862.23\ K = 589.1^{\circ}C} \quad .$$

Depending on the choice of elastic constants for alkali feldspars we therefore predict a critical temperature for the coherent solvus which is

72°C to 85°C below the critical temperature for the hydrostatic solvus.

Comparison with experimental observations

Tuttle and Bowen (1958, Table 2 and Figs. 7 and 9) (T and B) report a series of experiments in which they maintained several sanidine-high albite cryptoperthites ($0.42<X^{o}<0.55$) at successively higher temperatures for long periods of time, and determined the compositions of the coexisting lamellae from their ($\bar{2}01$) spacings. In all cases the crystals had become homogeneous at 610°C. Although T and B had no runs between 550°C and 610°C, they estimated a critical temperature of 570°C. T and B's cryptoperthite solvus broadens very rapidly with lowering temperature and is therefore not entirely contained within the hydrostatic solvus, whereas a coherent solvus should be. However, Smith and MacKenzie (1958) (S and M) questioned T and B's use of the ($\bar{2}01$) method for composition determinations of cryptoperthites. S and M carried out similar experiments and used α^* and γ^* to determine the composition of the sodium-rich phase in their samples and in those of T and B. The solvus they consequently drew (S and M, Figs. 3 and 4) has the same critical temperature, T_c = 570°C, but is much narrower than that of T and B; it is entirely contained within any of the various room pressure hydrostatic solvi given by Bowen and Tuttle (1950), Orville (1963), Luth and Tuttle (1966) and Müller (1971).

As shown earlier (Figure 7 and related discussion) composition determination by the ($\bar{2}01$) method does exaggerate the potassium-content of the K-rich phase and underrate the one of the Na-rich phase in cryptoperthites; it therefore leads to too broad a solvus. S and M's curve should therefore be preferred, although coherency stresses may also affect the parameters α^* and γ^* of the twinned albite.

The agreement between the critical temperature inferred from experimental data and the theoretical result presented above is surprisingly good. This agreement strongly suggests that the observed coherency of cryptoperthite lamellae is indeed a sufficient cause for their abnormal exsolution behavior.

DISCUSSION

Uniqueness of coherent solvus. Elastic constants and compositional strain coefficients have been assumed independent of composition, thus leading to a constant value of the coefficient k in (8). Because the compositional strain coefficients in particular are not quite constant, a more refined analysis would result in k being replaced by some linear function of X and X^o. By performing the calculations of Appendix E on the function $\bar{\phi}$ so obtained, it is easy to see that the coherent solvus would no longer be independent of the average composition X^o. The importance of this effect has not been explored.

Coherent spinodal. The coherent solvus gives the compositions of coexisting lamellae X^a and X^b in equilibrium within the constraint of coherency; the two types of lamellae are in particular fully equilibrated with respect to alkali-ion exchange. Let us now consider a homogeneous crystal of composition X^o whose temperature has been lowered so as to bring it within the coherent solvus. If, furthermore, X^o is within the coherent spinodal at that temperature, any arbitrarily small composition fluctuations within the crystal are energetically profitable and thus occur spontaneously. The coherent spinodal, therefore, refers to the bounds to the average composition X^o of an unstable phase within which the mechanism of coherent spinodal decomposition is possible; it should not be confused with the coherent solvus.

Because the lattice framework remains unbroken the energy associated with a coherent composition fluctuation also includes a strain energy term. To the extent that fluctuations can be considered to be along the 1-direction alone (that is, they preserve the symmetry of Appendix A) the relevant energy function is still the Cahn energy $\bar{\phi}$ given by Equation 15. The coherent spinodal can thus be calculated from the condition $(\partial^2\bar{\phi}/\partial X^2)_{P,T} = 0$, or $(\partial^2\bar{G}/\partial X^2)_{P,T} = -2k$, and is shown in Figure 10.

'End regions'. The coherent two-phase equilibrium, like the stress analysis on which it is based, assumes infinite parallel lamellae. Figures 3 and 4, however, show that the lamellae thin out and end, or, conversely, fork. In the 'end-regions' stress and strain components and the strain energy are not uniform. The strain energy in particular is higher than in the idealized lamellar structure. Boundary migration and diffusion will thus continue in such regions and lead to a closer and closer approximation of that idealized structure. This expansion or regression of lamellae along their edges must be an important mechanism leading to their overall thickening.

Loss of coherency. Although the coherent solvus is a stable solvus within the constraint of coherency, the loss of coherency (when possible) leads to a lowering of the total free energy. For example, at 500°C, 1 kbar and $X^o = 0.40$ (Figure 9), loss of coherency lowers the average free energy by 63 cal mol^{-1} (segment CH, Figure 9). To the extent that loss of coherency is considered possible our coherent equilibrium is therefore only a metastable equilibrium. It may happen on the other hand that unconstrained feldspars do not nucleate; in such case the strained cryptoperthite would set higher activities for the feldspar components and could thus cause metastable growth of other phases. We note that the activities of Or and Ab at a given temperature depend on the average

composition X^o of the cryptoperthite (See Figure 9).

Evolution of cryptoperthites

We can now sketch the cooling history of a high-temperature alkali feldspar as follows:

(i) composition fluctuations and spinodal decomposition;

(ii) formation of discrete lamellae having sharp boundaries;

(iii) thickening of these lamellae, together with gradual readjustment of their compositions as temperature drops;

(iv) monoclinic-triclinic transition of the albite phase and consequent twinning;

(v) monoclinic-triclinic transition of the potassium feldspar and consequent twinning.

Except for the displacive transition in Na-rich phases the monoclinic transition in alkali feldspars is accompanied by Al-Si ordering and by large changes in dimensions of the lattice cell. The temperatures of these transitions are therefore likely to be strongly affected by the constraint of coherency and may be quite different from corresponding temperatures in single phase crystals.

The above sequence of events can be quenched at any stage by rapid cooling (except again for the displacive transition in Na-rich phases). On the contrary, long term annealing at a sufficiently high temperature will allow a loss of coherency. Cryptoperthites are thus not found in large batholiths but are instead restricted to extrusive rocks or small intrusive bodies, in which cooling must have been slow enough to permit alkali-ion diffusion, but fast enough to prevent nucleation and growth of unstrained phases. There are intermediate situations where a cryptoperthitic feldspar coexists with

unstrained phases, the latter growing at the expense of the former. Several examples of coexisting macroperthites and cryptoperthites described in the literature [e.g. Moorhouse (1959): Plate 3-D and Fig. 159-B; Tschermak (1864), Brogger (1890), both reproduced by Barth (1969, Figs. 1-15 and 1-16)] can be interpreted in this manner.

OTHER MINERALS

The analysis presented here can be extended to other mineral systems in which coherent exsolution may occur.

Plagioclase feldspars. The peristerite solvus of sodium-rich plagioclases is a likely candidate. Indeed peristerites have many features in common with cryptoperthites. The Schiller effect which they exhibit was first interpreted by Laves (1951) as due to the coexistence of two plagioclase phases. Typical end-member compositions are An_2 and An_{22} (Wt.% of the $CaAl_2Si_2O_8$ component) with rather large variations (e.g. Ribbe, 1960). Fleet and Ribbe (1965) observed almost perfect peristerite lamellae in TEM. Although Fleet and Ribbe interpreted the electron diffraction patterns as the superposition of normal reciprocal lattices for the two end-member compositions (their Fig. 4); the actual patterns (their Fig. 2) are better interpreted as two anomalous reciprocal lattices which satisfy the relationship of Figure B1. Indeed anomalous lattice parameters have been recorded in peristerites, and Viswanathan and Eberhard (1968) assigned the anomalies to 'distortion'. Korekawa et al. (1970) studied an oligoclase ($An_{16.5}$) by X-ray and TEM, and interpreted the lattice parameter fluctuations observed as composition fluctuations; in the present terminology the latter would be called coherent (compare in particular their Figure 5 with the present Figure B1). Korekawa et al. may thus have

observed an early coherent spinodal decomposition stage of peristerite formation. Coexisting single-phase crystals of albite and oligoclase have been observed by Evans (1964) and Crawford (1966) and thus evidence the existence of a hydrostatic peristerite solvus. Iiyama (1966) observed the three-phase field sanidine-albite-oligoclase experimentally and determined that the crest of the peristerite solvus was between 700° and 800°C. The three distinct phases observed by X-rays in some single crystals (Viswanathan and Eberhard, 1968) may in fact be the coherent counterpart of the hydrostatic three-phase field.

Schiller effect and lamellar structures are also observed for more Ca-rich plagioclases and have been interpreted as exsolution lamellae; X-ray and TEM results are difficult to interpret however.

Clinopyroxenes. Robinson et al. (1971) noted that the assumption of continuity of lattices between host and lamellae in clinopyroxenes readily explained observed orientations of the lamellae in natural pyroxenes. TEM observations of lunar pyroxenes (Christie et al., 1971) are also fully compatible with coherency of the lamellae. Clinopyroxene exsolution may thus well be a coherent process in many cases, as suggested by Champness and Lorimer (1971). In Chapter 4 it is shown how the Mohr circle can be used to test the coherency of clinopyroxene lamellae.

Conclusion

Exsolution lamellae are observed in many other mineral systems; however, only a detailed study can determine in each case whether these lamellae are coherent or not.

Coherency, strain energy, and their thermodynamic implications, have wider applications than to coherent exsolution. If two or more phases coexist

within an unbroken lattice framework and are thus compelled to match along coherent interfaces, they in general acquire a strain energy which they would not have if coherency were not maintained. If, as in this paper, the phases can be considered to be in equilibrium with respect to well-defined mechanisms (migration of fluid components, cation ordering, displacive strain), the inclusion of strain energy in the thermodynamic analysis of such transformations is in principle straightforward. Such analysis is clearly required if these phase equilibria are to be used as reliable geothermometers or geobarometers.

APPENDIX A

Uniformity of stresses and strains within lamellae

Consider a set of lamellae which satisfy the following conditions:

1. The lattice framework behaves elastically, that is, it is not broken or disrupted by the stresses.
2. Boundaries between lamellae are coherent.
3. The boundaries are infinite, parallel planes.
4. Each lamella is characterized by a definite set of stress-free lattice parameters which is a function of its composition.
5. The thickness of the 'book' of lamellae is much larger than the thickness of an individual lamella and there is no systematic variation in the composition of the crystal (as averaged over many lamellae) when moving along a direction perpendicular to the lamellae.

We choose a cartesian coordinate system such that the 1-axis is perpendicular to the plane of the lamellae, the 2- and 3- axes being therefore parallel to the lamellae boundaries.

Because of Condition 3, the origin in the 2,3 plane is arbitrary, and thus

$$\sigma_{ij,2} = 0 \quad , \quad \sigma_{ij,3} = 0 \quad , \quad \text{for } i,j = 1,2,3,$$

where $\sigma_{ij,k} = \partial\sigma_{ij} / \partial x_k$.

The three equations of equilibrium reduce to

$$\sigma_{1i,1} = 0 \, . \qquad \text{for } i = 1,2,3.$$

Hence, σ_{11} , σ_{12} and σ_{13} are constant throughout the composite. If only a

hydrostatic pressure P is applied to the external boundaries, $\sigma_{11} = -P$ and $\sigma_{12} = \sigma_{13} = 0$.

Similarly, because of Conditions 1, 2 and 3, compatibility equations (e.g. Sokolnikoff, 1956, p. 28) reduce to

$$e_{22,11} = 0, \qquad e_{33,11} = 0, \qquad e_{23,11} = 0, \tag{A1}$$

where the strain, e_{ij}, can be of compositional as well as elastic origin and $e_{ij,kl}$ denotes $\partial^2 e_{ij}/\partial x_k \, \partial x_l$.

Within a lamella of constant composition (Condition 4) any strain variation must be of elastic origin. Equations A1 then become (in matrix notation)

$$\begin{bmatrix} s_{22} & s_{23} & s_{24} \\ s_{23} & s_{33} & s_{34} \\ s_{24} & s_{34} & s_{44} \end{bmatrix} \times \begin{bmatrix} \sigma_{2,11} \\ \sigma_{3,11} \\ \sigma_{4,11} \end{bmatrix} = \begin{bmatrix} 0 \\ 0 \\ 0 \end{bmatrix}. \tag{A2}$$

The assumption of linear infinitesimal elasticity is made in (A2); the result demonstrated here is more general however. A demonstration for finite strain and nonlinear elasticity would require care in defining instantaneous stress, strain and elastic constants.

All eigenvalues of a symmetric matrix of elastic coefficients such as in (A2), are positive; otherwise there would be combinations of non-zero stresses for which the strain energy would be zero or negative, which is impossible. The determinant of (A2) is therefore non-zero, and the only solution to (A2) is the trivial one:

$$\sigma_{2,11} = \sigma_{3,11} = \sigma_{4,11} = 0. \tag{A3}$$

Stress components σ_{22}, σ_{33} and σ_{23} can therefore only vary linearly with x_1 within a lamella. The sense along the 1-axis is arbitrary (Condition 5), and, therefore, by reason of symmetry, σ_{22}, σ_{33} and σ_{23} are constant within lamellae. They do not have the same value in lamellae of different compositions, however.

Part of the theorem demonstrated here is a special case of a more general theorem given by Eshelby (1957). Eshelby shows that if no stresses are applied at infinity, stresses and strains are uniform within coherent ellipsoidal inclusions. (Eshelby does not use the term coherent; in the present terminology, however, the problem he treats is the one of coherent inclusions.) In the general case, only one phase, the inclusion (or host), can be surrounded by an ellipsoid. Under the conditions of this appendix, where ellipsoids are reduced to the two parallel planes bounding a lamella, the distinction between host and matrix disappears: Eshelby's result consequently applies to all lamellae.

APPENDIX B

Reciprocal lattices of coherent lamellae

Consider a crystal made of lamellae of only two distinct compositions and satisfying conditions 1 to 5 of Appendix A. (In Appendix A the number of possible lamella compositions is not restricted to two). Each lamella is in a homogeneous state of strain and lattices in all lamellae of one kind are superposable by a parallel translation. The two lattices, corresponding to the two kinds of lamellae, are related to each other by a unique linear transformation which must leave the plane of the boundaries invariant, a direct consequence of the constraint of coherency. The linear transformation is thus an invariant plane strain (IPS) (e.g. Wayman, 1964). A

classic result of linear transformation theory is that linear transformations can be characterized in general by three distinct eigenvectors and associated eigenvalues. An eigenvector is a vector whose direction is unchanged in the transformation; its eigenvalue is the ratio of the length of the transformed vector to the original. In an IPS, any two non-colinear vectors in the invariant plane (IP) can be arbitrarily chosen as eigenvectors, and their corresponding eigenvalues are 1. Unless the transformation is an identity, the third eigenvector of an IPS is not arbitrary; in what follows, this third eigenvector is designated as the characteristic vector of the IPS.

Properties of an IPS can be restated as follows:

1. One lattice plane direction, (hkl), the direction of the lamellae boundaries, i.e. the IP, is identical in both kinds of lamellae; that is, (hkl) has the same orientation and the same repeat distances within it in both lattices. Its d-spacing is not the same, however.
2. One lattice direction, [pqr], direction of the characteristic vector, is also parallel to itself in the two lattices. Barring identity, repeat distance along [pqr] is not the same in the two lattiees. The ratio of these repeat distances is the eigenvalue associated to the characteristic vector and is also the ratio of the (hkl) spacings in the two lattices.

There is no reason, in general, for (hkl) and [pqr] to be rational.

Consider a lattice plane in real space, (mno), which contains the characteristic vector [pqr]. Neither the direction nor the spacing of (mno) are affected by the IPS, or, in other words, (mno), has the same direction and spacing in the two types of lamellae. Therefore, in reciprocal space, reciprocal points mno coincide for the two lattices. All such points define a plane P^* through 000 which is perpendicular to [pqr]. The two reciprocal

lattices are therefore related by an IPS, the IP of which is P^*.

Consider now, in real space, lattice planes (hkl) parallel to the IP. The (hkl) spacing is not the same in the two lamellae. In reciprocal space, the two corresponding hkl points lie on a line perpendicular to the (hkl) plane. The direction of this line is the direction of the characteristic vector of the IPS in reciprocal space.

The relationship between direct and reciprocal lattices for the two types of lamellae is shown in Figure B1.

APPENDIX C

Determination of composition of cryptoperthite lamellae from two (h0l) spacings.

Figure 7 is the Mohr circle for elastic strain, constructed from numerical values in Equations 3 and 5; we can measure from it that

$$\frac{1}{X-X^o}\frac{\delta d(\bar{2}04)}{d(\bar{2}04)} = -0.0095\ (-0.0087), \qquad \text{(C1a)}$$

$$\frac{1}{X-X^o}\frac{\delta d(\bar{2}01)}{d(\bar{2}01)} = +0.0137\ (+0.0146), \qquad \text{(C1b)}$$

where $d(h0l)$ is the $(h0l)$ spacing and $\delta d(h0l)$ is the change in spacing due to elastic strain.

Because variations in spacings, whether elastic or compositional, are small compared to the values of these spacings, Equations C1 can be combined into

$$0.0137\frac{\delta d(\bar{2}04)}{d^o(\bar{2}04)} + 0.0095\frac{\delta d(\bar{2}01)}{d^o(\bar{2}01)} = 0, \qquad \text{(C2)}$$

where $d^o(h0l)$ is some average value of the $(h0l)$ spacing for high temperature alkali feldspars. Taking $d^o(\bar{2}04)/d^o(\bar{2}01) = 0.435$, (C2) becomes

$$\delta d(\bar{2}04) + \underset{(0.26)}{0.30}\ \delta d(\bar{2}01) = 0 . \qquad \text{(C3)}$$

The combination of lattice parameters $d(\bar{2}04) + 0.30\ d(\bar{2}01)$ is therefore not affected by the elastic strain; its value (Figure C1) is function only of the composition of the lamella and can be used to determine that composition when the two spacings are known.

APPENDIX D

Expression for the chemical potential

By definition $\bar{\phi} = \bar{E} - T\bar{S} + P\bar{V}$,

and therefore, from (11a),

$$d\bar{\phi} = \bar{S}dT + \bar{V}\,\sigma_{ij}\,de_{ij} + P\,d\bar{V} + \bar{V}dP + \mu dX.$$

The constraint on any lamella which exsolves or changes composition is that it keeps matching the average crystal in the 2- and 3- directions. In any change of composition of the coherent lamella at constant P and T we therefore have

$$de_{22} = de_{33} = de_{23} = 0,$$

Because there are no shear stresses parallel to the boundaries, we thus have

$$\bar{V}\,\sigma_{ij}\,de_{ij} = \bar{V}\,\sigma_{11}\,de_{11} = -\,P\,d\bar{V} .$$

A variation of $\bar{\phi}$ at constant P and T is therefore given by

$$d\,\bar{\phi}\Big|_{P,T} = \mu dX,$$

hence (16).

APPENDIX E

Coexisting compositions on a coherent solvus

Equations giving the coherent solvus are obtained from $\bar{\phi}$ exactly as the hydrostatic solvus is obtained from $\bar{G}$ (Thompson, 1967). Coexisting compositions must satisfy the system

$$\left[\bar{\phi} - X_2\left(\frac{\partial\bar{\phi}}{\partial X_2}\right)_{P,T}\right]^{\underline{a}} = \left[\bar{\phi} - X_2\left(\frac{\partial\bar{\phi}}{\partial X_2}\right)_{P,T}\right]^{\underline{b}}, \quad (E1a)$$

$$\left[\bar{\phi} + X_1\left(\frac{\partial\bar{\phi}}{\partial X_2}\right)_{P,T}\right]^{\underline{a}} = \left[\bar{\phi} + X_1\left(\frac{\partial\phi}{\partial X_2}\right)_{P,T}\right]^{\underline{b}}. \quad (E1b)$$

Taking $\bar{\phi}$ as given in (15), with $\bar{G}$ as in (17), (E1) becomes

$$RT \ln X_1^{\underline{a}} + X_2^{\underline{a}2}(W_1 - k) + 2 X_1^{\underline{a}} X_2^{\underline{a}2}(W_2 - W_1)$$
$$= RT \ln X_1^{\underline{b}} + X_2^{\underline{b}2}(W_1 - k) + 2 X_1^{\underline{b}} X_2^{\underline{b}2}(W_2 - W_1), \quad (E2a)$$

$$RT \ln X_2^{\underline{a}} + X_1^{\underline{a}2}(W_2 - k) + 2 X_2^{\underline{a}} X_1^{\underline{a}2}(W_1 - W_2)$$
$$= RT \ln X_2^{\underline{b}} + X_1^{\underline{b}2}(W_2 - k) + 2 X_2^{\underline{b}} X_1^{\underline{b}2}(W_1 - W_2). \quad (E2b)$$

The system E2 is formally identical to the system of equations giving the hydrostatic solvus (Thompson, 1967, Eqs.81).

References

ABERDAM, D., and R. KERN (1962) Observations au microscope électronique de quelques feldspaths perthitiques. C.R. Acad. Sci. 255, 734-736.

_____, _____, P. LEYMARIE, AND M. PIERROT (1964) Etude cristallographique détaillée d'une orthose cryptoperthitique. C.R. Acad. Sci. 258, 1268-1271.

ARDELL, A. J. (1968) An application of the theory of particle coarsening: the γ' precipitate in Ni-Al alloys. Acta Metall. 16, 511-516.

_____ (1970) The growth of gamma prime precipitates in aged Ni-Ti alloys. Metall. Trans. 1, 525-534.

_____ , AND R. B. NICHOLSON (1966) The coarsening of γ' in Ni-Al alloys. J. Phys. Chem. Solids 27, 1793-1804.

BARTH, T. F. W. (1969) Feldspars. Wiley-Interscience, London.

BOLLMANN, N. W., AND H.-U. NISSEN (1968) A study of optimal phase boundaries: the case of exsolved alkali feldspars. Acta Crystallogr. A 24, 546-557.

BOWEN, N. L., AND O.F. TUTTLE (1950) The system $NaAlSi_3O_8$ - $KAlSi_3O_8$ - H_2O , J. Geol. 58, 489-511.

BROWN, W. L., C. WILLAIME AND C. GUILLEMIN (1972) Exsolution selon l'association diagonale dans une cryptoperthite: étude par microscopie électronique et diffraction des rayons X. Bull. Soc. franç. Minéral. Cristallogr. 95, 429-436.

CAHN, J. W. (1962) Coherent fluctuations and nucleation in isotropic solids. Acta Metall. 10, 907-913.

CHAMPNESS, P. E., AND G. W. LORIMER (1971) An electron microscopic study of a lunar pyroxene. Contr. mineral. petrol. 33, 171-183.

CHRISTENSEN, N. I. (1966) Compressional wave velocities in single crystals of alkali feldspar at pressures to 10 kilobars. J. Geophys. Res. 71(12), 3113-3116.

CHRISTIE, O. H. J. (1968) Spinodal precipitation in silicates. I. Introductory application to exsolution in feldspar. Lithos 1, 187-192.

CHRISTIE, J. M., J. S. LALLY, A. H. HEUER, R. M. FISHER, D. T. GRIGGS, AND S. V. RADCLIFFE (1971) Comparative electron petrography of Apollo 11, Apollo 12, and terrestrial rocks. Proc. Second Lunar Science Conf. 1, 69-89. M.I.T. Press, Cambridge, Massachusetts.

COOMBS, D. S. (1954) Ferriferous orthoclase from Madagascar. Mineral. Mag. 30, 409-427.

CRAWFORD, M. L. (1966) Composition of plagioclase and associated minerals in some schists from Vermont, U. S. A., and South Westland, New Zealand, with inferences about the peristerite solvus, Contr. Mineral. Petrol. 13, 269-294.

DELBOVE, F. (1971) Equilibre d'échanges d'ions entre feldspaths alcalins et halogènures sodi-potassiques fondus. Application au calcul des propriétés thermodynamiques de la série des feldspaths alcalins. Bull. Soc. franç. Minéral. Cristallogr. 94, 456-466.

DONNAY, G., AND J. D. H. DONNAY (1952) The symmetry change in the high-temperature alkali-feldspar series. Amer. J. Sci., Bowen vol., 115-132.

ESHELBY, J. D. (1957) The determination of the elastic field of an ellipsoidal inclusion, and related problems. Proc. Roy. Soc. London A241, 376-396.

EVANS, B. W. (1964) Coexisting albite and oligoclase in some schists from New Zealand. Amer. Mineral. 49, 173-179.

FLEET, S. G., AND P. H. RIBBE (1963) An electron-microscope investigation of a moonstone. Philos. Mag. 8 (91), 1179-1187.

_____, AND _____(1965) An electron-microscope study of peristerite plagioclases. Mineral. Mag. 35, 165-176.

FRISILLO, A. L., AND G. R. BARSCH (1972) Measurement of single-crystal elastic constants of bronzite as a function of pressure and temperature. J. Geophys. Res. 77 (32), 6360-6384.

GIBBS, J. W. (1906) The Scientific Papers of J. Willard Gibbs, Vol. I. Thermodynamics, Longmans, Green, and Company.

HEUER, A. H., R. F. FIRESTONE, J. D. SNOW, H. W. GREEN, R. G. HOWE, AND J. M. CHRISTIE (1971) An improved ion thinning apparatus. Rev. Scientific Instruments 42(8), 1177-1184.

HIRSCH, P. B., A. HOWIE, R. B. NICHOLSON, D. W. PASHLEY, AND M. J. WHEELAN (1965) Electron microscopy of thin crystals. Plenum Press, New York, N.Y.

IIYAMA, J. T. (1966) Contribution à l'étude des équilibres sub-solidus au système ternaire orthose-albite-anorthite à l'aide des réactions d'échange d'ions Na-K au contact d'une solution hydrothermale. Bull. Soc. franç. Minéral. Cristallogr. 89, 442-454.

KELLY, A., AND R. B. NICHOLSON (1963) Precipitation hardening. In B. Chalmers (ed.) Progress in Materials Science, Vol. 10. The Macmillan Company, New York, N. Y.

KOREKAWA, M., H.-U. NISSEN, AND D. PHILLIP (1970) X-ray and electron-microscopic studies of a sodium-rich low plagioclase. Z. Kristallogr. 131, 418-436.

LAVES, F. (1951) Relationships between exsolved plagioclase and its host (abstr.). Am. Crys. Ass. Meeting, Washington, D.C.

_____ (1952) Phase relations of the alkali feldspars, II. J. Geol. 60, 549-574.

LORIMER, G. W., AND P. E. CHAMPNESS (1973) Combined electron microscopy and analysis of an orthopyroxene. Amer. Mineral. 58, 243-248.

LUTH, W. C., AND O. F. TUTTLE (1966) The alkali feldspar solvus in the system Na_2O - K_2O - Al_2O_3 - SiO_2 - H_2O. Amer. Mineral. 51, 1359-1373.

_____, P. M. FENN, AND R. F. MARTIN (1970) Thermodynamic excess functions, relative activities, and solvus relations for synthetic alkali feldspars (abstr.). G. S. A. 83rd annual meeting, Milwaukee.

_____, R. F. MARTIN, AND P. M. FENN (1972) The peralkaline alkali feldspar solvus (abstr.) Feldspar conference progr., Manchester.

MACKENZIE, W. S., AND J. V. SMITH (1956) The alkali feldspars: III. An optical and X-ray study of high-temperature feldspars. Amer. Mineral. 41, 405-427.

MOORHOUSE, W. W. (1959) The study of rocks in thin section. Harper and Row, New York, N. Y.

MUIR, I. D., AND J. V. SMITH (1956) Crystallization of feldspars in larvikites. Z. Kristallogr. 107, 182-195.

MÜLLER, G. (1971) Der Einfluss der Al,Si-Verteilung auf die Mischungslücke des Alkalifeldspäte. Contr. Mineral. Petrol. 34, 73-79.

NABARRO, F. R. N. (1940) The strains produced by precipitation in alloys. Proc. Roy. Soc. London A175, 519-538.

NYE, J. F. (1957) Physical properties of crystals. Oxford University Press, London.

OFTEDAHL, C. (1948) Studies on the igneous rock complex of the Oslo region. XI. The feldspars. Skr. Norske Vidensk.-Akad. Oslo I Mat.-Naturvidensk 3, 1-77.

ORVILLE, P. M. (1963) Alkali ion exchange between vapor and feldspar phases. Am. J. Sci. 261, 201-237.

_____ (1967) Unit-cell parameters of the microcline-low albite and the sanidine-high albite solid solution series. Amer. Mineral. 52, 55-86.

RIBBE, P. H. (1960) X-ray and optical investigation of peristerite plagioclases. Amer. Mineral. 45, 626-644.

ROBIN, P.-Y. F. (1974) Thermodynamic equilibrium across a coherent interface in a stressed crystal. Amer. Mineral. (in press).

ROBINSON, P., H. W. JAFFE, M. ROSS, AND C. KLEIN, JR. (1971) Orientation of exsolution lamellae in clinopyroxenes and clinoamphiboles: considerations of optimal phase boundaries. Amer. Mineral. 56, 909-939.

RYZHOVA, T. V. (1964) The elastic properties of plagioclase. Bull. (Izv.) Acad. Sci. USSR, Geophys. series, 1049-1051. [Amer. Geophys. Union transl., 633-635.]

_____, AND K. S. ALEKSANDROV (1965) The elastic properties of potassium-sodium feldspars. Bull. (Izv.) Acad. Sci. USSR, Geophys. series, 98-102. [Amer. Geophys. Union transl., 53-56.]

SIMMONS, G. (1964) Velocity of compressional waves in various minerals at pressures to 10 kilobars. J. Geophys. Res. 69(6),1117-1121.

SMITH, J. V. (1961) Explanation of strain and orientation effects in perthites. Amer. Mineral. 46, 1489-1493.

_____, AND W. S. MACKENZIE (1958) The alkali feldspars: IV. The cooling history of high-temperature sodium-rich feldspars. Amer. Mineral. 43, 872-889.

_____, AND I. D. MUIR (1958) The reaction sequence in larvikite feldspars. Z. Kristallogr. 110, 11-20.

SOKOLNIKOFF, I. S. (1956) Mathematical Theory of Elasticity, 2nd ed.. McGraw-Hill Book Co., Inc., New York, N. Y., 476p.

STEWART, D. B., AND DORA VON LIMBACH (1967) Thermal expansion of low and high albite, Amer. Mineral. 52, 389-413.

THOMPSON, J. B., JR. (1967) Thermodynamic properties of simple solutions. In P. H. Abelson, ed. Researches in Geochemistry II, John Wiley and Sons, New York, N.Y., 340-361.

_____, AND D. R. WALDBAUM (1968) Mixing properties of sanidine crystalline solutions: I. Calculations based on ion-exchange data. Amer. Mineral. 53, 1965-1999.

_____, AND _____ (1969) Mixing properties of sanidine crystalline solutions: III. Calculations based on two-phase data. Amer. Mineral. 54, 811-838.

TUTTLE, O.F. (1952) Origin of the contrasting mineralogy of extrusive and plutonic rocks. Amer. J. Sci. 60(2), 107-124.

_____, AND N. L. BOWEN (1958) Origin of granite in the light of experimental studies in the system $NaAlSi_3O_8$ - $KAlSi_3O_8$ - SiO_2 - H_2O. Geol. Soc. Amer. Mem. 74, 153 pp.

VISWANATHAN, K., AND E. EBERHARD (1968) The peristerite problem. Schw. Miner. Petrogr. Mitt. 48, 803-814.

VOIGT, W. (1928) Lehrbuch der Kristallphysik, Teubner, Leipzig and Berlin.

WALDBAUM, D. R., AND J. B. THOMPSON, JR. (1968) Mixing properties of sanidine crystalline solution: II. Calculations based on volume data. Amer. Mineral. 53, 2000-2017.

_____, AND _____(1969) Mixing properties of sanidine crystalline solutions: IV. Phase diagrams from equations of state. Amer. Mineral. 54, 1274-1298.

WAYMAN, C. M. (1964) Introduction to the crystallography of martensitic transformations. MacMillan Company, New York, N.Y.

WILLAIME, C. (1973) Interprétation par des calculs d'énergie élastique des textures observées par microscopie électronique dans les cryptoperthites. Thèse de doctorat d'état ès sciences. Université de Paris VI, Paris, France.

_____, AND W. L. BROWN (1972) Explication de l'orientation des interfaces dans les exsolutions des feldspaths, par un calcul d'énergie élastique. C. R. Acad. Sci. (Paris) 275, 627-629.

_____, AND M. GANDAIS (1972) Study of exsolution in alkali feldspars. Calculation of elastic stresses inducing periodic twins. Phys. stat. sol. a9, 529-539.

_____, W. L. BROWN, AND M. GANDAIS (1973) An electron-microscopic and X-ray study of complex exsolution textures in a cryptoperthitic alkali feldspar. J. Mat. Sci. 8, 461-466.

WRIGHT, T. L., AND D. B. STEWART (1968) X-ray and optical study of alkali feldspar, I. Determination of composition and structural state from refined unit-cell parameters and 2V. Amer. Mineral. 53, 38-87.

YUND, R. A., AND R. H. MCCALLISTER (1970) Kinetics and mechanisms of exsolution, Chem. Geol. 6, 5-30.

TABLE 1. SELECTED STIFFNESS CONSTANTS OF ALKALI FELDSPARS[1]

c_{ij}	11	22	33	44	55	66
	12	13	23	15	25	35	46
No. 61[2]	0.596	1.581	1.049	0.139	0.203	0.370
	0.362	0.360	0.285	-0.118	-0.057	-0.129	-0.026
C[3]	0.750	1.720	1.280	0.170	0.300	0.370
	0.430	0.490	0.360	-0.170	-0.140	-0.190	-0.030
No. 61[4]	0.493	1.581	1.145	0.173	0.207	0.336
	0.324	0.364	0.326	-0.050	-0.069	-0.028	-0.086
C[4]	0.615	1.720	1.457	0.204	0.279	0.336
	0.346	0.469	0.444	-0.054	-0.136	-0.096	-0.081

[1] *Elastic constants measured by acoustic methods are adiabatic constants; the correction from adiabatic to isothermal is not large enough to be significant. Units are Mbar.*

[2] *Ryzhova and Aleksandrov (1965), Table 3. Conventional coordinates.*

[3] *Composite set of elastic constants from Ryzhova and Aleksandrov (1965), Table 3, and from Ryzhova (1964). Conventional coordinates.*

[4] *Elastic constants recalculated in new coordinate system, illustrated in Figure 6.*

CAPTIONS

FIG. 1. 'Large' region of larvikite alkali feldspar consisting solely of albite, regularly twinned according to the pericline law. Three isolated lattice dislocations are visible. The view is along the b axis. 100 kV Japan Electron Microscope.

FIG. 2. Irregular exsolution lamellae of K-feldspar, showing as dark areas. The periodicity of pericline twinning (alternating shades of gray) is variable. The view is along the b axis. 100 kV JEM.

FIG. 3. (a) Direct image of lamellar structure. Lamellae make an angle of 107^{o} with the basal cleavage. (b) Electron diffraction pattern. 100 kV JEM.

FIG. 4. Thin exsolution lamellae viewed under high magnification. Moiré fringes mark the lamellae boundaries, which are here viewed at an angle. The undulations visible in every other lamella are probably due to twinning of the sodium-rich phase. Siemens 101 Electron Microscope.

FIG. 5. Mohr circle for the stress-free compositional strain in the ac plane. Abscissas of a and c and the difference between their ordinates are given by Equations 1. The angle between the a and c axes is then sufficient to construct the Mohr circle. m: direction of the minimum principal axis of compositional strain; M: maximum principal axis.

FIG. 6. Coordinate systems. a, b, c: conventional crystallographic axes for a monoclinic feldspar (b = diad axis). X, Y, Z: conventional cartesian coordinate axes. 1, 2, 3: present choice of cartesian coordinate axes.

FIG. 7. Mohr circle for elastic strain in the ac plane. The relative change of d(h0l) spacing is equal to the longitudinal strain ε_{xx} in a direction normal to (h0l), noted here n(h0l). (Elastic constants of Ryzhova and

and Aleksandrov's crystal No. 61).

FIG. 8. Mohr circle for total strain between lamellae in the ac plane. The segment a.d. is equal to the angular deviation of a lattice direction [p0r] between the two lattices in cryptoperthites. (Elastic constants of Ryzhova and Aleksandrov's crystal No. 61).

FIG. 9. Energy-composition curves. The dashed curve is a plot of $\overline{G} - X_1 \mu_1^o - X_2 \mu_2^o$ using the equation of state of Thompson and Waldbaum (1969). The solid curve is a plot of $\overline{\phi} - X_1 \mu_1^o - X_2 \mu_2^o$, for k = 603.6 cal mol^{-1} (No. 61). Note that the slope of the common tangent to the $\overline{\phi}$ curve is a function of X^o.

FIG. 10. Temperature-composition diagram. The dashed curve is the hydrostatic solvus at 1 kbar. The solid curves are the coherent solvi corresponding to the elastic constants of Ryzhova and Aleksandrov's crystal No. 61 (k = 603.6 cal mol^{-1}) and of C (k = 704.6 cal mol^{-1}). The dotted curve is the spinodal for k = 603.6 cal mol^{-1}.

FIG. B1. Two-dimensional representation of the invariant plane strain (IPS) relating the two lattices across a coherent interface.
(a) Direct space. The plane of the interface is invariant in the linear transformation which relates one lattice to the other. The direction of the characteristic vector is that of the one lattice direction which has the same orientation in the two lattices.
(b) Reciprocal space. o: reciprocal lattice point of phase a. •: reciprocal lattice point of phase b. The line segments joining two reciprocal points of same index in a and b are all parallel to each other and perpendicular to the invariant plane in real space.

If the lines drawn in direct space are taken to represent directions of the vectors defining the primitive lattice cell, note that the invariant plane and

the characteristic vector both have simple rational indices; this is not necessarily so in a real situation.

FIG. C1. Determinative parameter for anomalous cryptoperthites. This linear combination of two lattice spacings is not affected by the elastic strain due to coherency. When the two spacings are known their linear combination can be calculated and the corresponding composition read from the curve. The coefficient in the linear combination depends to some extent on which elastic constants are held to be true; the elastic constants chosen here are those of Ryzhova and Aleksandrov's crystal No. 61. Lattice spacing data are from Orville (1967, Table 3C).

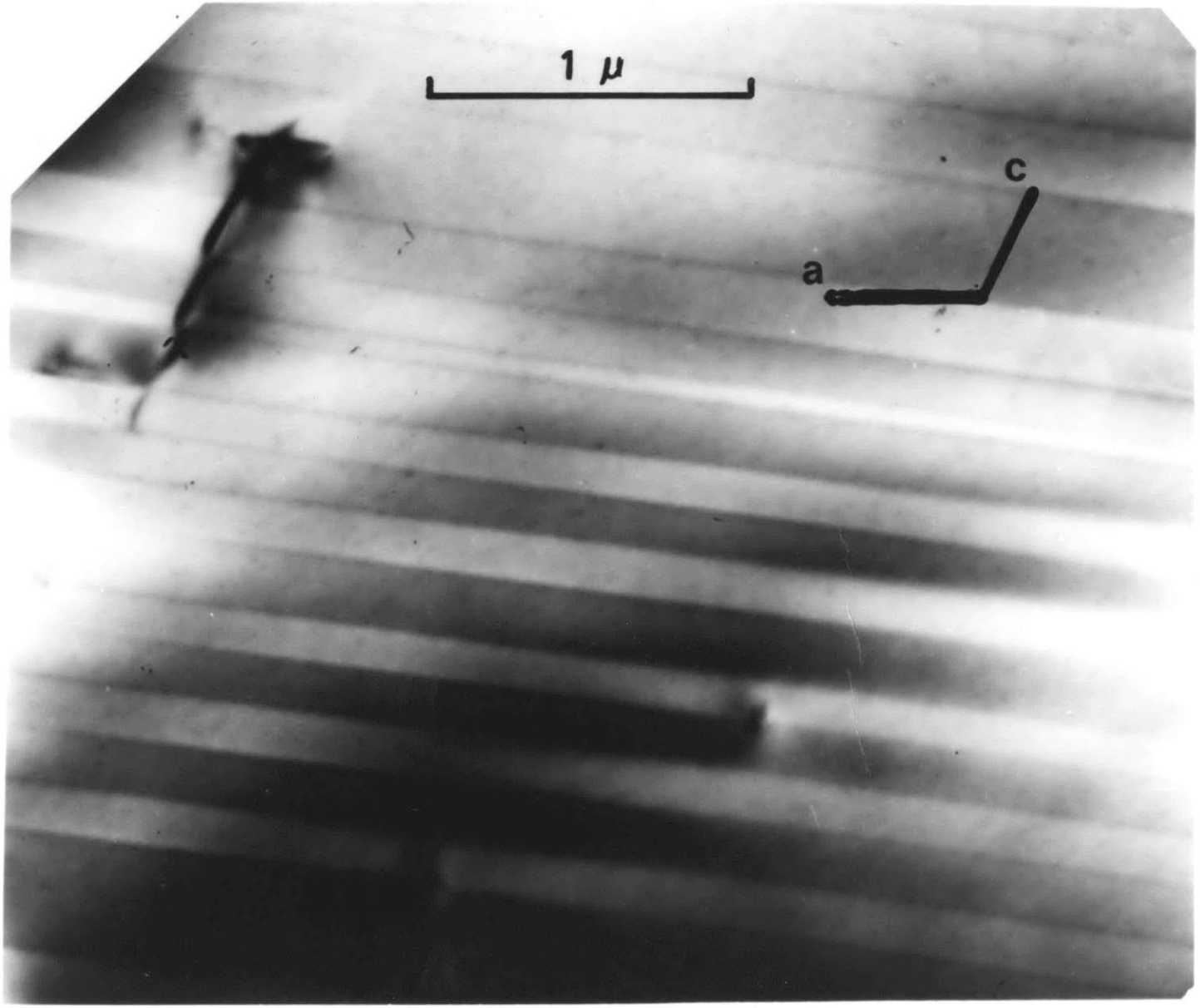
1 μ
c
a

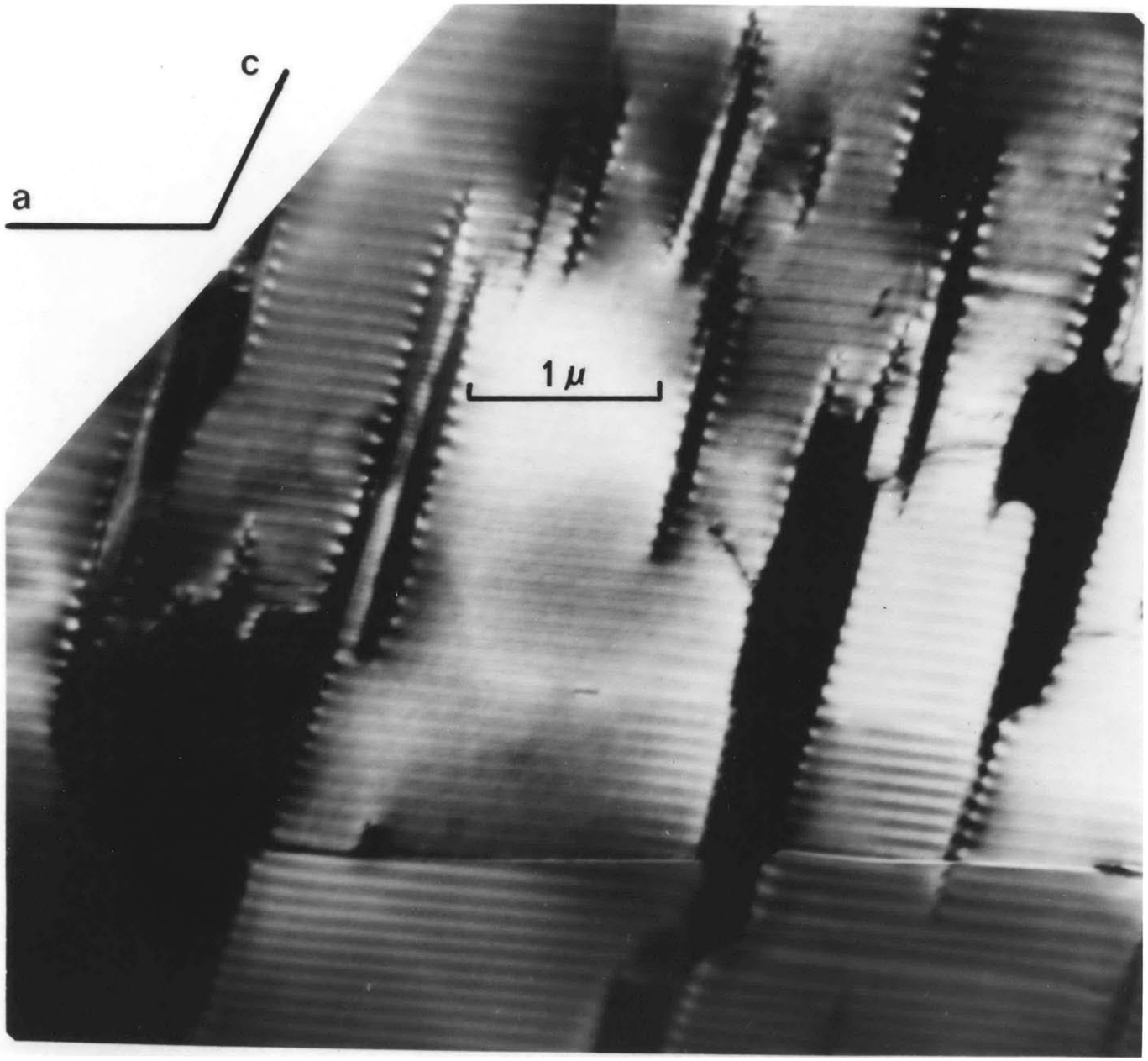
c
a
1 μ

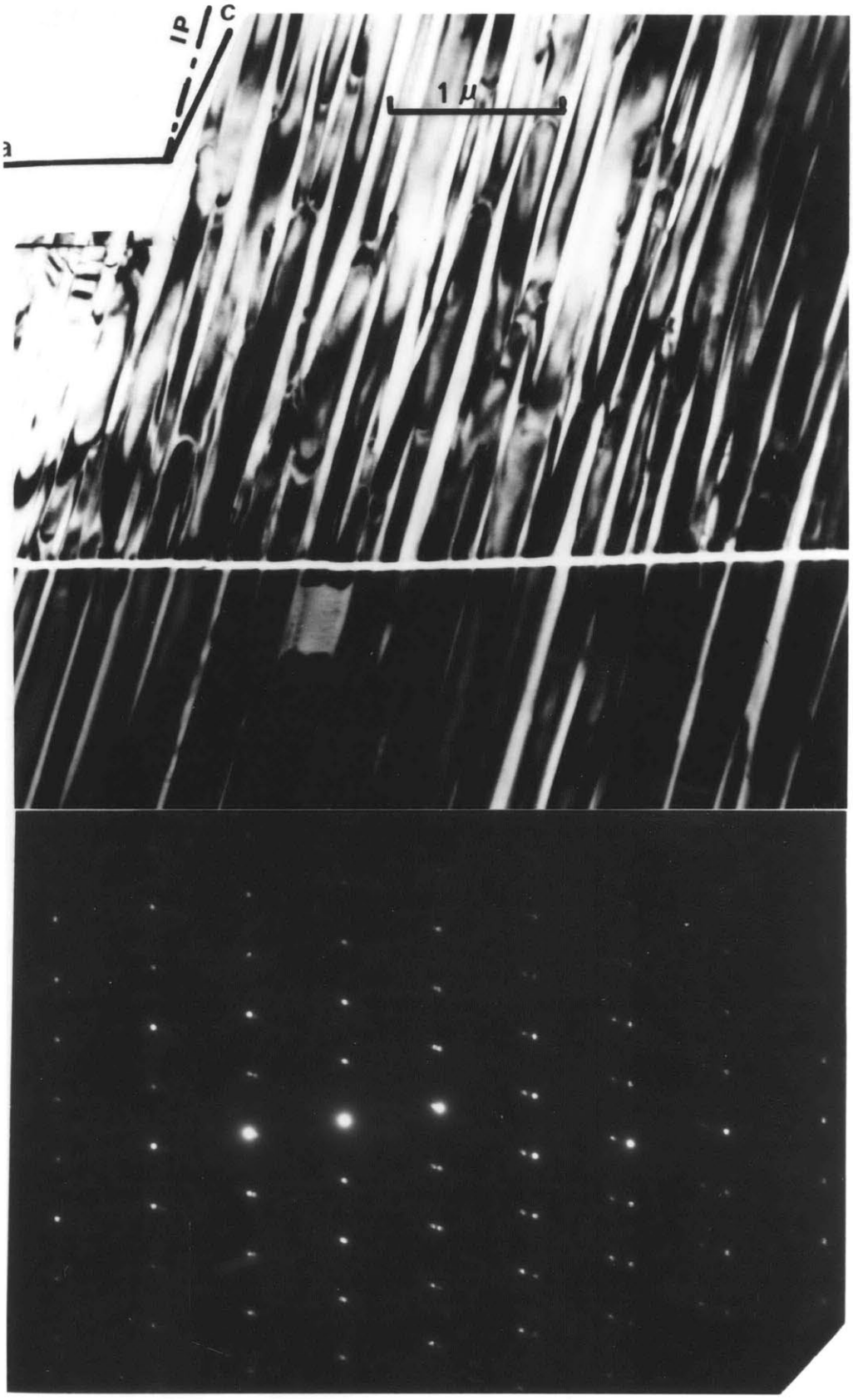
c
1 μ

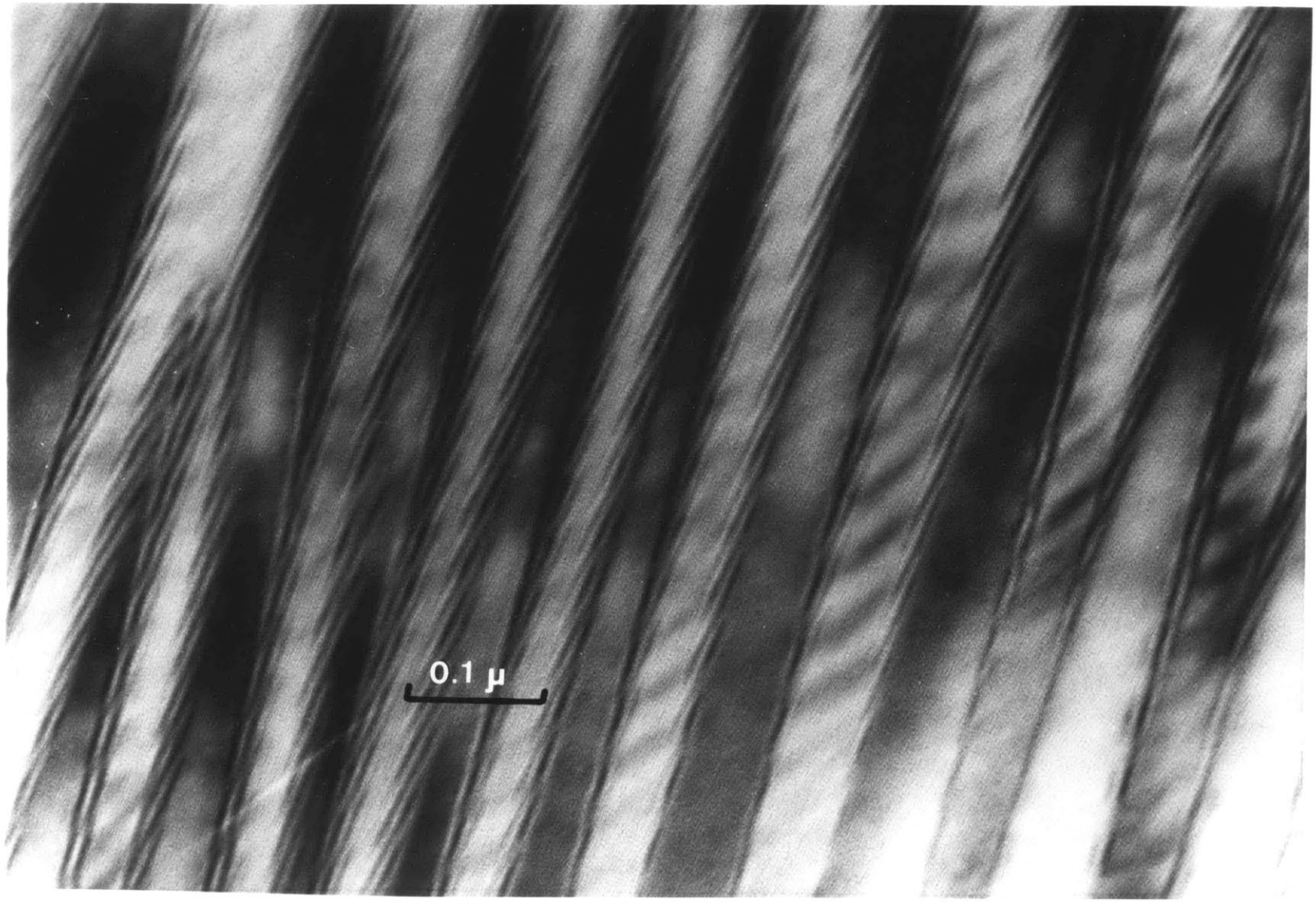
0.1 μ

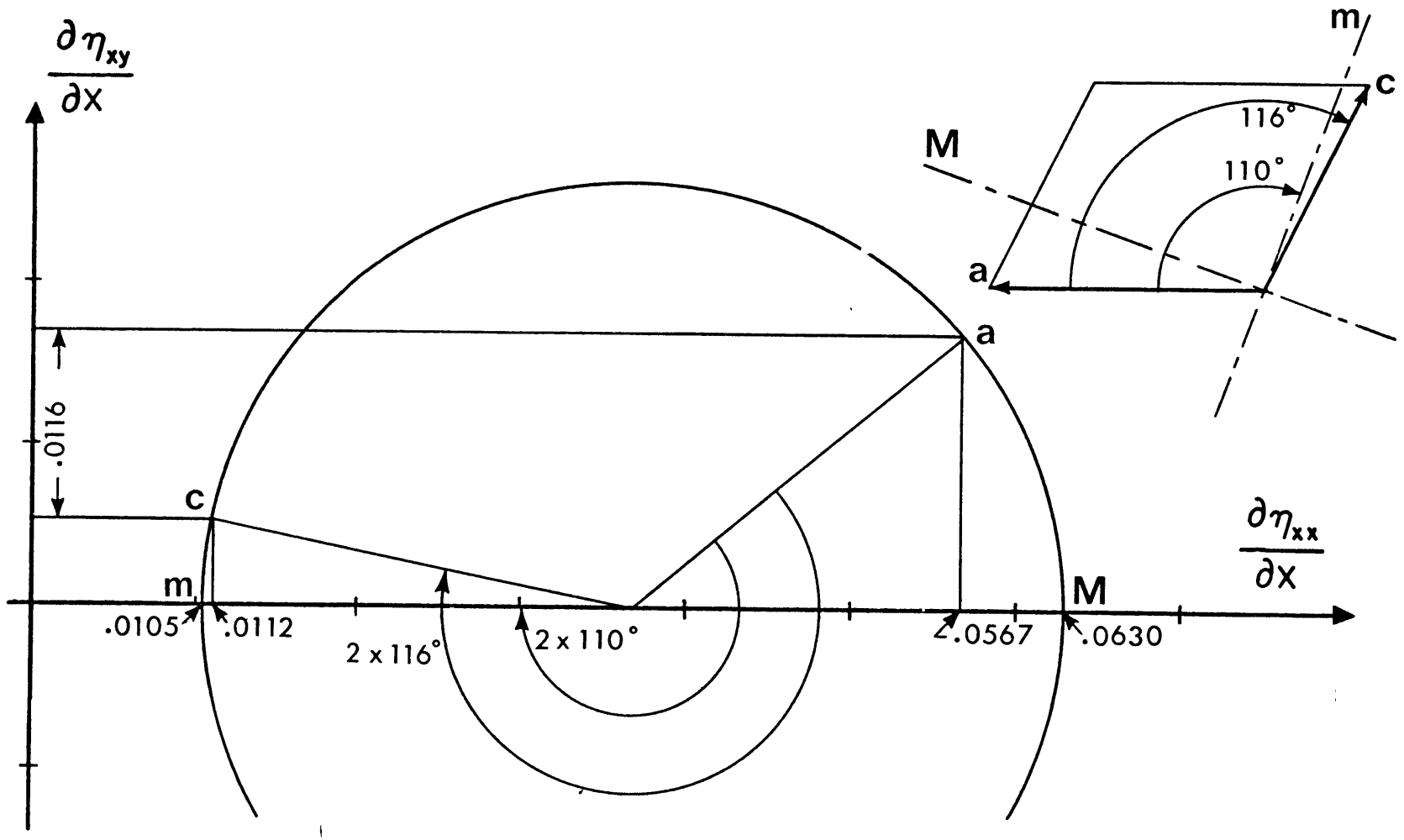
$\frac{\partial \eta_{xy}}{\partial x}$
.0116
c
m
.0105
.0112
2 x 116°
2 x 110°
a
M
.0567
.0630
$\frac{\partial \eta_{xx}}{\partial x}$
m
c
116°
110°
M
a

Fig.5

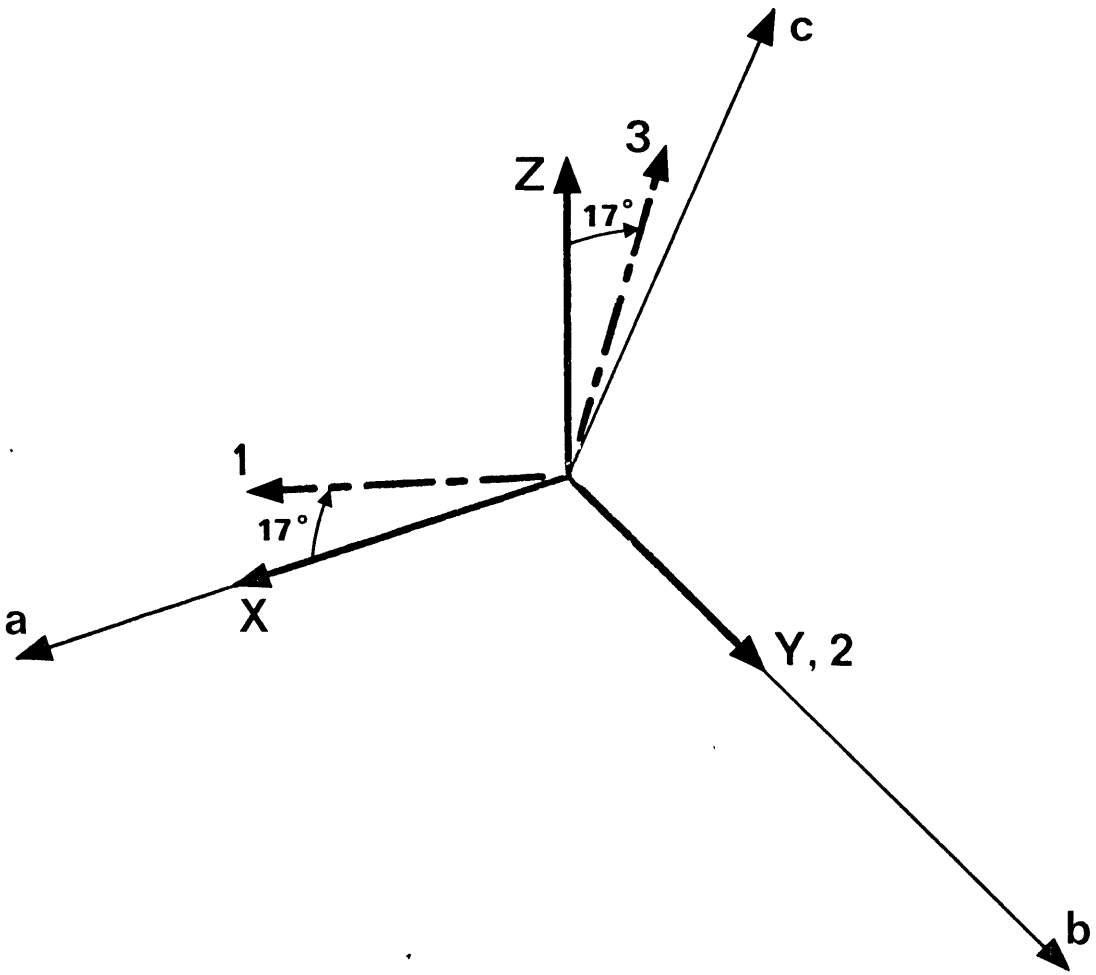

Fig. 6

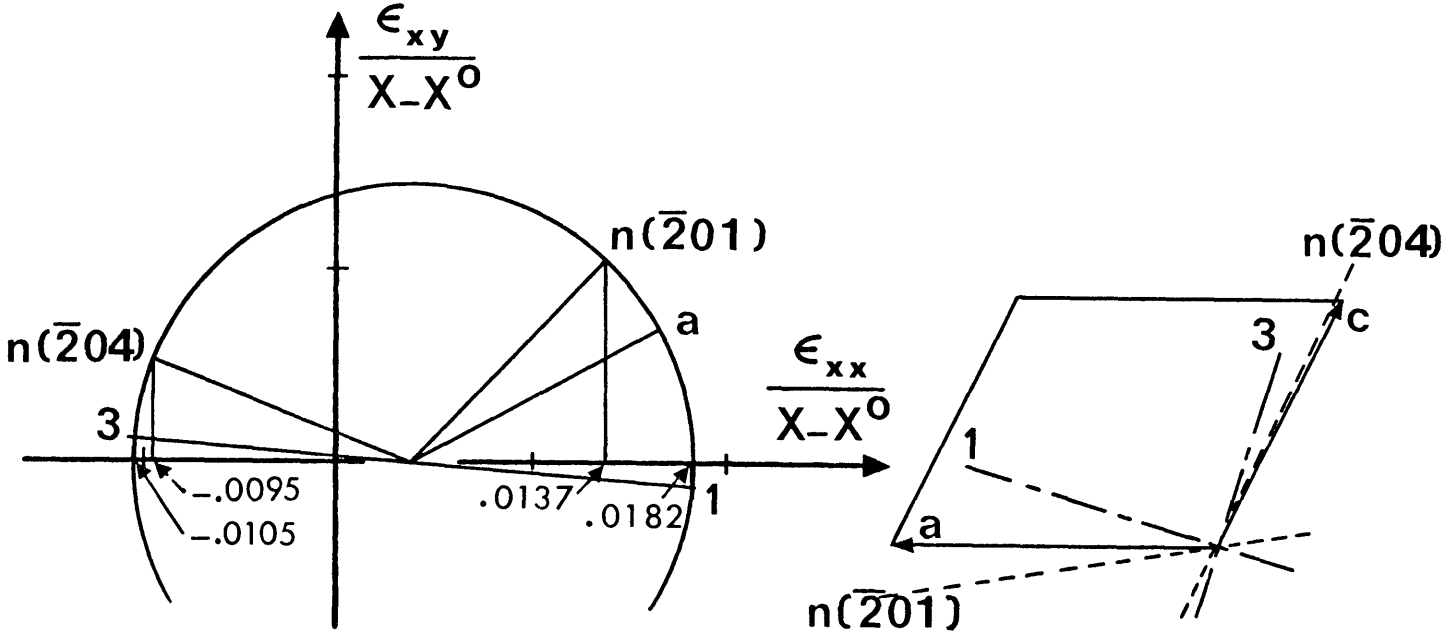
ϵ_{xy}
X-X°
n(2̄01)
n(2̄04)
a
ϵ_{xx}
X-X°
3
-.0095
-.0105
.0137
.0182
1
n(2̄04)
c
3
1
a
n(2̄01)

Fig. 7

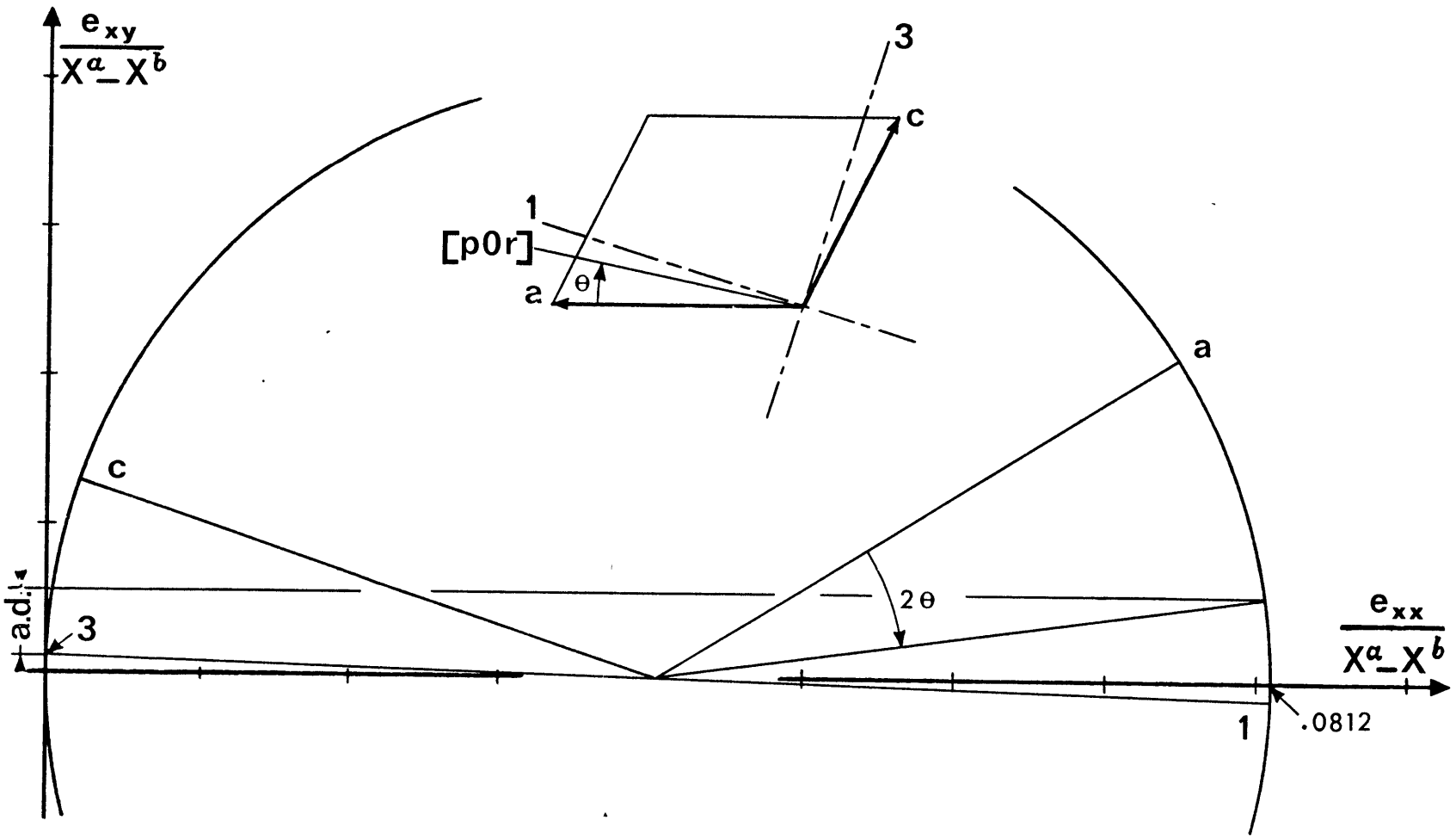

Fig.8

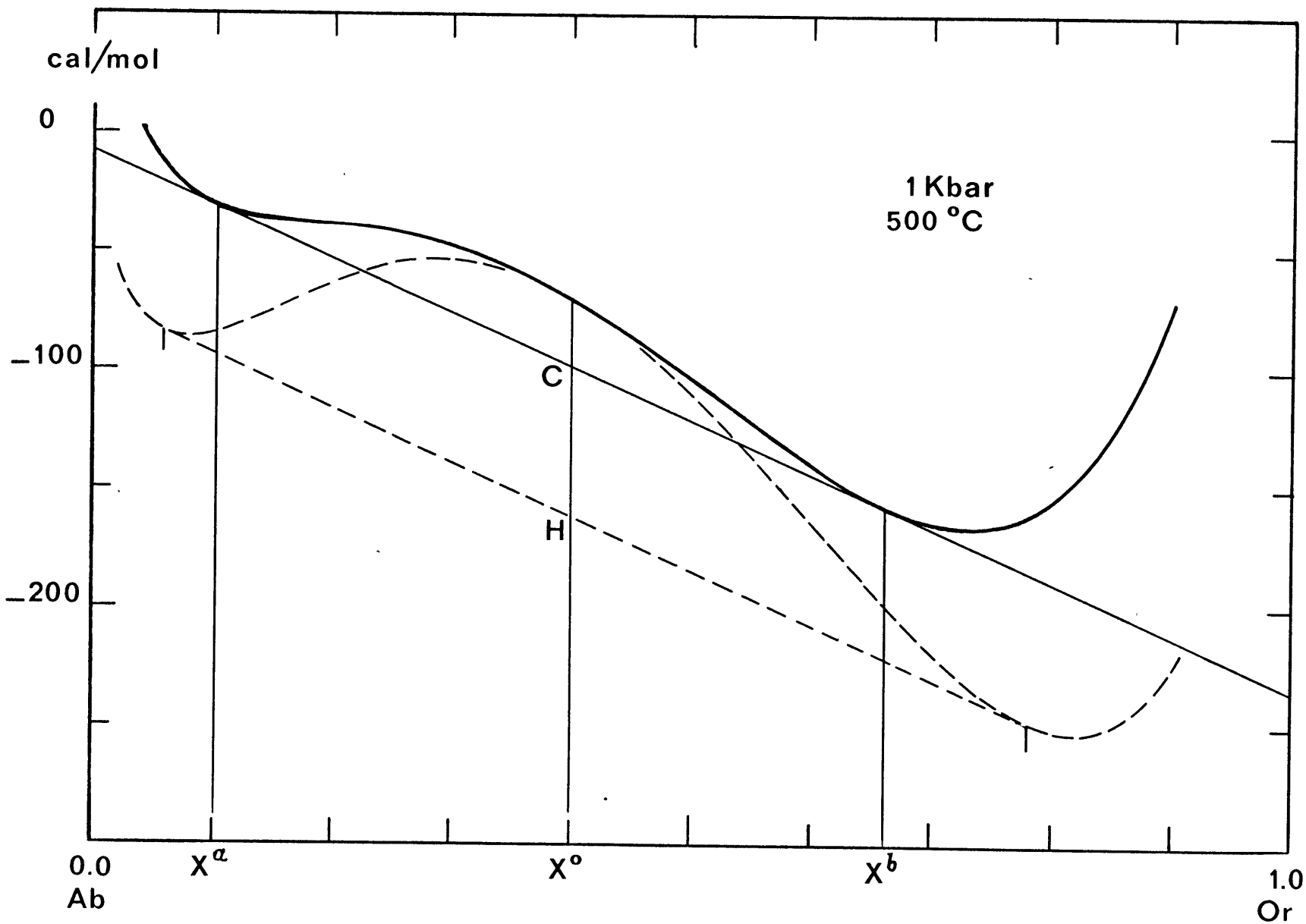

Fig. 9

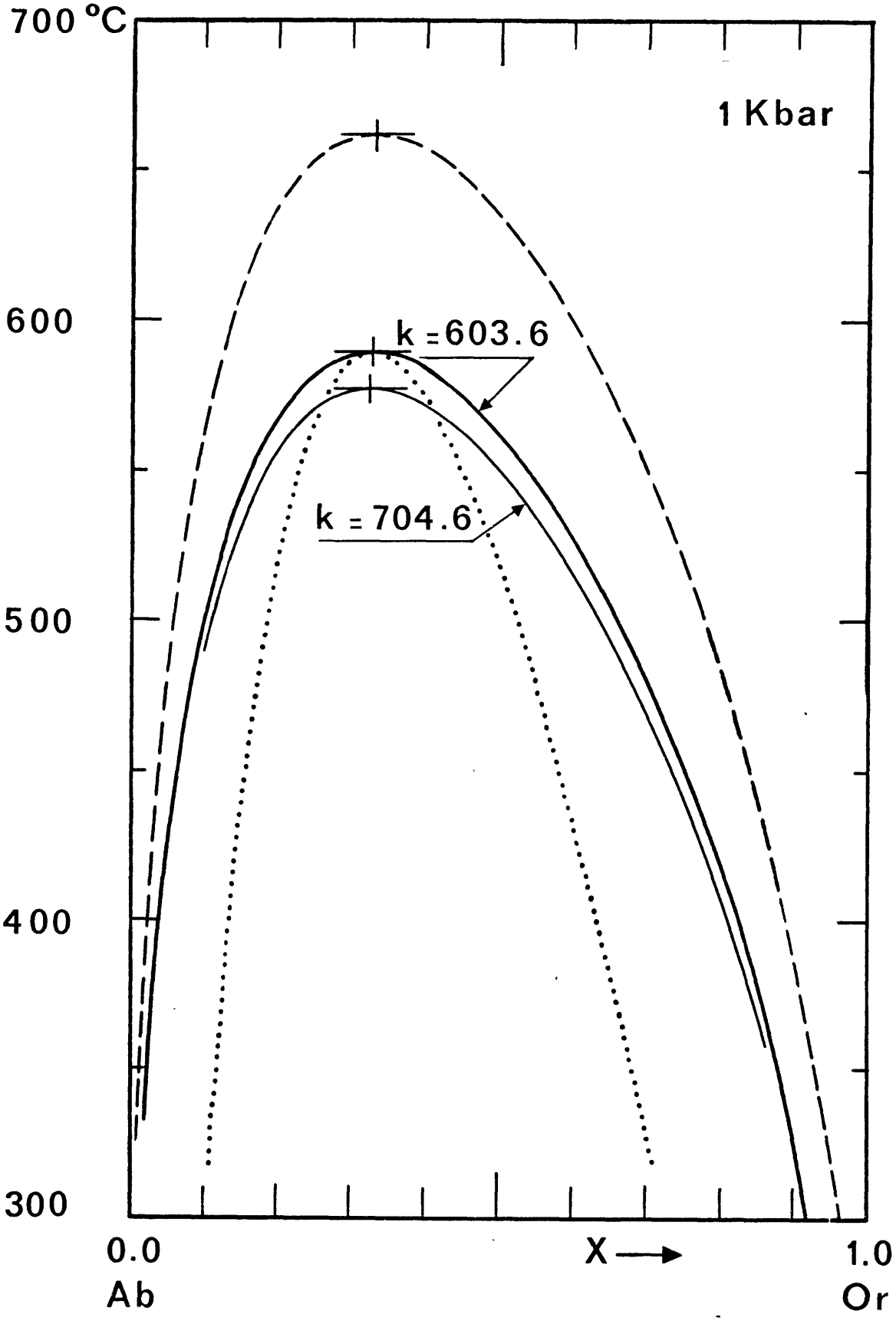

Fig. 10

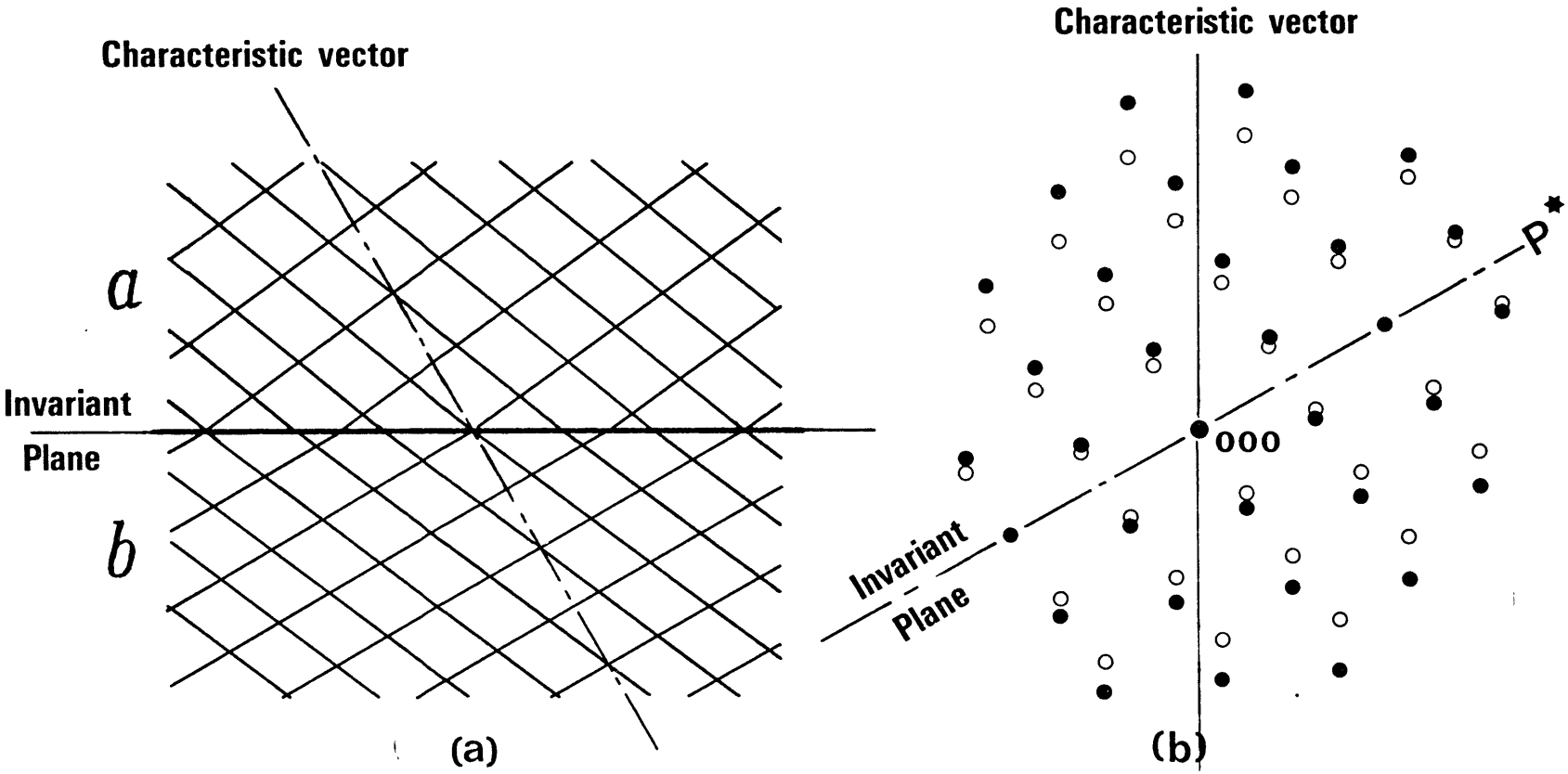
Characteristic vector
a
Invariant
Plane
b
(a)
Characteristic vector
P*
000
Invariant
Plane
(b)

Fig. B1

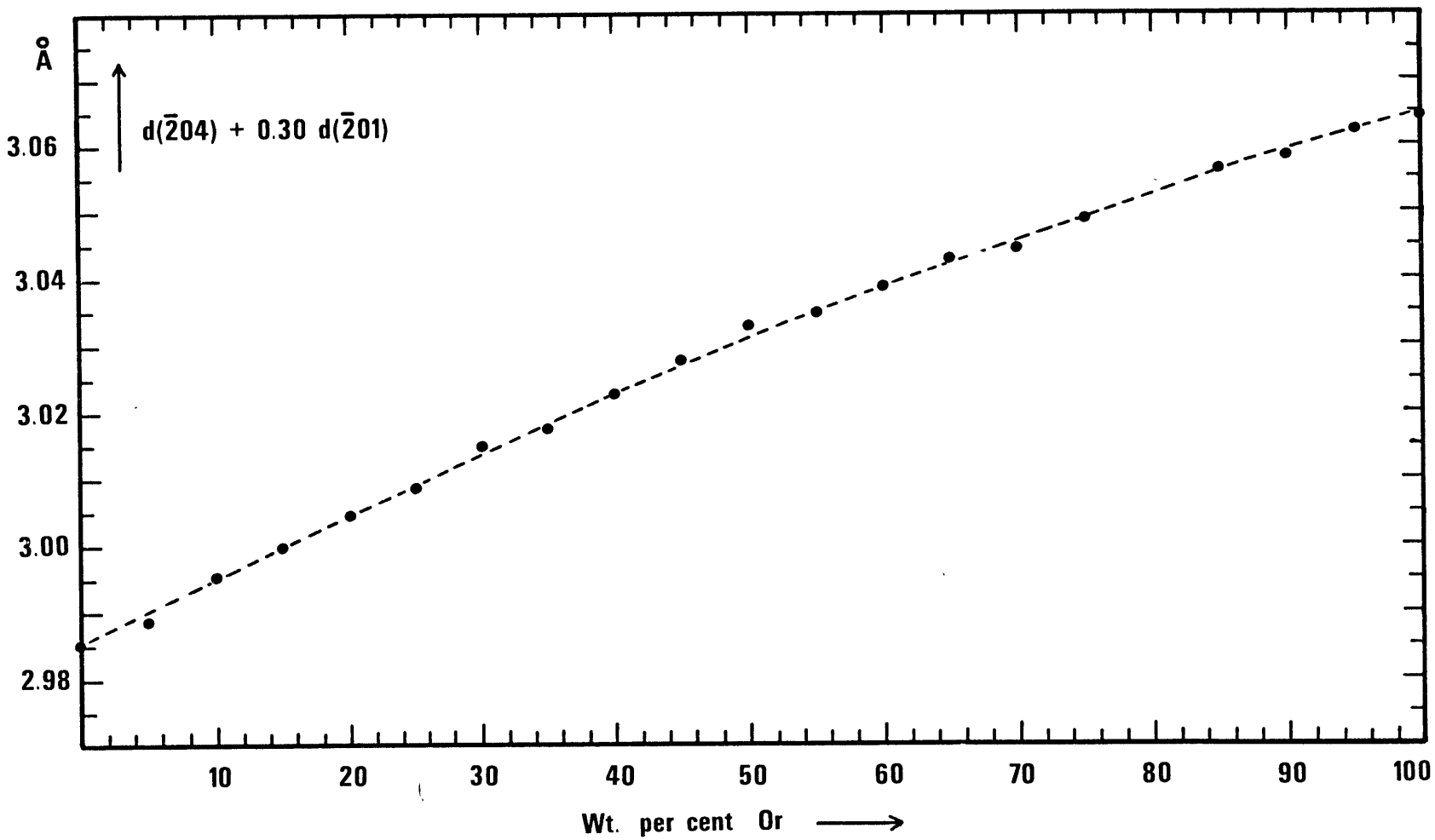
Å
d(2̄04) + 0.30 d(2̄01)
3.06
3.04
3.02
3.00
2.98
10
20
30
40
50
60
70
80
90
100
Wt. per cent Or

Fig. C1

CHAPTER 4

ANGULAR RELATIONSHIPS BETWEEN HOST AND EXSOLUTION LAMELLAE AND THE USE OF THE MOHR CIRCLE[1]

Abstract

The Mohr circle for strain provides a rapid, precise and calculation-free method of predicting angles of exsolution of clinopyroxene or clino-amphibole lamellae from the knowledge of their lattice parameters and of those of the host. Agreement between predicted and observed angles indicates that host and lamellae have maintained 'coherency' during cooling; disagreement, on the contrary, indicates the loss of 'coherency'. As suggested by Robinson and others this information may become very useful for unravelling the cooling history of these minerals.

---

[1] Submitted to Amer. Mineral. .

INTRODUCTION

Robinson et al (1971), Jaffe et al (1972), and Ross et al (1972) report clinoamphibole and clinopyroxene exsolution lamellae which are not oriented parallel to (100) and (001) as was previously often accepted (e.g. Deer et al, 1963). Robinson et al (1971) (RJRK) show that observed orientations are satisfactorily explained in many cases by the requirement that lattices of coexisting phases be 'matched' along the planes of contact.

In all cases [010] lies within the plane of the lamellae; only angles with the a and c axes vary among occurrences. Robinson and his co-workers predict this exsolution angles from measured values of lattice parameters for host and lamellae; their predictions agree generally well with observations. For finding that "plane of dimensional best fit" RJRK first used large scale graphic representations of the two lattices in (010) (their Figure 4), then used a numerical method based on that representation. The purpose of this note is to show that the Mohr circle for strain (e.g. Nye, 1957) provides the same result without any calculation. In addition the Mohr circle gives immediately the angular deviation of any lattice direction, [h 0 ℓ], between the two lattices.

Coherency. Boundaries along which two phases have maintained full continuity of their lattices are called coherent boundaries (e.g. Kelly and Nicholson, 1963). By extension, lamellae whose boundaries are coherent are called coherent lamellae (Chapter 3) . The clinopyroxene or clinoamphibole lamellae considered here would be truly coherent if the repeat distances in the two lattices were identical not only along the direction of the trace of the lamella on (010), but also along [010].

RJRK do show that the first condition is often satisfied; as to the

second, they only state that "generally the b dimensions of host and lamellae are nearly identical", without indicating to what extent the matter was investigated. If b dimensions of host and lamellae were not equal the lamellar boundaries would only be semi-coherent.

Much of the development presented here is applicable whether b dimensions of host and lamellae are equal (true coherency) or not (semi-coherency). However some statements are valid only if the boundaries are truly coherent. For simplicity of writing we shall distinguish between strictly coherent boundaries, for which true coherency is assumed, and, simply, 'coherent' boundaries when only the equality of repeat distances along the trace of the lamella on (010) is assumed.

THE MOHR CIRCLE FOR STRAIN

Lattice strain between host and lamella. Differences in lattice dimensions (say, respectively an augite and a pigeonite) define a strain, formally similar to a thermal expansion or an elastic deformation. Both augite and pigeonite are monoclinic and b is the diad axis; for symmetry reasons b is also a diad axis for the strain tensor. In practice this means that the b axis is a principal direction of strain, the two other principal directions therefore lying in (010). Like stress, strain can be represented on a Mohr diagram, a particularly convenient representation when dealing with a plane which, like (010), contains two principal directions.

Mohr circle (MC). Figure 1 is the MC for the lattice strain between a host augite and "001" pigeonite lamellae from the Hudson Highlands (Jaffe and Jaffe, 1971, cited by Robinson et al, 1971, Tables 3 and 5).

Lattice parameters for the augite are:

$\underline{a}_a = 9.77_6$ Å , $\underline{c}_a = 5.25_2$ Å , $\beta_a = 105^\circ 55'$ (Figure 1a) ; (1a)

for the pigeonite:

$$\underline{a}_p = 9.69_5 \text{ Å} , \quad c_p = 5.23_6 \text{ Å} , \quad \beta_p = 108^\circ 33' \quad . \tag{1b}$$

The $\underline{b}$ dimensions are equal: $\underline{b}_a = \underline{b}_p = 8.89_0$ Å . (1c)

The lattice strain in (010) is completely defined by

$$\frac{\Delta \underline{a}}{\underline{a}} = \frac{\underline{a}_p - \underline{a}_a}{\underline{a}_a} = \frac{-0.08_1}{9.77_6} = -0.008_3 \quad , \tag{2a}$$

$$\frac{\Delta \underline{c}}{\underline{c}} = \frac{-0.01_6}{5.25_2} = -0.003_0 \quad , \tag{2b}$$

$$\Delta\beta = \beta_p - \beta_a = 2^\circ 38' = 0.050_0 \text{ rad.} \tag{2c}$$

The host lattice is taken as reference state.

Construction of the Mohr circle from these data is explained in Figure 1 . If a lattice direction, $[\underline{h}\ 0\ \underline{\ell}]$, makes an angle θ with the $\underline{a}$ axis, Point D , which represents $[\underline{h}\ 0\ \underline{\ell}]$ on the MC , is at an angular distance 2θ from Point A . The abscissa of D is equal to the longitudinal strain along $[\underline{h}\ 0\ \underline{\ell}]$ of the lattice of the lamella with respect to that of the host; the ordinate difference between any two points, say A and D , is equal to the difference between the $[100]\cdot[\underline{h}\ 0\ \underline{\ell}]$ angle in the lamellae and that in the host, expressed in radians.

The MC in Figure 1b intersects the ordinate axis in two points, L and L' ; this means that there is no longitudinal strain along the corresponding lattice directions, or, in other words, that repeat distances along these directions are the same for both phases. L and L' are therefore the directions of "dimensional best fit" sought by RJRK. The angles between the L direction and the $\underline{a}$ and $\underline{c}$ axes are 9.6° and 115.5° respectively (half the angles

which L makes with A and C respectively, on the MC).

Optical measurements of the angle between the "001" lamellae and the c axis give $116^{o} \pm 1^{o}$ (RJRK, Table 3). Like the numerical calculations by RJRK the Mohr circle construction thus demonstrates that the "001" pigeonite lamellae are 'coherent' within the augite host.

Because $\underline{b}_a = \underline{b}_p$ (Equation 1c) the lamellae are in fact strictly coherent.

Deviation of lattice directions. Although L is not a rational lattice direction it differs from $[30\bar{1}]$ by only 0.3^{o} (and from $[32.0.\bar{11}]$ by 0.003^{o} !) . For practical purposes we can say that (103) is the direction of the plane of coherency; by necessity (103), and $[30\bar{1}]$, have the same orientation in the host and the "001" lamellae. Such is not the case for other lattice directions $[\underline{h}\ 0\ \underline{\ell}]$: the angular deviation of $[\underline{h}\ 0\ \underline{\ell}]$ between the two lattices, $\delta[\underline{h}\ 0\ \underline{\ell}]$, is equal to the difference between the ordinate of D and that of L . Thus we read directly that the a axis is only deviated by an angle $\delta[100] = 0.0030 = 3.4'$; $\delta[001] = 0.0470 = 2^{o}\ 41.6'$.

The lattice direction which undergoes the largest deviation between the two lattices is close to [1.0.10] (Point E on MC) with

$$\delta[1.0.10] = 0.0490 = 2^{o}\ 48.5' \ .$$

On the contrary, [805] (Point V on MC) undergoes no deviation.[2] The longitudinal strain along [805] (abscissa of V in Figure 1b) is - 0.0255; this is also the relative change in the (103)-spacing between the two lattices; because

---

[2] In Chapters 2,3 we called such undeviated lattice direction the characteristic vector of the [strictly] coherent boundary. Note that V and L' are necessarily at 180^{o} from each other on the MC ; the characteristic vector for the L boundaries is therefore perpendicular to the other predicted lamellar orientation L' .

strict coherency is maintained here, the abscissa of V is also the volumetric strain between the two lattices.

DISCUSSION

Representation of strain by a Mohr circle implies infinitesimal strain. The worse error introduced by this approximation is roughly the error in equating Cos(0.052) to 1 (where 0.052 radians is the diameter of the MC). Cos 0.052 = 0.99864 and the error is therefore 0.124% or $0^{o}05'$.

The error arising from the uncertainty in the data can be estimated empirically by redrawing the MC for slightly different values of the data in Equations 2a, b. For example if 0.008_3 is replaced by 0.008_1 in (2a), the predicted angle of the lamellae L with the c axis becomes 115.3^{o} instead of 115.5^{o}. This variation is larger than the worse error introduced by the assumption of infinitesimal strain; both predictions lie well within the limits of accuracy of optical measurements of exsolution angles ($\pm 1^{o}$). Use of the Mohr circle for infinitesimal strain seems therefore quite justified.

Applications

The Mohr circle construction, like the numerical method of RJRK, thus can serve to establish whether or not host and lamellae are 'coherent': they are 'coherent' if predicted and observed angles agree, they are not if prediction and observation disagree.

Now, when exsolution lamellae between clinopyroxenes first form it is always energetically advantageous for them to maintain 'coherency'. The stress-free (single phase) lattice parameters of coexisting clinopyroxenes are such that there always are two directions along which 'coherency' can be maintained with no elastic distortion[3] (and consequently no elastic strain energy) and

---

[3] In case of strictly coherent clinopyroxenes the maintenance of equal b

in this manner the high interfacial energy of incoherent boundaries can be saved. However, as RJRK point out, changes in compositions of the coexisting phases (solvus effect) and differences in thermal strain (thermal expansion effect) during cooling change the angles of 'stress-free coherency'. The directions of the existing lamellae are set and cannot be changed, and therefore, one of two things may happen.

1. 'Coherency' is not lost, for example as a result of rapid cooling. Lamellae may become elastically strained and acquire lattice parameters which are anomalous compared to those of homogeneous crystals of the same composition; if these anomalous parameters are used the MC will still predict the observed exsolution angle.

The lattice parameters of the two kinds of lamellae may be detectably different after cooling, because thermal contraction is not isotropic. Lattice parameters of the "100" pigeonite lamellae in the augite studied by Jaffe and Jaffe (1971) thus differ significantly from those of the "001" lamellae given in (1b). In such a case the lattice parameters of the "001" lamellae can only serve to predict the exsolution angle for the "001" lamellae themselves.

2. 'Coherency' is lost, as perhaps during slow cooling. Stresses which otherwise would slowly build up as a result of the solvus and thermal expansion effects are thus relieved. Further growth of these lamellae would require a migration of the now incoherent boundaries; this appears to be difficult and another set of

---

3(contin.)
parameters in the host and the lamellae requires nonhydrostatic stresses, mostly in the lamellae which therefore acquire some elastic strain energy. That strict coherency is nevertheless maintained in some cases means that loss of coherency is either themodynamically more costly or is prohibited for kinetic reasons. The effect of elastic strain energy on lamellar exsolution behavior has been examined in Chapter 3.

lamellae develops instead, which has the new angle of 'stress-free coherency'.

This second set may in turn lose 'coherency' during further cooling. Ross et al (1972) report examples of such multiple exsolution in which, characteristically, only the third (and last) set of lamellae has preserved 'coherency'.

Our present knowledge of thermal expansion in the pyroxene quadrilateral and our understanding of the kinetics of the loss of 'coherency' are not sufficient to give more than qualitative information on relative cooling rates. As our knowledge improves, analyses such as the one presented here may tell us much about complete cooling histories of minerals and rocks.

REFERENCES

DEER, W.A., R.A. HOWIE, and J. ZUSSMAN (1963) Rock-forming minerals. Vol.2 Chain silicates. Longmans, Green and Co. Ltd., London, 379 p.

JAFFE, H.W., and E.B. JAFFE (1971) Bedrock geology of the Monroe quadrangle, New York. N.Y. State Museum and Sci. Serv., Map and Chart Series No.20.

_____, P. ROBINSON, R.J. TRACY, and M. ROSS (1972) Correlation of angles of pigeonite exsolution lamellae, composition, and calculated optimal phase boundaries in metamorphic augites. Geol. Soc. Amer. Abstracts 4 (7), 552.

KELLY, A., and R.B. NICHOLSON (1963) Precipitation hardening. In B. Chalmers (ed) Progress in Materials Science, Vol. 10. The MacMillan Co., New York, N.Y.

NYE, J.F. (1957) Physical properties of crystals. Oxford Univ. Press, London, 322 p.

ROBIN, P.-Y.F. (1974a) Stress and strain in cryptoperthite lamellae and the coherent solvus of alkali feldspars. Amer. Mineral. (in press)

_____ (1974b) Thermodynamic equilibrium across a coherent interface in a stressed crystal. Amer. Mineral. (in press)

ROBINSON, P., H.W. JAFFE, M. ROSS, and C. KLEIN,Jr. (1971) Orientation of exsolution lamellae in clinopyroxenes and clinoamphiboles: consideration of optimal phase boundaries. Amer. Mineral. 56, 909 - 939.

ROSS, M., P. ROBINSON, and H.W. JAFFE (1972) Pigeonite lamellae in Bushveld augite sequentially exsolved on phase boundaries at angles controlled by differential thermal contraction. Geol. Soc. Amer. Abstracts 4(7), 644-645.

FIGURE CAPTIONS

FIG. 1. (a) a c plane of clinopyroxene lattice cell. Parameters are those of an augite crystal described by Jaffe and Jaffe (1971) and cited by Robinson et al (1971, Table 3, example 4 and Table 5).

(b) Mohr circle for the lattice strain between the augite host and the pigeonite lamellae. The circle is constructed as follows:

Abscissae of Points A and C (corresponding to a and c axes respectively) are given by Equations 2a and b . The ordinate of A can be arbitrarily set as zero; the ordinate of C is then equal to $\Delta\beta$ expressed in radians (Eq. 2c). The center O of the MC is obtained from the requirements (i) that it lie on the perpendicular bisector of AC , and (ii) that Arc AC (counted clockwise as is $\beta = \widehat{a\ O\ c}$ in Figure 1a) be equal to 2β (hence $|\widehat{CAO}| = \beta - 90° = 15°55'$).

The MC can thus be drawn, of center O and radius $|\overline{OA}| = |\overline{OC}|$. An ambiguity may arise in deciding whether C should be drawn above or below A. For an angle $\beta = \widehat{a\ O\ c}$ counted clockwise (the present case) the rule is that C is above A if $\Delta\beta$ (Eq. 2c) is positive, C is below A if $\Delta\beta$ is negative. The rule is reversed if β (and AC on the MC) is counted counter-clockwise.

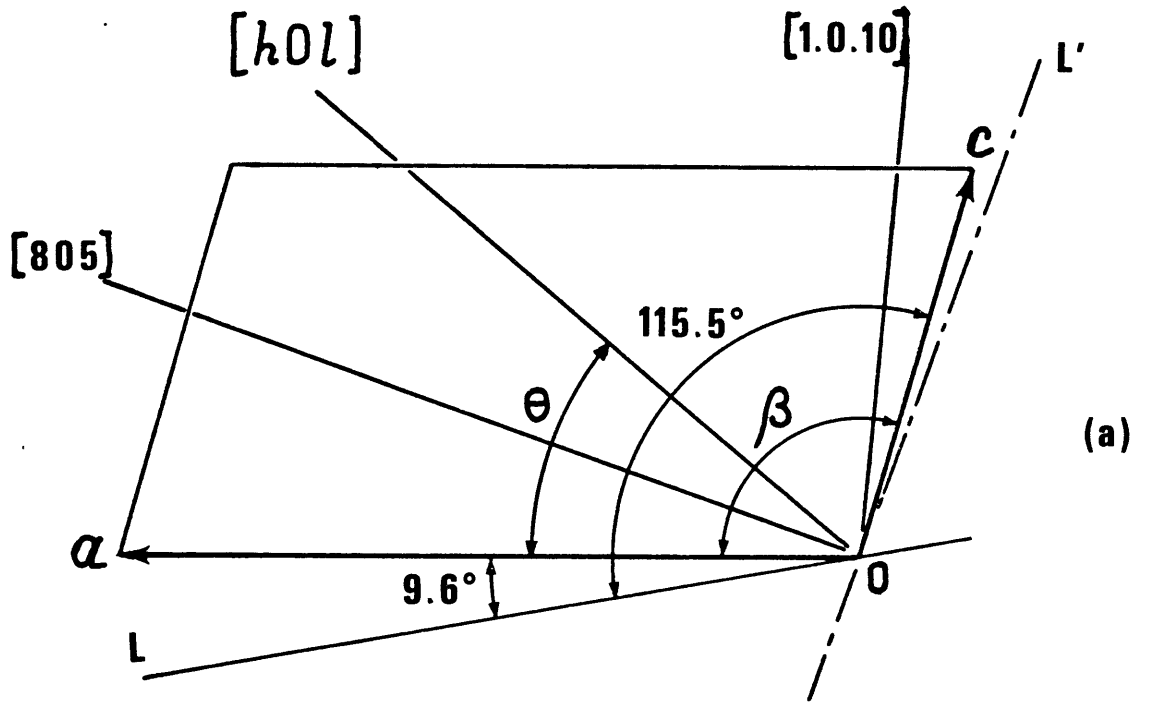
[hOl]
[1.0.10]
L'
c
[805]
115.5°
θ
β
a
9.6°
O
L

(a)

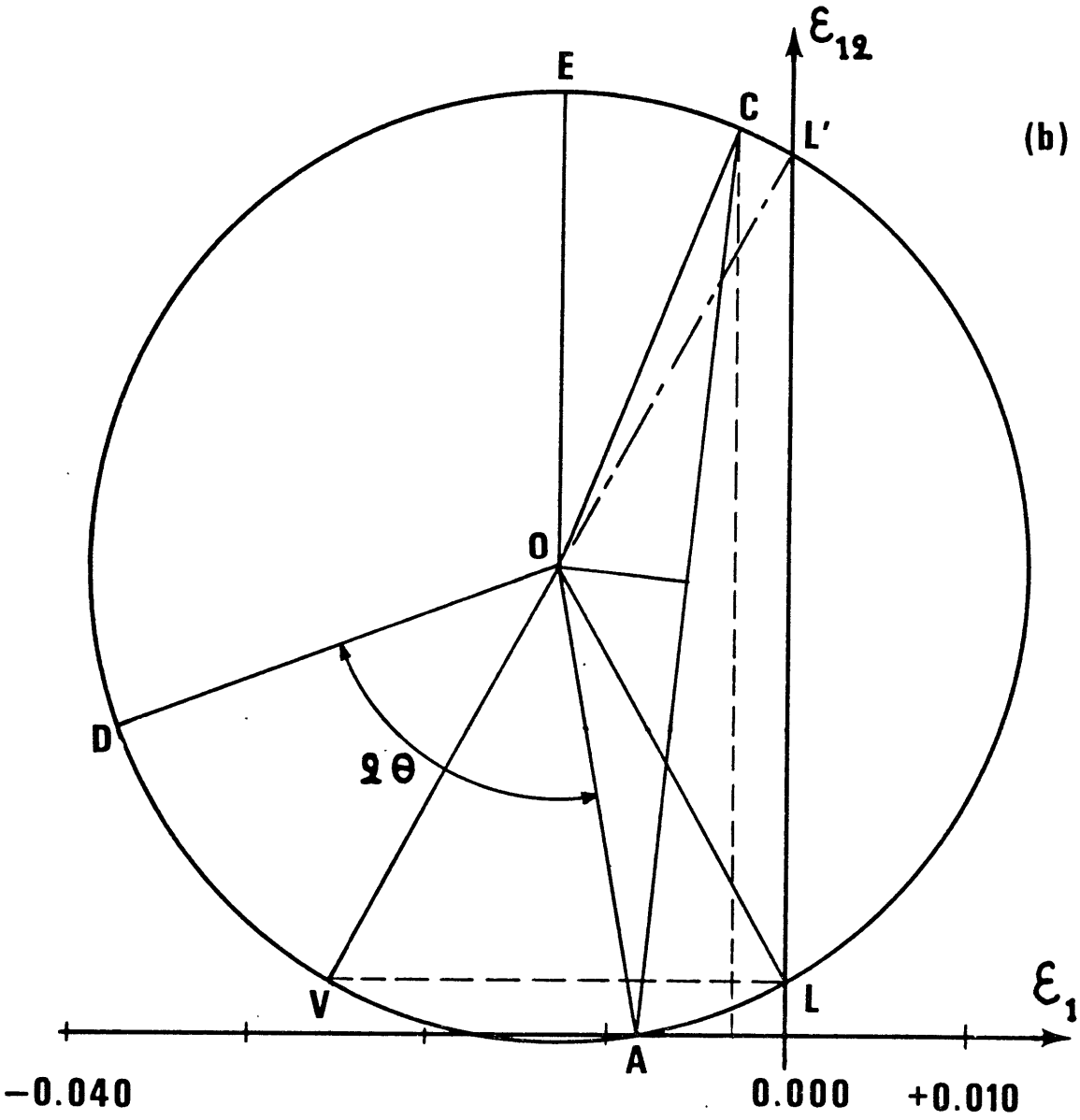
ε12
E
C
L'
O
D
2θ
V
L
A
ε11
−0.040
0.000
+0.010

(b)

CHAPTER 5

EFFECT OF A SHEAR STRESS ON A COHERENT TRANSFORMATION IN A BINARY SYSTEM, WITH POSSIBLE APPLICATIONS TO Fe,Mg PYROXENES

INTRODUCTION

This chapter is a theoretical development based on a result of Chapter 2 . The question considered is that of the effect of a resolved shear stress τ on the equilibrium between two phases α and β when (a) α and β maintain coherency along their common interface, (b) the transformation strain is large, and, (c) at least one component of the solid is fluid (see Chapter 2) and has a different concentration in α and β .

Coe (1970) (see also Chapter 2, Equations 26, 27 and 28) established the condition of equilibrium for a coherent transformation characterized by a finite simple shear across a planar interface in a one-component system. The purpose of this chapter is essentially to generalize Coe's result to the case in which cation diffusion through the framework can occur.

As one application of the theory the shear-induced transformation from orthopyroxene (OP, or O) to clinopyroxene[1] (CP, or C) is used as example throughout the chapter. Some assumptions which are made here regarding the transformation mechanisms must be justified, for any particular system, before the results can be considered applicable. Although this author regards these assumptions as very likely to be valid in the OP-CP system and will argue in their favor, the evidence probably leaves room for debate; this should be kept in mind.

---

[1] Clinopyroxene means here the clinoenstatite-clinoferrosilite solid solution series with the crystallographic symmetry of pigeonite, $P2_1/c$ (see Smith, 1969).

ASSUMPTIONS

They can be divided into essential assumptions and assumptions of convenience.

The essential assumptions are, in effect, that under appropriate conditions (1) the silicate framework can support the applied stress without plastic flow, (2) the variational migrations of an interface between OP and CP fit the description given in Chapter 2, and (3) the metal ions can diffuse through the silicate framework.

The high mechanical strength of pyroxenes is probably most strikingly demonstrated by experiments performed by W. Durham (personal communication) at M.I.T. Axial stresses of about 2 kbar were applied onto unconfined orthopyroxene crystals at 1320°C for almost three hours; the crystallographic orientation chosen was such that the resolved shear stress was maximum on (100)[001], held to be the easiest glide system in pyroxene; yet no shortening of the sample could be detected.

That diffusion of Fe, Mg and Ca through the pyroxene framework is possible and does not require the rupture of the lattice is demonstrated by the fact that coherent exsolution lamellae are observed both between orthopyroxene and pigeonite or between augite and pigeonite (see Chapters 2 and 4). Coherent exsolution requires that diffusion of the cations over distances of several microns be able to occur at temperatures as low as 800°C or even less (Virgo and Hafner, 1970, conclude "that diffusion paths of the order of a few lattice constants are possible down to temperatures of 480°C") .

Shear-induced transformation of OP to CP at temperatures between 25°C and 1000°C is reported by many authors (for a review see Coe, 1970, and Coe and Müller, 1973). No X-ray work appears to have been done on the resulting 'two-phase crystals', but electron diffraction and transmission electron

microscopy (Coe and Müller, 1973) confirm earlier suggestions that the two pyroxenes coexist coherently along their common (100) plane.

However, it is not sufficient to show that OP-CP interfaces are coherent, it must further be established that their migration under a shear stress, satisfies the reversibility criterion discussed in Chapter 2 . The evidence here is less compelling. Kirby and Coe (1974 ; also Kirby, 1974 , personal communication) observe a high density of stacking faults (and associated partial dislocations) in Bamble bronzite - and induced clinobronzite - deformed at temperatures up to 800°C and a resolved shear stress which they estimate to be between 3 and 10 kbar[2].

Dislocation glide violates the assumption of solid behavior (no flow) made above. If motion of dislocations or partial dislocations along the interfaces is possible and accompanies the growth of either phase, this would indicate also that the framework is broken at the interface; irreversible gliding along the interface then being possible, no unique characteristic vector for the transformation could be defined (see Chapter 2), and growth of CP would not be a truly coherent process.

The following remarks can be made in defense of the coherency of the process however :

(1) Glide dislocations observed by Kirby and Coe indeed contradict experiments such as those by W. Durham. The shear stresses used were significantly higher and would thus have exceeded the limit for 'solid behavior'.

(2) Two-lattice-layer thick CP lamellae (≈ 18Å) should cause the same displacement field as a stacking fault. The apparent displacement vector of

---

[2] This large uncertainty is inherent to the solid medium confining pressure apparatus which they used (Kirby, 1974, personal communication).

such a 'stacking fault' would in fact be approximately $\frac{3}{4}[001]$, compatible with the displacement vectors measured by Kirby and Coe (Kirby, 1974, personal communication).

(3) Similarly, reversible growth of, say, CP at the expense of OP should occur by areal expansion of successive 18 Å thick layers along the interfaces. The edges of such expanding layers should also have the same strain field and TEM image as partial dislocations, although the framework would remain unbroken.

After their runs, in fact, Kirby and Coe (1974) annealed their samples at 1100°C and observed the total disappearance of CP and a strain reversal. In the light of this last observation and of the remarks above, together with the known strength of pyroxenes and observed coherency of their interfaces, the essential assumptions appear quite reasonable over a broad range of temperature and stresses.

The assumptions of convenience are those which are not fundamental to the theory presented here. They are chosen so as to simplify the details of the development; however, as discussed later, they can easily be replaced by other ones if our information so requires. It is first assumed that the pyroxenes belong to the pure enstatite-ferrosilite series; Fe and Mg are the only diffusing species, and, because of site constraints (see Thompson, 1969), there is only one independent fluid component. The chemical formula of these pyroxenes can therefore be written as $(FeMg_{-1})_X.MgSiO_3$ (see Chapter 3, Footnote 6).

CP is assumed to have a stability field at low temperature. For pure enstatite, Grover's (1972) transition temperature of 566°C is accepted; following Kuno's (1966) hypothetical phase diagram based on natural occurrences, 800°C is chosen as the transition temperature for pure ferrosilite.

Both OP and CP are assumed to be ideal solutions, a reasonable

approximation at temperatures above 550°C and for $X < 0.6$ (Virgo and Hafner, 1970). The entropy difference between orthoenstatite and clinoenstatite or between orthoferrosilite and clinoferrosilite is arbitrarily taken to be

$$\Delta\bar{S} = \bar{S}^{o}_{M} - \bar{S}^{c}_{M} = \bar{S}^{o}_{F} - \bar{S}^{c}_{F} = 1 \text{ cal mol}^{-1} \text{ deg}^{-1} \quad , \tag{1}$$

$$= 41.84 \text{ bar cm}^{3} \text{ mol}^{-1} \text{ deg}^{-1} \ ,$$

where superscripts o and c stand for OP and CP, and subscripts M and F stand for Mg end-member and Fe end-member. Assuming an entropy difference independent of temperature and composition can perhaps be justified by the fact it is mostly a configurational entropy change. The enthalpy change, $\Delta\bar{H}$, is also independent of temperature, but not of composition.

Because the change in volume is very small (Smith, 1969) it can be neglected; the transformation is thus essentially a simple shear along (100) parallel to [001]. The angle of shear, ψ (Chapter 2, Eq. 26 and Fig. 2), is taken to be $\psi = 13.3^{o}$ (Coe, 1970; Coe and Müller, 1973). Elastic strains can justifiably be neglected in comparison to the large transformation strain.

THERMODYNAMIC DESCRIPTION OF THE TRANSITION UNDER HYDROSTATIC CONDITIONS

Equilibrium between ortho- and clinoenstatite at 566°C ($T_M = 849K$) implies that

$$\Delta\bar{H}_{M} = T_{M} \, \Delta\bar{S} \quad . \tag{2a}$$

Similarly, for ferrosilite ($T_F = 1073K$),

$$\Delta\bar{H}_{F} = T_{F} \, \Delta\bar{S} \quad . \tag{2b}$$

Gibbs energies for the pure end-members at any temperature T are

therefore given by

$$\bar{G}_M^c \quad , \tag{3a}$$

$$\bar{G}_M^o = \bar{G}_M^c + (T_M - T)\ \Delta\bar{S} \quad , \tag{3b}$$

$$\bar{G}_F^c \quad , \tag{3c}$$

and $$\bar{G}_F^o = \bar{G}_F^c + (T_F - T)\ \Delta\bar{S} \quad . \tag{3d}$$

Gibbs energies of formation of OP and CP with intermediate compositions from pure clinoenstatite and pure clinoferrosilite are given by

$$\delta\bar{G}^c = \bar{G}^c - X_M^c\ \bar{G}_M^c - X_F^c \bar{G}_F^c = RT(X_M^c \ln X_M^c + X_F^c \ln X_F^c) \quad , \tag{4a}$$

$$\delta\bar{G}^o = \bar{G}^o - X_M^o\ \bar{G}_M^c - X_F^o\ \bar{G}_F^c$$

$$= X_M^o(T_M - T)\Delta\bar{S} + X_F^o(T_F - T)\Delta\bar{S} + RT(X_M^o \ln X_M^o + X_F^o \ln X_F^o) \quad . \tag{4b}$$

OP and CP compositions coexisting at equilibrium under hydrostatic pressure are given by the rule of common tangent to the two curves (4a) and (4b) (eg. Gordon, 1968, pp. 75-78):

$$X^o/X^c = \exp\left[\frac{\Delta\bar{S}}{R}(1 - T_F/T)\right] \quad , \tag{5a}$$

$$(1-X^o)/(1-X^c) = \exp\left[\frac{\Delta\bar{S}}{R}(1 - T_M/T)\right] \quad , \tag{5b}$$

where $X^o = X_F^o = 1 - X_M^o$ and $X^c = X_F^c = 1 - X_F^c$. Figure 1 shows the corresponding phase diagram for the numerical values assumed.

EQUILIBRIUM UNDER AN APPLIED SHEAR STRESS

Preliminary considerations

Equilibrium between OP and CP under stress, like the one between cryptoperthite lamellae in Chapter 3, could be better described as the equilibrium

of their common, coherent interface with respect to migration. Thus a CP lamella is in equilibrium only if all the coherent boundaries bounding it satisfy the equilibrium conditions demonstrated in Chapter 2. When a uniform stress is applied on the composite crystal, only infinite parallel boundaries can in fact be in equilibrium everywhere; indeed all the parameters in the equation expressing equilibrium (Chapter 2, Eq. 18b) then maintain a constant value everywhere, and the equilibrium condition, if satisfied, is satisfied everywhere.

Electron micrographs (Coe and Müller), show that CP lamellae are indeed very large compared to their thickness. They are in that respect much closer to ideal lamellae than the cryptoperthite lamellae examined in Chapter 3; this is no doubt a consequence of the much larger transformation strain. For the principle, however, it is important to remember that equilibrium is not obtained in the 'end regions'.

A portion of coherent interface between OP and CP is represented schematically in Figure 2. The resolved shear stress τ on (100)[001] is, by definition, the component along the c direction of the shear stress on (100) . By convention τ may be considered positive when it is oriented in the sense shown in Figure 2a, and therefore when 'it favors' the CP phase. On the other hand a negative value of τ , in Figure 2a , would 'favor' the OP phase. However, for one orientation of the orthopyroxene there are two clinopyroxenes possible; in Figure 2b a negative τ 'favors' the CP phase. Consequently any non-zero resolved shear stress favors one of the two possible CP over the OP phase. Only positive values of τ need therefore be considered.

Equilibrium conditions

Equation 18 of Chapter 2 can be rewritten

$$(\bar{E}^c - T\bar{S}^c + P\bar{V}^c)-(\bar{E}^o - T\bar{S}^o + P\bar{V}^o + \tau\bar{V}\tan\psi) = \mu(X^c - X^o) \quad . \tag{6}$$

It is shown in the Appendix that, because the finite transformation strain is large compared to any elastic strain, (6) simplifies to

$$\bar{G}^c - (\bar{G}^o + \tau\bar{V}\tan\psi) = \mu(X^c - X^o) \quad , \tag{7}$$

where $\bar{G}^c$ and $\bar{G}^o$ are the Gibbs energies of OP and CP having the same compositions, at the same temperature T, but under a hydrostatic pressure equal to the normal component of compressive stress, P, acting on the boundaries. The Appendix also shows that the chemical potential of the fluid component, as defined by Gibbs (1906, Eq. 467) or in Chapter 2 (Eq. 17), is also equal to

$$\mu^c = \left(\frac{\partial\bar{G}^c}{\partial X^c}\right)_{P,T} \quad \text{and} \quad \mu^o = \left(\frac{\partial\bar{G}^o}{\partial X^o}\right)_{P,T} \quad . \tag{8}$$

Equation 6 and the implicit additional equilibrium condition, $\mu = \mu^c = \mu^o$, therefore amount to a rule of common tangent to the curves $\bar{G}^c$ and $(\bar{G}^o + \tau\bar{V}\tan\psi)$, or, equivalently, to the curves $\delta\bar{G}^c$ and $(\delta\bar{G}^o + \tau\bar{V}\tan\psi)$. $\delta\bar{G}^c$ and $\delta\bar{G}^o$ are given by Equations 4a and b, and therefore

$$\delta\bar{G}^c = RT(X_M^c \ln X_M^c + X_F^c \ln X_F^c) \quad , \tag{9a}$$

$$\delta\bar{G}^o + \tau\bar{V}\tan\psi = X_M^o\left[\frac{\tau\bar{V}\tan\psi}{\Delta\bar{S}} + T_M - T\right]\Delta\bar{S} + X_F^o\left[\frac{\tau\bar{V}\tan\psi}{\Delta\bar{S}} + T_F - T\right]\Delta\bar{S}$$

$$+ RT(X_M^o \ln X_M^o + X_F^o \ln X_F^o) \quad . \tag{9b}$$

Equation 9b differs from 4b only in that T_M and T_F are respectively replaced by

$$T_M' = T_M + \frac{\tau\bar{V}\tan\psi}{\Delta\bar{S}} \tag{10a}$$

and

$$T_F' = T_F + \frac{\tau\bar{V}\tan\psi}{\Delta\bar{S}} \quad . \tag{10b}$$

In other words, the phase diagram in presence of a constant resolved shear stress τ is identical to that of a 'hydrostatic' reaction between two ideal solutions having the same entropy difference, $\Delta\bar{S}$, but having transition temperatures for the pure end-members higher by $\frac{\tau\bar{V}\tan\psi}{\Delta\bar{S}}$. For the end members the transition does not involve the fluid component; the above rise in temperature is indeed the same as the one established by Coe (1970; see also Chapter 2, Eq. 28) for one-component systems.

For τ = 1 kbar and the numerical values assumed earlier, Equations 10 give

$$T'_M = 849 + 177 = 1026K = 753^oC \quad ,$$

and $$T'_F = 1073 + 177 = 1250K = 977^oC \quad .$$

The corresponding phase diagram is shown in Figure 1 (dashed curve). The two-phase field for equilibrium under the shear stress τ is somewhat narrower than for hydrostatic equilibrium, and the two diagrams are therefore not exactly related by a translation of 177^o. Because of the temperature rise, $\Delta\bar{S}$ may also deviate from the constant value assumed; the narrowing of the two-phase field noted above may in fact be insignificant in comparison with changes due to these variations in $\Delta\bar{S}$.

Rapid strain

When the strain is applied rapidly, diffusion of cations may not be possible. The transition is then purely displacive and another, shorter term equilibrium may be reached. Instead of the requirement that the chemical potential of a fluid component be the same in both phases, the new constraint is that

$$X^o = X^c = X \quad . \tag{11}$$

Equilibrium is then given by

$$\delta\bar{G}^c = \delta\bar{G}^o + \tau\bar{V}\tan\psi \quad ,$$

or, using (9a,b) and (11) ,

$$T = T_M + X(T_F - T_M) + \frac{\tau \bar{V} \tan\psi}{\Delta \bar{S}} \quad , \tag{12a}$$

or

$$T = T'_M + X(T'_F - T'_M) \quad . \tag{12b}$$

The equilibrium temperature for the displacive transition under a resolved shear stress τ is therefore a linear function of composition; it is represented in Figure 1 (dotted line) . In effect there is no longer a fluid component; (12) could also be obtained from Coe's result if we imagine that the hydrostatic two-phase field is replaced by a straight, single-line displacive transition boundary.

DISCUSSION

Choice of $\Delta \bar{S}$

The value of 1 cal mol^{-1} deg^{-1} assumed for the entropy difference between OP and CP is probably a maximum value; the real value could just as well be 0.2 cal mol^{-1} deg^{-1} or less. Everything else being maintained equal, one consequence of a smaller value for $\Delta \bar{S}$ is a narrowing of the two-phase field. For example at the median temperature between T_F and T_M the composition difference between CP and OP is given to a very good first-order approximation, by

$$|\Delta X_{med}| = (X^c - X^o)_{med} \simeq \frac{1}{2} \frac{\Delta \bar{S}}{R} \frac{T_F - T_M}{T_F + T_M} \tag{13}$$

(T_F and T_M must be replaced by T'_M and T'_F when $\tau \neq 0$) . Thus, for $\Delta \bar{S}$ = 1 cal mol^{-1} deg^{-1} , (13) gives at $\tau = 0 (T_{med} = 961K)$: $|\Delta X_{med}|$ = 2.93 mol% ; at τ = 1 kbar (T_{med} = 1138K): $|\Delta X_{med}|$ = 2.47 mol% . By contrast, for $\Delta \bar{S}$ = 0.2 cal mol^{-1} deg^{-1}, (13) gives,

for $\tau = 0$: $|\Delta X_{med}| = 0.59$ mol% ;

for $\tau = 1$ kbar : $|\Delta X_{med}| = 0.49$ mol% .

If $\Delta\bar{S}$ were smaller, composition differences between coexisting lamellae would become difficult to detect (J.C. Rucklidge, U. of Toronto, personal communication); in practice the transition would then be undistinguishable from a purely displacive one.

If $\Delta\bar{S}$ is smaller than 1 cal mol^{-1} deg^{-1} another consequence is that a same shear stress τ 'raises' the phase diagram by a larger amount (Eqs. 10a, b) . Thus, for $\Delta\bar{S} = 0.2$ cal mol^{-1} deg^{-1} , a resolved shear stress of only 200 bars raises the phase diagram by the same 177^{o} .

The rise in temperature of the OP-CP equilibrium under an applied shear stress could in fact be used to estimate $\Delta\bar{S}$. In a series of experiments mentioned earlier W. Durham (1974, personal communication) applied axial stresses on orthoenstatite crystals at about $1320^{o}C$. The resolved shear stress reached 975 bars in Runs 7308P-8 and 7308P-10 , and went as high as 1165 bars in 7308P-9 ; failure of the pistons generally terminated the runs. No permanent strain could be detected (within 0.1%) in 7308P-8 and 10 ; a small (0.2%) strain was measured in 7308P-9. Some lamellae, tentatively identified as CP, were observed in cursory TEM examinations.

At $1300^{o}C$ Kirby and Coe (1974) annealed CP lamellae out of their crystals in times as short as 2 minutes; complete disappearance of CP was even obtained at $1100^{o}C$. Therefore, in view of the temperature and duration of Durham's runs it may perhaps be assumed that the lamellae he observed were in approximate equilibrium under the highest shear stress applied. Taking $600^{o}C$ as the temperature of hydrostatic equilibrium (very uncertain because of the unknown Ca content of the samples) the following equality must then

have been approximately satisfied[3] :

$$\frac{\tau \bar{V} \tan\psi}{\Delta \bar{S}} \approx 1320^{o} - 600^{o} = 700^{o} \qquad (14)$$

or, for τ = 1000 bars,

$$\Delta \bar{S} = 10.3 \text{ bar cm}^3 \text{ mol}^{-1} \text{ deg}^{-1} = 0.25 \text{ cal mol}^{-1} \text{ deg}^{-1} \quad .$$

Equation 14 is crude in that it relies on the assumption that $\Delta \bar{S}$ is independent of temperature; the principle underlying it remains valid however.

Generalizations

The theoretical development presented above can be extended to less simple assumptions if further data so require. Even for ideal solutions, the entropy difference $\Delta \bar{S}$ may not be the same for the two end-members; this is easily taken into account by appropriate substitutions of $\Delta \bar{S}_F$ and $\Delta \bar{S}_M$ to $\Delta \bar{S}$ in Equations 9b, 10a and 10b . The approximate translation of the phase diagram to higher temperature becomes a linear function of composition instead of being uniform.

A more drastic generalization is when the solutions are no longer assumed to be ideal. Figure 3 illustrates a hypothetical phase diagram with a maximum. A resolved shear stress τ should again result in 'raising' the two-phase field. The single line corresponding to the rapid (diffusionless) shear-induced transformation is always within the two-phase field. Analytically, excess energy

---

[3] It may be argued instead that Durham's runs were well into the stability field of CP under shear stress but that most of the CP was annealed out (and the associated strain recovered) at the end of the run, between removal of the axial load and lowering of the temperature.

and entropy terms can simply be added to Equations 9a, b in the same way they would be added to Equations 4a, b .

The generalization to several fluid components is also straightforward in principle. Indeed the calcium content of pyroxenes can also vary without disruption of the silicate framework (see Chapter 4). Compositions of ternary pyroxenes can be written for instance $(Fe_2Mg_{-2})_X(CaMg_{-1})_Y.Mg_2Si_2O_6$; X and Y are mole fractions of the fluid components (subject to the following limits: $0 \leq X$, $0 \leq Y \leq 1$, $2X + Y \leq 2$) . In the theoretical development $\mu(X^c - X^o)$ must then be replaced by $\mu^x(X^c - X^o) + \mu^y(Y^c - Y^o)$, and the analysis of equilibrium for binary systems must be replaced by that for ternary ones (eg. Gibbs, 1906, pp.63-134) . The qualitative result would remain that a resolved shear stress τ raises the temperature of stability of the monoclinic-pyroxene.

As discussed earlier there is some question as to whether the composition difference, $(X^c - X^o)$, could be detected in practice in the binary Enstatite-Ferrosilite joint. On the other hand there is no doubt that coexisting pigeonite and orthopyroxene have significantly different compositions; detection of the higher Calcium content of 'shear-induced pigeonite lamellae' compared to the orthopyroxene host should thus be easier.

Applications

The theory developed in this paper suggests the intriguing possibility of exploring some equilibrium phase diagrams at temperatures significantly higher than for hydrostatic equilibrium! Differences with classical hydro-thermal runs lie in the use of uniaxial or triaxial equipment on oriented single crystals of sufficient size. In addition to X-ray diffraction, the results can be studied by microprobe analysis, optical and electron microscopy, and electron diffraction.

A crude analysis can give us an idea of when such 'nonhydrostatic runs' may become advantageous. Uniaxial or triaxial experiments are more delicate than hydrothermal runs; they require in particular a constant supervision. Consequently their duration cannot exceed say 6 hours in practice, as opposed to the 100 days or so which are possible in hydrothermal runs (time ratio = 1/400). If the kinetics of the reaction were controlled in both sets of conditions by a same, simply activated process having an Arrhenius energy E_o, nonhydrostatic runs would progress more than hydrostatic ones if

$$\frac{E_o}{R}\left(\frac{1}{T_H} - \frac{1}{T_S}\right) \geq \ln 400 \quad ;$$

(H : hydrostatic ; S : 'stressed') .

Taking T_H = 850K (≈ 580°C , as near the Mg-end of the OP-CP diagram) and E_o = 50 kcal mol^{-1} , nonhydrostatic runs would become more efficient than hydrostatic ones if $T_S \geq$ 1070K (≈ 800°C) . This temperature, in turn, requires that the crystal be able to support a resolved shear stress of 250 bars, if $\Delta\bar{S}$ = 0.2 cal mol^{-1} deg^{-1} , or of 1250 bars if $\Delta\bar{S}$ = 1 cal mol^{-1} deg^{-1} .

Clearly such 'quantitative' analysis is very questionable, because of its many implicit or explicit assumptions, and of the arbitrary value given to E_o ; it shows however that the possibility of 'nonhydrostatic runs' should perhaps not be hastily discarded. In fact, the estimate of $\Delta\bar{S}$ from W. Durham's uniaxial experiments already is a preliminary exploration of the OP-CP equilibrium.

IS CLINOPYROXENE A STRESS MINERAL ?

A. Harker (1939, p.150) defined a stress mineral as a mineral phase for which "... the introduction of a shearing stress as an additional condition causes an extension of the [stability] field ..." The extension of the CP

stability field by the shear stress τ (Figure 1) therefore appears to be a sufficient theoretical demonstration of the validity of Harker's concept. However many of the physical constraints in the 'coherent reaction' studied here strongly restrict the meaning of a 'stability field' . Let us recall them.

1. The most fundamental assumption, one which must always be made when considering the stability of any solid under stress is the assumption of solid behavior. Implications of this assumption follow from Gibbs' original analysis and have been examined in Chapter 2. Briefly, it is only because the migration of a 'solid component' of the pyroxene through the pyroxene framework is not considered possible that the state reached can be referred to as one of equilibrium. If it were not for the existence of that solid component any stressed solid would be fundamentally unstable. A practical consequence of the existence of the solid component has been that only chemical potentials corresponding to the fluid components were defined (and held to be constant throughout the system at equilibrium). This is in direct contradiction to the usual criterion of chemical equilibrium during metamorphism, which is that chemical potentials for all chemical components present maintain a constant value in the system (see Turner and Verhoogen, 1960, p.16) at least locally (see Thompson, 1959). In conclusion therefore, there is no stability field of a stressed mineral phase under the usual assumptions made by the metamorphic petrologist.

2. As was also discussed earlier, the OP-CP equilibrium under stress refers only, strictly speaking, to the equilibrium of parallel coherent interfaces. That is, CP under stress is stable only to the extent that it indeed exists as infinitely large and thin lamellae; like the cryptoperthite lamellae of Chapter 3, the 'end-regions' are not in equilibrium. This fact

restricts even further the meaning of 'stable phase'.

3. Finally, Harker (1939, p.150) referred to a 'measure of shearing stress' and apparently considered that such measure, like hydrostatic pressure, would be an intensive parameter, the same for the whole rock. In the present study, the 'measure of shearing stress' which affects the equilibrium is the resolved shear stress on (100)[001] . Now let us consider for example a rock submitted to a differential stress σ_D = 1 kbar and assume that each pyroxene crystal is under the same uniform stress. For the simple case where the pyroxene grains are randomly oriented with respect to the stress field, the resolved shear stress τ reaches its maximum value of 500 bars in only a vanishingly small proportion of the crystals; instead the value of τ varies among crystals from 0 to 500 bars; there is therefore no unique OP-CP equilibrium diagram in a rock under a given differential stress σ_D .

It is clear from the above restrictions that chemical equilibrium under stress, this new chemistry called for by Harker (1939, p.146; see Chapter 1), differs more from the classical chemistry than Harker himself probably imagined.

APPENDIX : EQUILIBRIUM OF A COHERENT INTERFACE WHEN THE TRANSFORMATION STRAIN IS FINITE , THE ELASTIC STRAINS ARE INFINITESIMAL AND ONE CHEMICAL COMPONENT IS FLUID .

For one fluid component, the equilibrium condition (Chapter 2, Eq. 18b) becomes

$$(\bar{E}^c - T\bar{S}^c + P\bar{V}^c)-(\bar{E}^o - T\bar{S}^o + P\bar{V}^o) - \tau_i\gamma_i = \mu(X^c - X^o) \quad , \tag{A1}$$

where, it is recalled, γ_i is the tangential component of the characteristic vector v_i , and τ_i the shear stress component on the interface (Figure A1). If coordinates are chosen such that the 1-axis is perpendicular to the interface the scalar product reduces to (matrix notation: $\tau_2 = \sigma_{21} = \sigma_6$, $\tau_3 = \sigma_{31} = \sigma_5$)

$$\tau_i \gamma_i = \sigma_6 \gamma_2 + \sigma_5 \gamma_3 \quad .$$

Let us call $\gamma_{2,o}$, $\gamma_{3,o}$ the components of γ_i at the same temperature but under a hydrostatic pressure P alone. In presence of a shear stress along (001) the components of γ_i become

$$\gamma_2 = \gamma_{2,o} + \bar{V}^c \varepsilon_6^c - \bar{V}^o \varepsilon_6^o \quad , \tag{A2a}$$

$$\gamma_3 = \gamma_{3,o} + \bar{V}^c \varepsilon_5^c - \bar{V}^o \varepsilon_5^c \quad , \tag{A2b}$$

where ε_5^o , ε_6^o , ε_5^c and ε_6^c are components of elastic strain corresponding to the shear stress. Equation A1 can therefore be rewritten

$$\left[\bar{E}^c - T\bar{S}^c + P\bar{V}^c - \bar{V}^c(\sigma_5\varepsilon_5^c + \sigma_6\varepsilon_6^c)\right] \tag{A3}$$

$$- \left[\bar{E}^o - T\bar{S}^o + P\bar{V}^o - \bar{V}^o(\sigma_5\varepsilon_5^o+\sigma_6\varepsilon_6^o)\right]-(\sigma_6\gamma_{2,o}+\sigma_5\gamma_{3,o}) = \mu(X^c-X^o) \quad .$$

The chemical potential has been defined by the variational equation (Gibbs' Equation 467, or Chapter 2, Eq. 17)

$$\delta\bar{E} = T\,\delta\bar{S} + \bar{V}\,\sigma_i\delta\varepsilon_i + \mu\delta X \ ,$$

$$\text{or} \quad \delta\bar{E} = T\,\delta\bar{S} - P\,\delta\bar{V} + \bar{V}\sum_{i=2}^{6}\sigma_i\delta\varepsilon_i + \mu\delta X \ . \tag{A4}$$

Let us call $\bar{C}^c$ and $\bar{C}^o$ the bracketed quantities in (A3) :

$$\bar{C} = \bar{E} - T\bar{S} + P\bar{V} - \bar{V}(\sigma_5\varepsilon_5 + \sigma_6\varepsilon_6) \quad .$$

At constant T , P , σ_5 and σ_6, a variation of $\bar{C}$ is , using (A4) ,

$$\delta\bar{C}\Big|_{P,T,\sigma_5,\sigma_6} = \mu\delta X + \bar{V}(\sigma_2\delta\varepsilon_2 + \sigma_3\delta\varepsilon_3 + \sigma_4\delta\varepsilon_4) \quad .$$

However, the constraint of coherency imposes

$$\delta\varepsilon_2 = \delta\varepsilon_3 = \delta\varepsilon_4 = 0 \quad ,$$

and therefore

$$\mu = \left(\frac{\partial\bar{C}}{\partial X}\right)_{P,T,\sigma_5,\sigma_6,\ \text{coherency}} \ . \tag{A5}$$

Let $\bar{G}$ be the Gibbs energy of the same phase at the same temperature T and under a hydrostatic pressure P .

$$\bar{C} = \bar{G} + \Delta\bar{F}^{el} + P\ \Delta\bar{V} - \bar{V}(\sigma_5\varepsilon_5 + \sigma_6\varepsilon_6) \ , \tag{A6}$$

where, like in Chapter 2, $\Delta\bar{F}^{el}$ and $\Delta\bar{V}$ are the molar Helmholtz elastic strain energy and molar elastic volume change corresponding to the application of the shear stress. As argued in Chapter 2, the last three terms in (A6) are very small compared to $(\sigma_6\gamma_{2,0} + \sigma_5\gamma_{3,0})$ and their differences for the two phases are likely to be even smaller; consequently, to a good approximation

$$\bar{C}^c - \bar{C}^o - \tau_i \gamma_{i,o} \simeq \bar{G}^c - \bar{G}^o - \tau_i \gamma_{i,o} \quad .$$

The last three terms in (A6) are not only very small, they are also likely to vary very little with composition. Therefore

$$\mu = \left(\frac{\partial \bar{C}}{\partial X}\right)_{P,T,\sigma_5,\sigma_6} \simeq \left(\frac{\partial \bar{G}}{\partial X}\right)_{P,T} \quad . \qquad (8)$$

References

COE, R.S. (1970) The thermodynamic effect of shear stress on the ortho-clino inversion in enstatite and other coherent phase transitions characterized by a finite simple shear. Contr. Mineral. Petrol. 26, 247-264.

_____, and W.F. MÜLLER (1973) Crystallographic orientation of clino-enstatite produced by deformation of orthoenstatite. Science 180, 64-66.

GIBBS, J.W. (1906) The collected works of J. Willard Gibbs, Ph.D., Ll.D. Vol. I, Thermodynamics. Longmans Green, and Co., New-York, 434 p.

GORDON, P. (1968) Principles of phase diagrams in materials systems. McGraw-Hill Book Co., New York, 232 p.

GROVER, J. (1972) The stability of low-clinoenstatite in the system $Mg_2Si_2O_6$-$CaMgSi_2O_6$. Amer. Geophys. Union Trans.(Abstracts) 53, 539.

HARKER, A. (1939) Metamorphism. Methuen and Co. Ltd., London, 362 p.

KIRBY, S.H., and R.S. COE (1974) The rôle of crystal defects in the enstatite iversion. Amer. Geophys. Union Trans. (Abstracts) 55, 419.

KUNO, H. (1966) Review of pyroxene relations in terrestrial rocks in the light of recent experimental work. Mineral. J. [Tokyo] 5, 21-43.

SMITH, J.V. (1969) Crystal structure and stability of the $MgSiO_3$ polymorphs; physical properties and phase relations of Mg,Fe pyroxenes. Mineral. Soc. Amer. Spec. Paper 2, 3-29.

TURNER, F.J., and J. VERHOOGEN (1960) Igneous and metamorphic petrology, second edition. McGraw-Hill Book Co., Inc., New York, 694 p.

THOMPSON, J.B., Jr., (1959) Local equilibrium in metasomatic processes. In Researches in geochemistry (ed. P.H. Abelson), J. Wiley & Sons, Inc., New York, 427-457.

VIRGO, D. and S. HAFNER (1970) Fe^{2+},Mg order-disorder in natural orthopyroxenes. Amer. Mineral. 55, 201-223.

FIGURE CAPTIONS

FIG. 1. Theoretical equilibrium phase diagram between orthopyroxene and clinopyroxene ($P2_1/\underline{c}$) along the enstatite-ferrosilite joint. Ideal solution is assumed in both phases; the assumed entropy difference and transition temperatures for the end-members are given in the text. The lower temperature diagram corresponds to equilibrium under hydrostatic conditions. The upper diagram (dashed lines) corresponds to equilibrium under a resolved shear stress τ = 1 kbar. The dotted line is the displacive transition line corresponding to rapid strain and absence of cation diffusion (see text).

FIG. 2. Schematic representation of an orthopyroxene (OP) - clinopyroxene (CP) interface. There are two possible CP which can develop coherently from one OP ; as a result, any resolved shear stress τ always 'favors' one of the two possible CP over the OP .

FIG. 3. Hypothetical phase diagram showing a possible equilibrium between two non-ideal solutions. As in Figure 1, a resolved shear stress τ raises the equilibrium temperatures.

FIG. A1. Schematic representation of coherent interface between OP and CP . The transformation strain is large and not assumed to be a simple shear in this appendix. γ_i is the tangential component of the characteristic vector, $\mathbf{v}_i$. Its absolute value is $\gamma = \bar{V}^C \tan\psi$. When the strain is a simple shear $\bar{V}^C = \bar{V}^O = \bar{V}$ and therefore $\gamma = \bar{V} \tan\psi$.

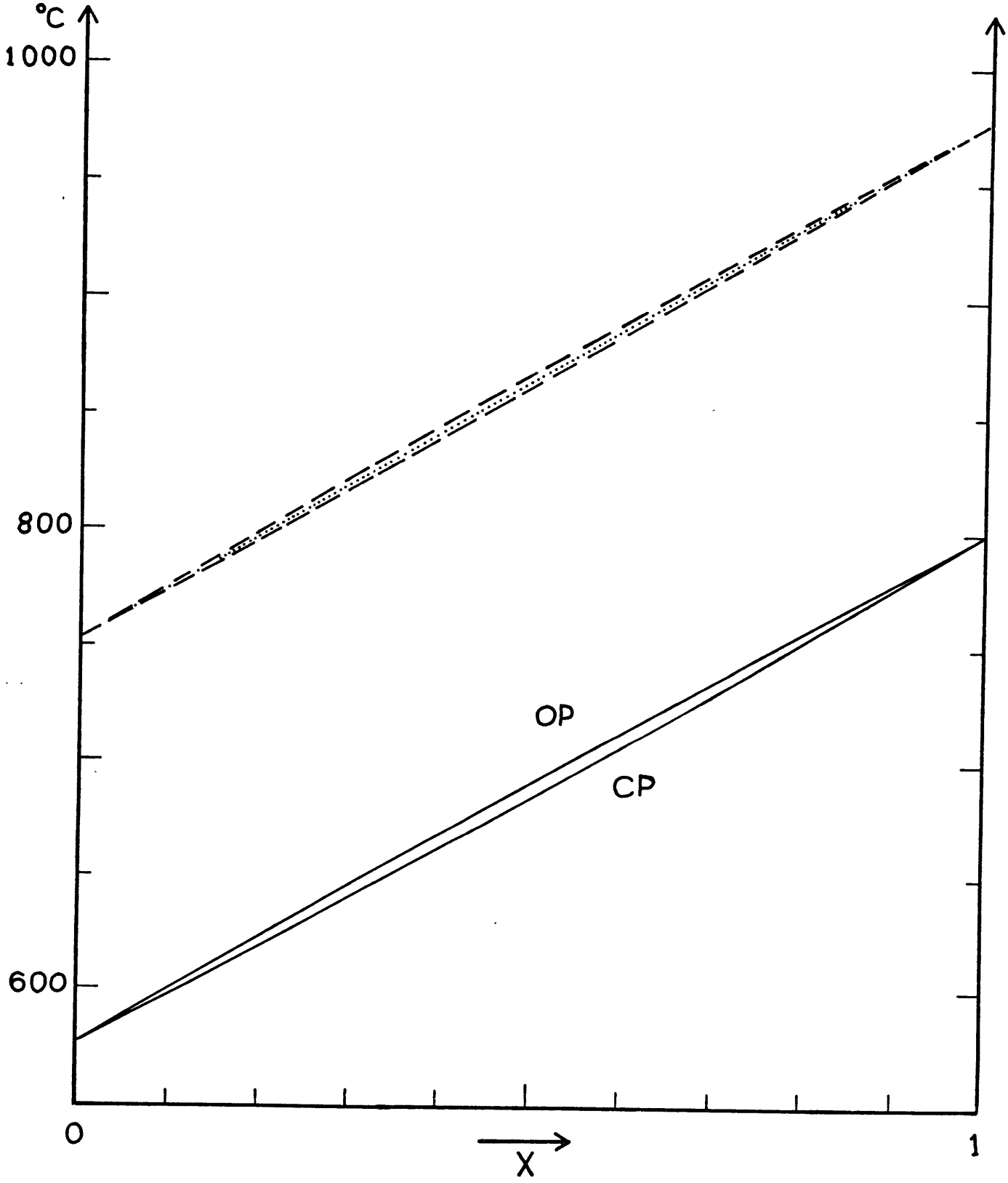

Fig. 1

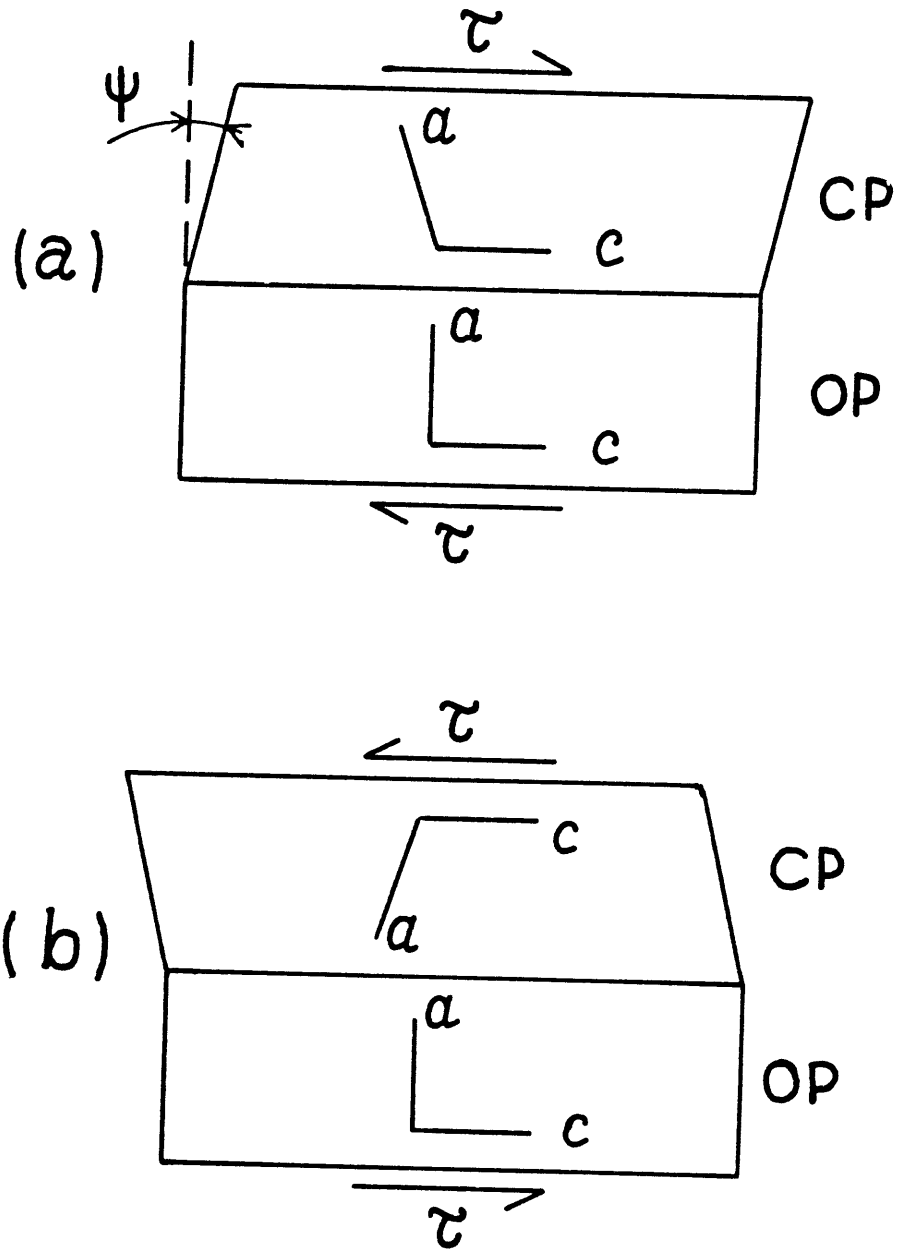

Fig.2

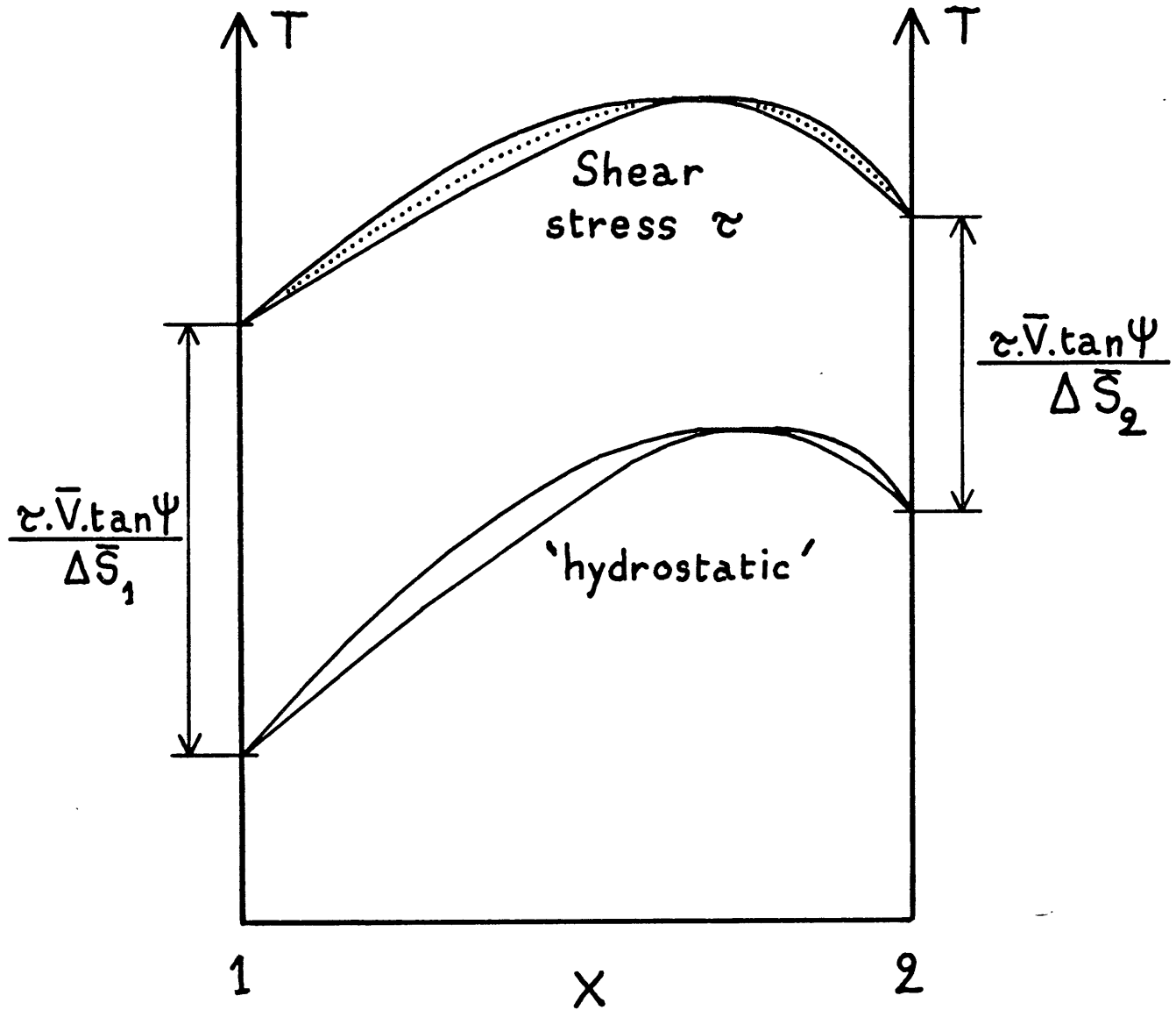

Fig. 3

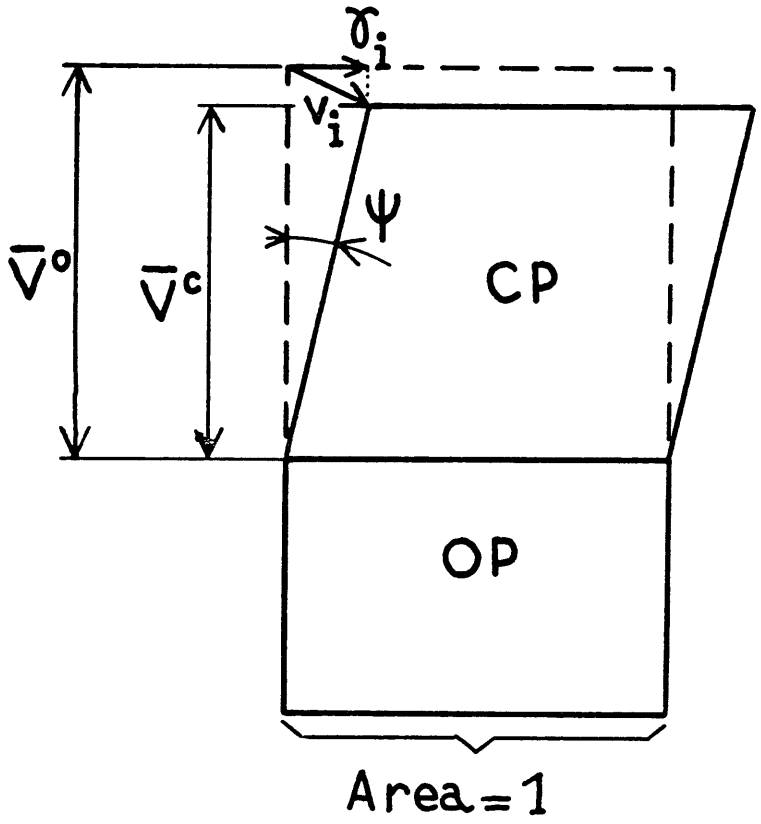

Fig. A1

CHAPTER 6

NONHYDROSTATIC STRESS AND 'THERMODYNAMIC PRESSURE'

INTRODUCTION

It was demonstrated in Chapters 2 and 5 that equilibrium of a solid under stress requires restrictions on possible transports of chemical components, and that these restrictions contradict the equilibrium criteria normally taken by petrologists. The argument, expressed in terms of solidity or fluidity of components, may look abstract and too indirect. The temptation is thus strong to ask the following question:

> Consider a transformation $\alpha \longleftrightarrow \beta$ which is in equilibrium at a temperature T_o and a hydrostatic pressure P_o. If a nonhydrostatic stress is applied, at the same temperature T_o, what values of stress components maintain the equilibrium?

The answer which is the most often given to that question (e.g. Turner and Verhoogen, 1960, pp. 474 - 477) can be stated as follows:

> Equilibrium is obtained when

$$\frac{1}{3}(P_1 + P_2 + P_3) = P_o \quad , \tag{1a}$$

> where P_1, P_2 and P_3 are principal components of compressive stress.

As a result $\frac{1}{3}(P_1 + P_2 + P_3)$ is sometimes called the 'thermodynamic pressure' in the stressed rock. For our purpose (1a) can be rewritten

$$\Delta P_1 + \Delta P_2 + \Delta P_3 = 0 \quad , \tag{1b}$$

where $\Delta P_i = P_i - P_o$.

An alternative answer suggested by some authors (see Brace et al, 1970)

is

$$P_1 = P_o \quad , \tag{2a}$$

$$\text{or } \Delta P_1 = 0 \quad , \tag{2b}$$

where P_1 is the maximum compressive stress.

In this chapter it is shown that the above question has no unique answer. Further specifications must be added; the answer depends on which specifications are so chosen. Some of the results are also used in a discussion of preferred orientations in monomineralic aggregates.

EQUILIBRIA BETWEEN TWO LINEARLY ELASTIC PHASES.

The example used for the demonstration is a first-order, reconstructive, transition[1] in a one-component system: $\alpha \longleftrightarrow \beta$. Elastic strains are assumed infinitesimal and linear functions of stresses. Equilibrium at T_o, P_o is expressed by

$$\bar{F}^{\alpha,0} + P_o \bar{V}^{\alpha,0} = \bar{F}^{\beta,0} + P_o \bar{V}^{\beta,0} \tag{3}$$

where $\bar{F}$ and $\bar{V}$ denote molar Helmholtz energy and volume respectively.

Let us therefore consider a rectangular parallelepiped of one phase, say α, submitted to pressures P_1, P_2, P_3 by fluids acting on its faces (Figure 1a). As Gibbs (1906) showed (see Chapter 2 for a review), α will neither grow from, nor dissolve into, the fluids if the chemical potential of the component of the solid is given in each fluid by

---

[1] A coherent transition would correspond to quite different constraints and is specifically excluded in this chapter. The effect of a stress on a coherent transition has been treated in Chapters 2 and 5 and also by Garland (1964) and Coe and Paterson (1969).

$$\mu_1^\alpha = \bar{F}^\alpha + P_1 \bar{V}^\alpha \quad , \tag{4a}$$

$$\mu_2^\alpha = \bar{F}^\alpha + P_2 \bar{V}^\alpha \quad , \tag{4b}$$

$$\mu_3^\alpha = \bar{F}^\alpha + P_3 \bar{V}^\alpha \quad . \tag{4c}$$

These equations can be rewritten

$$\mu_k^\alpha = \bar{F}^{\alpha,0} + P_o \bar{V}^{\alpha,0} + \Delta\bar{F}^\alpha + P_o \Delta\bar{V}^\alpha + \Delta P_k \bar{V}^{\alpha,0} + \Delta P_k \Delta\bar{V}^\alpha \ , \quad k = 1, 2 \text{ and } 3 \ , \tag{4d}$$

where $\Delta\bar{F}$ and $\Delta\bar{V}$ are respectively the changes in Helmholtz energy and volume of a mole when the stress is changed from P_o to P_1, P_2, P_3 at constant temperature T_o.

As Gibbs noted, μ_1^α, μ_2^α and μ_3^α are always higher than the chemical potentials necessary for equilibrium of α under hydrostatic pressure P_1, P_2 or P_3 respectively. Values given by (4) are therefore maintained in the fluids only if nucleation and growth of α in each fluid does not occur.

Choosing axes perpendicular to the faces of the parallelepiped, the longitudinal components of strain are, from Hooke's law,

$$\varepsilon_i^\alpha = - \sum_j s_{ij}^\alpha P_j \quad , \tag{5}$$

where: $i = 1, 2$ and 3, the summation is over $j = 1$ to 3, and s_{ij} are the matrix components of isothermal compliance (see Nye, 1957). The Helmholtz strain energy added to the crystal from P_o to the stressed state is

$$\Delta\bar{F} = \bar{V}^{\alpha,0} \sum_i \sum_j (P_o + \frac{1}{2} \Delta P_i) s_{ij}^\alpha \Delta P_j \quad . \tag{6}$$

The change in volume is

$$\Delta\bar{V} = - \bar{V}^{\alpha,0} \sum_i \sum_j s_{ij}^\alpha \Delta P_j \quad . \tag{7}$$

Using (6) and (7) , (4d) can be rewritten

$$\mu_k^\alpha = \bar{F}^{\alpha,0} + P_o \bar{V}^{\alpha,0} + \bar{V}^{\alpha,0} \left[\Delta P_k + \sum_i \sum_j \left(\frac{\Delta P_i}{2} - \Delta P_k \right) s_{ij}^\alpha \Delta P_j \right] \quad . \quad (8)$$

If $\Delta P_1 = \Delta P_2 = \Delta P_3$, (8) becomes

$$\mu^\alpha = \bar{F}^{\alpha,0} + P_o \bar{V}^{\alpha,0} + \bar{V}^{\alpha,0} \Delta P_1 \left(1 - \frac{\Delta P_1}{2K^\alpha} \right) \quad , \quad (9)$$

where K^α is the bulk modulus $\left(\frac{1}{K^\alpha} = \sum_i \sum_j s^\alpha{}_{ij} \right)$. The same equations can be written for β .

Several equilibria can now be envisaged. In Figure 1b for example, α is under stress whereas β is under hydrostatic pressure P_1 . This configuration may be a crude equivalent of the situation in which a new phase β has just appeared and is somehow 'sheltered' from the nonhydrostatic stress supported by α . For α and β to be in equilibrium with the fluid, there must be $\mu_1^\beta = \mu^\alpha$. Using (3) , (8), and (9) (transformed for β) , this equilibrium condition is

$$\bar{V}^{\beta,0} \Delta P_1 \left(1 - \frac{\Delta P_1}{2K^\beta} \right) - \bar{V}^{\alpha,0} \left[\Delta P_1 + \sum_i \sum_j \left(\frac{\Delta P_i}{2} - \Delta P_1 \right) s_{ij}^\alpha \Delta P_j \right] = 0 \quad . \quad (10)$$

This equilibrium condition is similar to (1b) or (2b) in that it is a relationship between the various principal components of stress. Other conditions are obtained by simply replacing ΔP_1 by ΔP_2 or ΔP_3 for when β is seeded instead in the second or the third fluid. Although similar these three conditions are not satisfied at the same time if ΔP_1 , ΔP_2 , $\Delta P_3 \neq 0$, and are in principle different if α is not isotropic.

Another possible equilibrium which will be studied in more detail is illustrated in Figure 1c ; α and β are both submitted to the same stress and are in contact through the fluid at P_1 . Equilibrium with respect to that fluid is obtained when

$$\bar{V}^{\alpha,0}\left[\Delta P_1 + \sum_i \sum_j \left(\frac{\Delta P_i}{2} - \Delta P_1\right) s_{ij}^{\alpha}\, \Delta P_j\right]$$

$$- \bar{V}^{\beta,0}\left[\Delta P_1 + \sum_i \sum_j \left(\frac{\Delta P_i}{2} - \Delta P_1\right) s_{ij}^{\beta}\, \Delta P_j\right] = 0 \qquad (11)$$

To get an idea of the practical significance of condition 11 , α and β are now assumed to be both elastically isotropic, with a same Poisson's ratio $\nu = \frac{1}{4}$. For further simplification let us make $\Delta P_2 = \Delta P_3$. Equation 11 reduces to

$$(\bar{V}^{\alpha,0} - \bar{V}^{\beta,0})\Delta P_1 + \frac{3}{4}\left(\frac{\bar{V}^{\alpha,0}}{E^{\alpha}} - \frac{\bar{V}^{\beta,0}}{E^{\beta}}\right)\Delta P_2(\Delta P_2 - 2\Delta P_1) = 0 \qquad . \qquad (12)$$

Now let α be the high-pressure phase, that is, α has a smaller molar volume; in general α also has a greater Young's modulus. For example we can take

$$\bar{V}^{\beta,0} = 1.10\ \bar{V}^{\alpha,0} \quad \text{and} \quad E^{\alpha} = 1.09\ E^{\beta} \qquad .$$

Condition 12 then becomes

$$\Delta P_1 + \frac{3}{2}\frac{\Delta P_2^{\,2}}{E^{\alpha} - 3\ \Delta P_2} = 0 \qquad . \qquad (13)$$

Therefore, given a value of ΔP_2 , always small compared to E^{α} , the equilibrium condition reduces to

$$\Delta P_1 \approx 0 \qquad . \qquad (14)$$

For example, taking $E^{\alpha} = 10^6$ bar and $\Delta P_2 = -100$ bar , $\Delta P_1 = -0.015$ bar! If $\Delta P_2 = -1$ kbar , $\Delta P_1 = -1.5$ bar . If, as in the two calculations above, P_1 is the maximum compressive stress, (14) is equivalent to (2b) . By contrast $(\Delta P_1 + \Delta P_2 + \Delta P_3)$ equals -67 bars and -667 bars respectively.

However, this equilibrium criterion only applies to the configuration of Figure 1c ; for that shown in Figure 1d it would be found that equilibrium

requires that $\Delta P_2 \approx 0$. Consequently it would be reasonable to take P_1 as the 'thermodynamic pressure' only if it can be shown (by some additional argument) that the reactions on the 2-faces can be ignored.

DISCUSSION

It is now possible to speculate on the conditions which a rock must satisfy for the above considerations to be applicable. Real mineral grains are clearly not rectangular parallelepipeds and no seals such as in Figure 1 exist along their edges. The fluid phase itself does not occur in large pockets but rather as thin films partially adsorbed along the grain boundaries.

However, it is conceivable that under mild temperatures the following conditions may be satisfied:

i) Crystals do not deform plastically under the applied stress.

ii) Chemical species which constitute the solid component of the reacting phases do not diffuse significantly either through the crystals themselves (Nabarro-Herring creep) or along the boundary layers (Coble creep). This constraint restricts the possible reaction to one in which the two minerals have the same composition, or at least share the same solid component; this justifies the choice of a one-component system in the analysis presented above.

iii) As briefly argued at the end of Chapter 2, sliding along incoherent grain boundaries is likely to occur much faster than any coupled solution-growth across it. It is therefore a fair assumption that one principal component of stress, P_1 , acts normal to a boundary between two reacting grains.

Subject to the latter boundary condition the stress-field in each grain must therefore be non-uniform if the rock is under stress. Principal stress

components P_2 and P_3 at points of two crystals on either side of a boundary have no reason to have the same value. The local equilibrium equation therefore becomes (see Equation 11)

$$\bar{V}^{\alpha,0}\left[\Delta P_1 + \sum_i \sum_j \left(\frac{\Delta P_i^{\alpha}}{2} - \Delta P_1\right) s_{ij}^{\alpha}\, \Delta P_j^{\alpha}\right] - \bar{V}^{\beta,0}\left[\Delta P_1 + \sum_i \sum_j \left(\frac{\Delta P_i^{\beta}}{2} - \Delta P_1\right) s_{ij}^{\beta}\, \Delta P_j^{\beta}\right] = 0 \qquad (15)$$

where all ΔP's vary along an interface, $\Delta P_2^{\alpha} \neq \Delta P_2^{\beta}$, $\Delta P_3^{\alpha} \neq \Delta P_3^{\beta}$, but $\Delta P_1^{\alpha} = \Delta P_1^{\beta} = \Delta P_1$.

Despite its theoretical variations along an interface, Condition 15 reduces in practice to

$$\Delta P_1 \approx 0 \quad , \qquad (16)$$

for the same reason that (12) reduced to (14) : for compliance moduli s_{ij} of the order of 10^{-5} to 10^{-6} bar^{-1} the summation terms within each bracket of (15) are negligible.

Therefore, as P_1 cannot be uniformly equal to P_o along the grain boundary if the rock is under stress, equilibrium is not reached in general. The high-pressure mineral, α, grows at the expense of β wherever $\Delta P_1 > 0$; β grows from α where $\Delta P_1 < 0$; it is only along discrete lines on the boundaries that $P_1 = P_o$ and no growth occurs.

For the rock as a whole it is difficult to decide what could be called 'equilibrium'. It could simply mean for example that the amounts of each mineral are maintained constant. Let us assume that the kinetics of growth of α and β are identical and isotropic. If the reacting grain boundaries are randomly oriented this 'equilibrium' would be reached approximately when

$$< P_1 > + < P_2 > + < P_3 > \approx P_o \quad , \qquad (17)$$

where $< P_i >$ are principal components of stress applied to the rock, as averaged over many grains. This is because the variable pressure P_1 normal to the boundaries would then approximately average to P_o. On the other hand, if all reacting grain boundaries were oriented approximately perpendicular to $<P_1>$ the 'equilibrium' would be reached for $< P_1 > \approx P_o$. (18)

Other possibilities, different assumptions would lead to yet other conditions. In truth, the difficulties encountered to define a 'thermodynamic pressure' all stem from the fact that there really is no metamorphic equilibrium under stress.

PREFERRED ORIENTATIONS IN MONOMINERALIC ROCKS.

In his theory of preferred orientations Kamb (1959) assumed that grain boundaries would be able to support shear stresses and that stresses were uniform in all grains. If it is accepted that in fact reacting grain boundaries are not likely to support any shear stress, Kamb's theory must be reviewed[2] .

Equilibrium Condition 15 can easily be applied to grains of a same mineral having different orientations. In this case $\bar{V}^{\alpha,0} = \bar{V}^{\beta,0}$, and hydrostatic equilibrium pressure P_o is arbitrary; it can conveniently be chosen as P_1 , and then $\Delta P_1 = 0$. Condition 15 thus reduces to

$$\frac{1}{2} s^{\alpha}_{22}(P_2{}^{\alpha} - P_1)^2 + \frac{1}{2} s^{\alpha}_{33}(P_3{}^{\alpha} - P_1)^2 + s^{\alpha}_{23}(P_2^{\alpha} - P_1)(P_3{}^{\alpha} - P_1)$$
$$= \frac{1}{2} s^{\beta}_{22}(P_2{}^{\beta} - P_1)^2 + \frac{1}{2} s^{\beta}_{33}(P_3{}^{\beta} - P_1)^2 + s^{\beta}_{23}(P_2{}^{\beta} - P_1)(P_3^{\beta} - P_1) \quad , \quad (19)$$

in which the two sets of compliance moduli are those calculated for the local coordinate system: 1-axis is perpendicular to the boundary, 2- and 3-axes are parallel to the other principal axes of stress (and are not necessarily the

---

[2] Kamb also assumed an equilibrium equation for the grain boundaries which the present author deems unfounded when shear stresses are acting on them. See Chapter 2.

same in the two grains). Condition 19 can of course also be obtained from Kamb's (1951) Equation 15.

If $P_2^{\alpha} = P_3^{\alpha} = P_2^{\beta} = P_3^{\beta}$, (19) reduces to

$$s_{22}^{\alpha} + s_{33}^{\alpha} + 2s_{23}^{\alpha} = s_{22}^{\beta} + s_{33}^{\beta} + 2s_{23}^{\beta} \quad . \tag{20}$$

Because equilibrium is clearly not met in general, the grain to grow is the one with the smallest value of $(s_{22} + s_{33} + 2s_{23})$, or, equivalently, the largest value of $(s_{11} + 2s_{12} + 2s_{13})$ (as $\sum_i \sum_j s_{ij} = \frac{1}{K}$ is invariant).

At most points on the boundaries, however, $P_2^{\alpha} \neq P_2^{\beta}$ and $P_3^{\alpha} \neq P_3^{\beta}$. The sense of growth, as deduced from the sense in which (19) is not satisfied, can only be predicted if the stresses in the two grains are known everywhere along their boundary. In practice the solution of such problems may be in computer elastic analyses of idealized grain shapes (e.g. Heinze and Goetze, 1973).

REFERENCES

BRACE, W.F., W. G. ERNST, AND R. W. KALLBERG (1970) An experimental study of tectonic overpressure in Franciscan rocks. Geol. Soc. Amer. Bull. 81, 1325-1338.

COE, R.S., AND M. S. PATERSON (1969) The α-β inversion in quartz: a coherent phase transition under nonhydrostatic stress. J. Geophys. Res. 74, 4921-4948.

GARLAND, C.W. (1964) Generalized Pippard equations, J. Chem. Phys. 41, 1005-1008.

GIBBS, J.W. (1906) The collected works of J. Willard Gibbs, Ph.D., LL.D., Vol. I. Thermodynamics, Longmans, Green, and Cy., New York, N.Y., 434 p.

HEINZE, W.D., AND C. GOETZE (1973) Computer simulation of stresses in a polycrystalline solid, A.G.U. Trans. (abstract) 54, 450.

KAMB, W.B. (1959) Theory of preferred crystal orientation developed by crystallization under stress, J. Geol. 67, 153-170.

———— (1961) The thermodynamic theory of nonhydrostatically stressed solids, J. Geophys Res. 66, 259-271.

NYE, J.F. (1957) Physical properties of crystals, Oxford University Press, London, 322 p.

TURNER, F.J., AND J. VERHOOGEN (1960) Igneous and metamorphic petrology, second ed., McGraw-Hill Book. Cy., Inc., 694 p.

CAPTION

FIG. 1. Stressed crystals in equilibrium with fluids and with each other. See text.

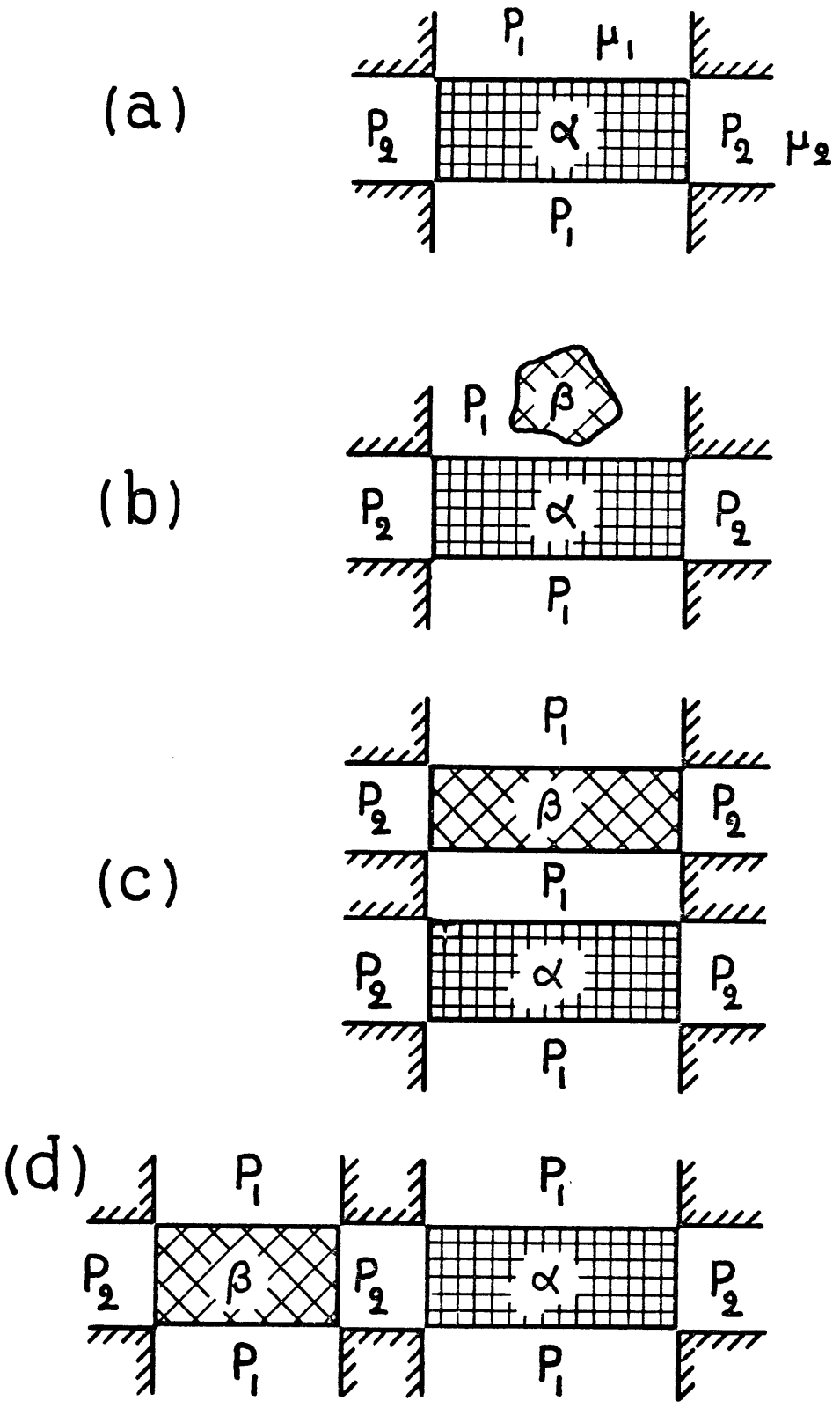
(a)
P1
μ1
P2
α
P2
μ2
P1
(b)
P1
β
P2
α
P2
P1
(c)
P1
P2
β
P2
P1
P2
α
P2
P1
(d)
P1
P1
P2
β
P2
α
P2
P1
P1

Fig. 1

CHAPTER 7

MIGRATION OF AN INTERFACE BETWEEN TWO AXIALLY STRESSED QUARTZ CRYSTALS HAVING DIFFERENT CRYSTALLOGRAPHIC ORIENTATIONS. ATTEMPTS AT EXPERIMENTAL DETERMINATION OF RATES.

INTRODUCTION

Kamb (1959) developed a thermodynamic theory of preferred orientations in stressed rocks based on Gibbs' (1906, Eq. 386) equilibrium conditon for stressed solids in contact with a fluid. Kamb reasoned that when two stressed crystals face each other across a grain boundary, the one which requires the lowest value of its chemical potential for equilibrium of that boundary will grow at the expense of the other one.

In order to develop the theory fully, Kamb (1959) assumed

(1) that the stress was uniform within each grain and the same in all the grains of the stressed polycrystalline aggregate;

(2) that Gibbs' Equation 386 could be generalized to grain boundaries supporting a shear stress, by merely replacing the pressure in the fluid by the normal component of stress;

(3) that grain growth rates were isotropic and linearly proportional to the difference in chemical potentials between the two grains.

In Chapter 2 it was noted that grain growth across the high-angle boundaries of a polycrystalline aggregate cannot generally be a reversible process when the boundaries support a shear stress. Consequently no generalization of Gibbs' equilibrium equation is possible for such boundaries. In Chapters 2 and 4, it was also argued that, in fact, reacting grain boundaries were not likely to be able to support any shear stress, and that therefore the stresses could not be uniform within each grain of the stressed aggregate.

Several of the assumptions made by Kamb (1959) thus do not appear justified. However, the basic idea that some grains may grow at the expense of others as a result of differences in elastic strain energies and molar volumes remains sound. In fact, Kamb's argument for monomineralic aggregates is exactly valid for the idealized situation represented in Figure 1a. A maximum compressive stress acts normal to the boundaries of many parallel 'wafers' of a mineral, each wafer having a different crystallographic orientation with respect to the stress. The stress has axial symmetry ($P_2 = P_3$) and is the same in all crystals. The wafers are assumed sufficiently thin relative to their lateral extent so that the only 'reactions' of importance are the ones along the parallel boundaries of the wafers. The orientation of the crystal which will then grow at the expense of any other one in contact with it is the one with the <u>smallest value</u> of $(s'_{22} + s'_{33} + 2s'_{23})$, or, equivalently, the <u>largest value</u> of $(s'_{11} + 2s'_{12} + 2s'_{13})$ (Chapter 6, Eq. 20). The primed elastic constants are those calculated for each crystal in a laboratory coordinate system having its 1-axis parallel to the stress axis P_1.

The importance of specifying which reactions are considered (Kamb, 1961) is well illustrated by analysing the situation represented in Figure 1b. There, individual crystals are in the shape of long cylindrical rods with polyhedric sections; the stress has axial symmetry ($P_2 = P_3$) and is also the same in all rods. When the rods are sufficiently long, only the reactions along the cylindrical surfaces may be considered important. The crystal orientation which will then grow at the expense of any other one is the one corresponding to the <u>lowest value</u> of s'_{11} (regardless of whether P_1 is larger or smaller than P_2).

Another possible reaction which can be considered is exemplified by Tullis and Tullis (1972). When a crystal of α-quartz is compressed axially, Dauphiné twinning is induced mechanically. Tullis and Tullis demonstrated

both theoretically and experimentally that for a given crystal, the one of the two possible twin orientations which develops is the one with the highest value of s'_{11}. (Note that mechanically induced Dauphiné twinning is a coherent transformation.)

However, it can be argued that in metamorphic rocks the flattening of grains normal to the maximum compressive stress results in configurations approximating that of Figure 1a. The Kamb criterion for monomineralic aggregates would therefore apply.

The driving force for such boundary migration is very small. In the experiments reported here I attempted to measure the migration rate of an interface between two uniaxially stressed crystals of quartz having different orientations. The aim was to evaluate whether such a migration could be geologically significant.

THE DRIVING FORCE FOR MIGRATION

Let a and b be the two crystals of different orientations under a same axial stress P_1, $P_2 = P_3$. The difference between the chemical potentials required at the interface to maintain equilibrium with a and b respectively is given by (see Chapter 6, Eqs. 8, 15 and 19):

$$\mu_1^a - \mu_1^b = \bar{V}^o(P_1 - P_2)^2\left[\left(\tfrac{1}{2}s_{22}^a + \tfrac{1}{2}s_{33}^a + s_{23}^a\right) - \left(\tfrac{1}{2}s_{22}^b + \tfrac{1}{2}s_{33}^b + s_{23}^b\right)\right] \qquad (1)$$

For compliances of the order of 10^{-6} bar^{-1}, stress differences of the order of 10^2 bars, and molar volumes of the order of $10^2 cm^3$, this potential difference is of the order of 0.01 cal mol^{-1}.

For example, choosing quartz as the mineral, let us take as crystal a one with its c-axis parallel to the axial stress, and, as crystal b, one with its c-axis perpendicular to the axial stress. Then

$$\Delta\xi = (\tfrac{1}{2}s^{a}_{22} + \tfrac{1}{2}s^{a}_{33} + s^{a}_{23}) - (\tfrac{1}{2}s^{b}_{22} + \tfrac{1}{2}s^{b}_{33} + s^{b}_{23})$$

$$= \tfrac{1}{2}(s_{11} - s_{33}) + s_{12} - s_{23} \qquad (2)$$

(Compliance moduli with neither prime nor superscripts are those corresponding to the conventional coordinate system for quartz: x_1 parallel to the crystallographic a-axis (diad axis) x_3 parallel to the c-axis, and x_2 in the basal plane, perpendicular to x_1 and x_3)

At 400°C, $\Delta\xi = 0.215 \times 10^{-6}$ bar^{-1} and $\bar{V}^{o} = 23.11$ cm^{3}mol^{-1}. For $P_1 - P_2 = 500$ bars,

$$\mu^{a}_{1} - \mu^{b}_{1} = 1.24 \text{ bar cm}^3 \text{ mol}^{-1},$$

or

$$\simeq 0.03 \text{ cal mol}^{-1} .$$

For comparison, it can be noted that in metamorphic reactions the driving force provided by a departure from the equilibrium temperature of 1° is often of the order of 10 cal mol^{-1} or more. In many cases no significant reaction is even obtained until this departure reaches several degrees.

The differential stress supported by the crystals enters as a squared quantity in the expression of the chemical potential difference (Eq. 1); in order to have as large a driving force as possible it is necessary to have a strong mineral. This was the main reason to choose quartz in these experiments; another reason was that extensive data are available on its elastic constants, mechanical behavior, natural and experimental preferred orientations, crystal growth, polishing, etc. Also, Fairbarn (1954) noted that quartz appears to readily acquire a preferred orientation under stress conditions which leave

most other minerals randomly oriented. Fairbarn's observation would therefore suggest that quartz responds relatively rapidly to differential stresses.

Variation of μ_1 with orientation in quartz

For quartz at 400°C the maximum value of $\left|\mu_1^a - \mu_1^b\right|$ is not for orientations of the c-axis parallel and perpendicular to the stress axis. To find the orientations which would provide the largest driving force it is necessary to calculate how μ_1 varies with orientations of the crystal. Let us call μ_o the value of the chemical potential at the temperature of the run, but under a hydrostatic pressure equal to P_1. From Chapter 6, or Kamb (1961, Eq. 15),

$$\frac{\mu_1 - \mu_o}{\bar{V}^o(P_1 - P_2)^2} = \xi = \frac{1}{2}s'_{22} + \frac{1}{2}s'_{33} + s'_{23} \quad . \tag{3}$$

For α-quartz (trigonal, class 32)

$$\xi = (\tfrac{1}{2}s_{11} + \tfrac{1}{2}s_{33} + s_{13}) + (-s_{33} + \tfrac{1}{2}s_{44} + s_{12})\cos^2\theta + (\tfrac{1}{2}s_{11} + \tfrac{1}{2}s_{33} - s_{13} + \tfrac{1}{2}s_{44})\cos^4\theta$$

$$+ 2s_{14}\cos\theta\cos\phi(3 - 4\cos^2\phi - 3\cos^2\theta), \tag{4}$$

where θ and ϕ are the angles which the principal direction of stress makes with the x_3 (c-axis) and x_2 axes of the crystal respectively. Figure 2 shows how ξ varies with the orientation of the crystal when the stress axis lies within two particular crystallographic planes of the quartz:

i) x_1x_3 plane ($\cos\phi = 0$);

ii) x_2x_3 plane ($\cos\phi = \sin\theta$).

The maximum value of ξ (and therefore, for a given stress, of μ_1) is indeed obtained when the c-axis is parallel to the maximum stress axis: $\xi = 1.270 \times 10^{-6}$ bar^{-1}. However, the minimum value is reached for crystals

oriented such that the maximum stress axis is in the x_2x_3 plane and makes an angle of 65° with the x_3 (c) direction: $\xi = 0.914 \times 10^{-6}$ bar^{-1}. Therefore the maximum possible value of $\Delta\xi$ at 400°C is for these two orientations: $\Delta\xi = 0.356 \times 10^{-6}$ bar^{-1}; for a differential stress of 500 bars,

$$\Delta\mu = 2.06 \text{ bar cm}^3 \text{ mol}^{-1} = 0.049 \text{ cal mol}^{-1}.$$

Thus the two orientations above would appear to be a good choice for maximizing the driving force. However, an interesting phenomenon occurs, which interferes with the 'Gibbs-Kamb mechanism'. The compliance modulus s'_{11} is given as a function of orientation by

$$s'_{11} = s_{11}\sin^4\theta + s_{33}\cos^4\theta + (2s_{13} + s_{44})\sin^2\theta\cos^2\theta + 2s_{14}\cos\theta\cos\phi(3 - 4\cos^2\phi - 3\cos^2\theta). \quad (5)$$

The orientation with the lowest value of ξ (and therefore the most favorable orientation for a Gibbs-Kamb mechanism) is also close to the one with the lowest compliance s'_{11}. Under the applied load, Dauphiné twinning would therefore occur in this crystal, resulting in a higher value of the compliance. The values of ξ and s'_{11} for the newly developed twin are obtained by changing the sign of $\cos\phi$ in (4) and (5). The new value of ξ (1.204×10^{-6} bar^{-1}) is no longer minimum. We thus see that, of the two twin orientations, the Gibbs-Kamb mechanism favors one while coherent Dauphiné twinning favors the other!

To avoid such problems the crystallographic orientations chosen were therefore those with the c-axis parallel and perpendicular to the stress axis.

Variation of $\Delta\mu$ with temperature; choice of temperature

$\Delta\mu$ is now taken to designate the quantity $\mu_1^{\parallel c} - \mu_1^{\perp c}$.

From (1) $$\Delta\mu = \bar{V}^{o}(P_1 - P_2)^2\Delta\xi \ , \qquad (6)$$

where (Eq. 2) $$\Delta\xi = \frac{1}{2}(s_{11} - s_{33}) + s_{12} - s_{23} \ .$$

Variations of $\bar{V}^{o}$ with temperature can justifiably be neglected here. However, as Figure 3 shows, $\Delta\xi$ increases substantially with temperature, from 0.100 $Mbar^{-1}$ at 100°C to 0.450 $Mbar^{-1}$ at 550°C (1 $Mbar^{-1} = 10^{-6}$ bar^{-1}). Factors influencing the choice of temperature for the experiments are thus the following:

i) For a given value of $\Delta\mu$ a higher temperature should cause a faster migration of the interface.

ii) For a given stress difference $(P_1 - P_2)$, $\Delta\mu$ increases with temperature as a result of the increase of $\Delta\xi$ shown in Figure 3.

iii) The stress difference which the crystals can support over a long period of time without plastic or brittle failure is expected to decrease with an increase in temperature.

iv) As temperature is raised close to the α-β transition ($\sim$ 573°C at atmospheric pressure) the thermal expansion coefficients become very large (and in fact infinite at the transition). The thermal stresses which are then associated with even small temperature gradients cause the crystals to fracture.

Clearly, if equations giving the dependence on temperature of growth rares and long-term strength were known, optimum temperature and stresses for the experiments could be calculated. Such is not the case, however. Our only detailed knowledge of the growth kinetics of quartz comes from hydrothermal growth (see following section) and may not be relevant to the present situation. Baeta and Ashbee (1970 a,b) do report a series of deformation experiments on unconfined artificial quartz crystals; they calculate activation energies

for plastic deformation on several glide systems. On the basis of Baeta and Ashbee's data it was originally believed that at 500°C, differential stresses of more than 1 kbar could easily be supported by crystals with the orientations chosen. As it turned out, failure occurred by propagation of brittle fractures; not much was known about this process in quartz when the present experiments were started although more work has been done since (Scholz and Martin, 1971; Martin, 1972).

It was thus the desire to avoid thermal stresses which limited the run temperatures to about 500°C.

RATE ESTIMATION FROM HYDROTHERMAL GROWTH OF QUARTZ CRYSTALS

As mentioned previously, the kinetics of quartz growth under hydrothermal conditions are relatively well known. The subject is reviewed by Laudise and Nielsen (1961). For the following discussion it is necessary to briefly describe the method used in hydrothermal growth.

Hydrothermal growth of quartz is achieved by surrounding a seed, at an absolute temperature T, with an aqueous solution supersaturated in silica, under pressures of the order of a kilobar. The supersaturation is obtained by dissolving quartz in another part of the vessel at a temperature $T + \Delta T$. Transfer of fluid between the two chambers is effected by convection. Variable amounts of Na_2CO_3, or more often NaOH (0.5 to 1.5 M) are added to the water.

Laudise and Nielsen (1961, p. 197) report that growth rates obey a law of the form

$$r = K e^{-\frac{\Delta E}{RT}} \Delta T \ . \qquad (7)$$

K is roughly independent of temperature, varies with pressure, increases somewhat with concentration in NaOH and is strongly dependent on the crystallographic orientation of the growing face. At pressures between 1.2 and 2.0 kbar and in 0.5 M NaOH solutions, K varies between 180×10^3 and 280×10^3 mm day^{-1} deg^{-1} for growth on the basal plane. Growth on m faces, of greater interest to us, is about 60 times slower, that is, K is between 3×10^3 and 4.5×10^3 mm day^{-1} deg^{-1}. The Arrhenius energy, ΔE, is about 20 kcal mol^{-1}.

We need to translate ΔT into an excess chemical potential $\Delta\mu$ in the supersaturated solution. If the solution is assumed ideal

$$\Delta\mu = RT\left(\frac{\partial \ln x}{\partial T}\right)_P \Delta T,$$

and

$$\left(\frac{\partial \ln x}{\partial T}\right)_P = \frac{\bar{L}}{RT^2} \quad \text{(eg. Denbigh, 1966, p.259)},$$

where $\bar{L}$ is the molar heat of solution of quartz in the aqueous phase. Therefore

$$\Delta\mu = \bar{L}\,\frac{\Delta T}{T} \tag{8}$$

This is assuming of course that the solution has reached equilibrium with the quartz in the hot part of the vessel. At temperatures of 300 to 400°C, and pressures up to 2 kbar, $\bar{L} \simeq 1$ kcal mol^{-1}.

For our purpose, the rate equation can therefore be rewritten, using (7) and (8),

$$r = KT\,\frac{\Delta\mu}{\bar{L}}\,e^{-\frac{\Delta E}{RT}}. \tag{9a}$$

Numerically, for growth on an m face,

$$r_{(mm/day)} \simeq 4\ T\ e^{-\frac{10^4}{T}}\ \Delta\mu_{(cal\ mol^{-1})} \cdot \qquad (9b)$$

For the present experiments, eg. at 500°C, $P_1 - P_2 = 500$ bars, $\Delta\mu = 0.044$ cal mol^{-1}, the rate predicted from (9b) is 0.3 μm/day, or 3 μm in 10 days. Such a growth is quite small and its occurrence would be hard to detect. It is indeed unfortunate that in the similar calculations made during planning of these experiments the writer took the value of K for growth on the basal plane and assumed a differential stress of 1 kbar; accordingly, the predicted rate was 240 times higher, and thus appeared to be a more reasonable bet.

As Laudise and Nielsen (1961) point out, the large anisotropy of the growth rate under hydrothermal conditions indicates that the rate-controlling mechanism must be related to the positioning of SiO_2 molecules on favorable sites of the pre-existing surface (probably screw dislocation steps), rather than to the diffusion of silica to the surface through the fluid. The faceted crystals obtained are in sharp contrast with the anhedral shapes of quartz grains observed in metamorphic or igneous rocks. This difference suggests that even if the aqueous phase is abundant in the rock ($P_{aqueous} = P_{total}$) the rate of growth of quartz crystals is limited by the availability of silica reaching their interface. Such a rate may consequently be much slower than the ones observed during hydrothermal growth.

DESCRIPTION OF THE EXPERIMENTS

Principle

Essentially the purpose of the programme was to reproduce for two crystals the situation sketched in Figure 1a. Experiments had to be under uniaxial stress because their expected duration made runs under confining pressure impractical.

Early on, it was envisaged to seal water between the two axially stressed crystals. Such an arrangement seemed to insure that no shear stresses would develop along the interface, and that the above analysis of the kinetics of hydrothermal growth would apply. The idea was abandoned, however, for the following reasons. (a) It appeared unavoidable that the seals themselves would introduce large stress concentrations along their contacts with the quartz crystals; these stress concentrations would then result in a much larger supersaturation of the fluid phase than the one under study. (b) Under no confining pressure, hydraulic fracturing of the crystals by the fluid seemed likely. (c) New crystals could have grown within the fluid under the hydrostatic pressure P_1 alone.

It was therefore decided to simply put the polished surfaces of the two crystals in direct contact, raise the temperature, and apply the load. One hope was that a sufficient amount of adsorbed water would remain on the surfaces to provide the means of transport of silica from one face to the other. The two polished faces were expected to adhere to each other under the load, a state often called 'optical contact'. Lord Rayleigh (1936) estimated the separation between polished glass surfaces in optical contact to be between 10 and 30 Å; it was thus also hoped that transport problems would be reduced to a minimum over such short distances.

Equipment

The basic loading frame and ram were those of a piston-and-anvil 'squeezer'. The applied load was maintained constant over a long period of time by insertion into the oil line of a pressure-regulating bladder (Greer, A107-200).

Various combinations of hard steel spheres and/or hemispheres were put in the column to provide an even pressure on the interface in spite of the unavoidable lack of parallelism of samples, spaces, and pistons.

The furnace was also a ready-made part of the squeezer. Rather than design a new one, temperature gradients over the sample length were minimized by surrounding the samples with a thick aluminum or copper sleeve (see later discussion).

The temperature was regulated by a Honeywell "Pyr-O-Vane' indicating millivoltmeter controller' (model 105C204). Daily line variations of several volts made it necessary at first to have a large difference between the high and the low power controlled by the Pyr-O-Vane (Low/High $\simeq$ 2/3). The resulting temperature oscillations were judged to be detrimental because of the large difference in thermal expansion parallel to the interface of the two crystal orientations. The difference between high and low was therefore reduced by taking the power from a Wanlass voltage regulator (Parax AC line conditioner PEC-500). The third run was terminated by the failure of that regulator. Although this failure has not been definitely explained, any interruption of 10 or more periods in the line voltage could have deactivated the secondary circuit of the instrument. The likelihood of such a power interruption during a run lasting several days is high enough to limit the usefulness of this type of voltage regulator.

The thermocouple for the controller was placed below the sample or in the thick sleeve. The output of a second thermocouple, placed either above the sample or also in the thick sleeve, was fed into a Moseley strip-chart recorder. Both thermocouples were read with a potentiometer from time to time.

Sample assembly

The artificial quartz crystal from which samples were cored has been kindly supplied by Dr. N.C. Lias (Western Electric, North Andover, Mass.). It is a fast grown, low Q crystal with a high water content (never measured, however). After heat treatment of oriented cores under pressure (one to two

hours at 600°C and 3 kbar) to homogenize the water distribution (Hobbs, 1968), the samples were prepared commercially from the cores (World Optics, 145 Newton St., Waltham, Mass.); diameter = 0.2500 ± 0.0001"; length: 0.500 ± 0.002". The 'reacting' faces were ground flat 'within one wavelength', and given a 'high-precision optical pitch polish' (10/5 Military specification).

The sample assembly was modified somewhat for each run. The configuration in the third run (Figure 4) is fairly representative. Temperature gradients along the length of the samples near 500°C were measured by moving a thermocouple along the axial hole of a dummy sample of fused silica. In spite of the thick copper or aluminum sleeve, the temperature near the center was 10 to 20°C higher than near the ends. Lucalox spacers, which were meant to 'trap' the heat within the sleeve and the samples and thus reduce the gradients, did not improve the situation significantly.

To prevent any offset of the crystals with respect to each other until the load was applied, a thin (0.002" to 0.003") aluminum sleeve was used to hold them together.

Surface preparation

As mentioned above the quartz used was an artificially grown, water-rich crystal; a high water content seemed desirable to improve the kinetics of the reaction studied. Some precautions in preparing the 'reacting' surfaces also seemed important.

Many authors report on defects and distortions of the lattice near the surface, introduced in the process of polishing crystals. Ida and Arai (1960) in particular made a thorough study of the residual stresses in polished quartz surfaces, and of the depth of such disturbed layers. They concluded that the 'residually stressed layer' extended to a depth of 100 to 1000 Å, although some flaws reached as far as 3 μm. The local strain

energy associated with such residual stresses is probably larger than the $\Delta\mu$ under study. The crystals were accordingly cleaned (trichloroethylene, and warm, concentrated NaOH solution) and then etched slightly, either with ammonium bifluoride [$(NH_4)HF_2$] or by argon-ion-bombardment. The thickness removed (0.25 to 1 μm) was estimated from Ida and Arai's (1960) etching rate calibrations for the chemical method, and, for the ion bombardment method, from a preliminary calibration of the erosion rate of a quartz thin section. The amount of etching by either method was kept low for fear of losing the flatness and polish of the surfaces. Samples were then stored in distilled water until the run.

RUNS AND RESULTS

In spite of the considerable amount of designing, machining, sample preparation, and the large number of calibrations which went into them, only three actual experiments were run. In the first run, the crystals were maintained under an axial stress of 900 bars (± 30 bars) at a temperature of 500°C (± 4°C) for 45 hours. Similarly the second run (490°C, 640 bars) lasted 209 hours, and the third (505°C, 640 bars) 90 hours.

'Creep' of the samples, measured on an Ames dial gauge attached to the piston, occurred each time. The first run was actually interrupted because the load was about to be carried by the thick sleeve rather than the samples. On retrieval all specimens were intensely fractured, leaving little hope that the stress could have been uniform along the surface.

The crystals from the second (and longest) run were nevertheless examined in detail by optical and scanning electron microscopy. Except for many pits and fractures the original polish was retained. It was expected that if any growth had occurred the original position of the interface would be marked by many impurities and defects. The crystal whose c-axis was

perpendicular to the load axis was thus sectioned lengthwise and the damage due to the saw removed by ion bombardment. Neither optical nor scanning electron microscopy of the section gave any evidence that growth had occurred.

These runs were abandoned in August 1972.

GROWTH OF QUARTZ FROM FUSED SILICA

In another series of four experiments, quartz was grown from fused silica, at hydrostatic pressures around 4 kbar and temperatures around 600°C. The object was to obtain some growth of quartz under a large chemical potential difference $\Delta\mu$, and, more generally, to check on the range of applicability of the growth rate equation established for hydrothermal conditions (Eqs. 9 a, b).

Conditions of the four runs were as follows:

QS - 1	wet	625 ± 15°C	4010 ± 20 bars	7 hours
QS - 2	dry	595 ± 15°C	3370 to 4080 bars	2 hours
QS - 3	wet	602 ± 10°C	4010 ± 20 bars	6 hours
QS - 4	wet	602 ± 10°C	3995 ± 20 bars	3 min[1]

---

[1]Precautions were taken to stay below the α-β transition when raising or lowering pressure and temperature. Consequently, in addition to the time listed here, it took between two and three hours from the time of first application of pressure to the time run conditions were reached; similarly it took one hour beyond the end of the run to bring temperature and pressure back down to room conditions. Run QS - 4 was meant to determine how much reaction occurred during these transient periods.

One-quarter-inch-long segments of a fused silica rod (Spectrosil, Thermal American Fused Quartz Co., Montville, N.J.) were used as starting samples after cleaning and etching for 5 minutes in concentrated solution of ammonium bifluoride. The diameter of the rod was 0.615 ± 0.001", while the inner diameter of the thick-walled copper tube in which the sample was held was 0.625" (Figure 5). In the three 'wet' runs the space between silica and tube was filled with distilled water; in QS -3, the sample was room-dry. The pressure (argon) was applied on the copper tubing.

No growth was detected in the dry run. In the three wet runs abundant quartz developed, with a typical 'chalcedony' structure: radiating, 'fan' patterns of many small needles of quartz elongated radially, parallel to their c - direction. Although a quartz crystal had been inserted with the fused silica to serve as seed, the chalcedony structure developed approximately evenly on all walls surrounding the sample, whether copper, stainless steel or quartz, and along cracks within the silica. The voids between the quartz and the fused silica, visible after dismantling, gave conclusive evidence that free vapor had remained trapped with the sample during the run. The crystal growth had therefore occurred by vapor transport, and was thus hydrothermal.

From the discussion by Scherer et al (1970), the difference in Gibbs energy between fused silica and quartz at 600°C can be calculated to be approximately

$$\Delta\mu = 800 \text{ cal mol}^{-1}.$$

The disorderly precipitation of quartz which is obtained under such a large driving force cannot easily be compared with the regular growth of artificial quartz crystals. Indeed, Equation 9 would predict, for the growth along the c direction in the time and conditions of the longest run (QS - 1), a thickness of 115 mm! The average thickness of the chalcedony layer which developed was only 0.5 mm.

CONCLUSION

A growth rate equation would be useful not only for the Kamb theory of preferred orientations but also for interpreting other metamorphic textures such as those of recrystallization recovery observed in strained rocks. Of the two sets of experiments described in this chapter, the first one gave rise to too low, the second one to too high a driving force to establish such an equation. A study of the migration of curved interfaces between crystals in hydrothermal vessels could perhaps provide an adequate answer.

In the meantime we may temporarily accept Equation 9b, and use it to evaluate the effectiveness of a Gibbs-Kamb mechanism in nature. We find for example that at 400°C and for $P_1 - P_2 = 50$ bars,

$$\Delta\mu = 0.3 \quad 10^{-3} \text{ cal mol}^{-1} ,$$

and

$$r = 0.1 \text{ mm per thousand years.}$$

A differential stress of one hundred bars would quadruple that rate. Analyses of lattice dislocation densities and grain size in quartz from metamorphic terranes suggest that their deformation might have been under stresses as high as several kilobars (C. Goetze, 1974, personal communication). Under such stresses, the assumption of solid behavior is no longer valid. However, for less drastic conditions, the possibility that the Gibbs-Kamb mechanism might be important in the development of natural preferred orientations cannot be discarded.

REFERENCES

BAETA, R.D., AND K.H.G. ASHBEE (1970 a) Mechanical deformation of quartz I. Constant strain-rate experiments. Philos. Mag. 22, 601-623.

_____ AND _____ (1970 b) Mechanical deformation of quartz II. Stress relaxation and thermal activation parameters. Philos. Mag. 22, 625-635.

COE, R.S., AND M.S. PATERSON (1969) The α-β inversion in quartz: a coherent phase transition under nonhydrostatic stress. J. Geophys. Res.74, 4921-4948.

DENBIGH, K. (1966) The principles of chemical equilibrium, second ed., Cambridge University Press, Cambridge, 494 p.

FAIRBARN, H.W. (1954) The stress-sensitivity of quartz in tectonites. Tschermaks mineral. u. petr. Mitt. 4, 75-80.

GIBBS, J.W. (1906) The collected works of J. Willard Gibbs, Ph.D., LL.D., Vol. I. Thermodynamics, Longmans, Green, and Co., New-York, N.Y., 434 p.

IDA, I., AND Y. ARAI (1960) VHF crystal polishing and the nature of polished quartz surfaces. Electr. Comm. Labor. Tech. J. (Tokyo) 8 (3-4), 119-174.

KAMB, W.B. (1959) Theory of preferred crystal orientation developed by crystallization under stress. J. Geol. 67 (2), 153-170.

_____ (1961) The thermodynamic theory of nonhydrostatically stressed solids. J. Geophys. Res. 66, 259-271.

LAUDISE, R.A.,AND J.W. NIELSEN (1961) Hydrothermal crystal growth. Solid state physics, Adv. in res. and app. 12,

MARTIN, R.J., III (1972) Time-dependant crack growth in quartz and its application to the creep of rocks. J. Geophys. Res. 77, 1406-1419.

RAYLEIGH, LORD (1936) A study of glass surfaces in optical contact. Proc. Roy. Soc. London A156, 326.

SCHERER, G., P.J. VERGANO, AND D. R. UHLMANN (1970) A study of quartz melting. Phys. chem. glasses 3, 53-58

SCHOLZ, C. H., AND R.J. MARTIN III (1971) Crack growth and static fatigue in quartz. J. Amer. Ceram. Soc. 54, 474.

TULLIS, J., AND T. TULLIS (1972) Preferred orientation of quartz produced by mechanical Dauphiné twinning: thermodynamics and axial experiments. In: Flow and fracture of rocks, Geoph. Monog. 16, Heard, Borg, Carter and Raleigh, eds., Amer. Geophys. Union, 67-82.

FIGURE CAPTIONS

FIG. 1. Crystals of different orientations coexisting (and reacting) in a uniform stress field. In the text the stress field is assumed to have axial symmetry. (a) Stack of parallel 'wafers'. (b) Bundle of parallel polyhedric 'rods'. Any disequilibrium, and possible reactions along the edges of the wafers, or at the ends of the rods, are assumed unimportant.

FIG. 2. Variation of $\xi = \frac{1}{2} s_{22} + \frac{1}{2} s_{33} + s_{23}$ as a function of the orientation of the crystal with respect to the axis of stress at 400°C. Full curve: $x_1 x_3$ section; dashed curve: $x_2 x_3$ section. The relative variations appear larger than they really are because the length of the radius vector plotted is proportional to ξ - 0.8 $Mbar^{-1}$, rather than to ξ. Elastic constants used are from Coe andPaterson's (1969, Fig. 3) compilation.

FIG. 3. Variation of $\Delta\xi = \xi^{\parallel c} - \xi^{\perp c} = \frac{1}{2}(s_{11}-s_{33}) + s_{12} - s_{23}$ in quartz as a function of temperature. Elastic constants are taken from Coe and Paterson (1969, Fig. 3).

FIG. 4. Sample assembly for the uniaxial runs.

FIG. 5. Sample assembly in the hydrostatic runs in which quartz grew from silica.

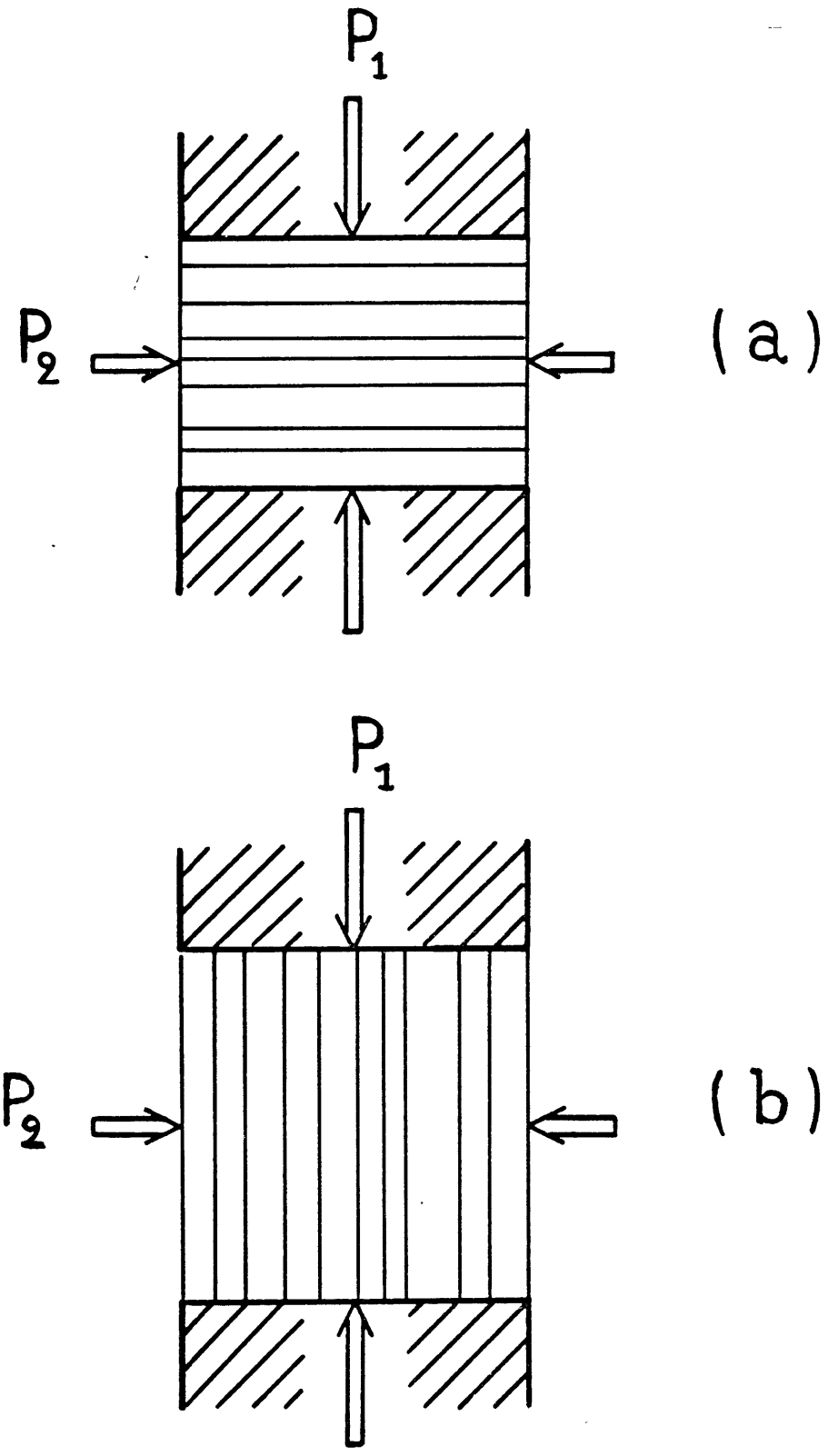

Fig. 1

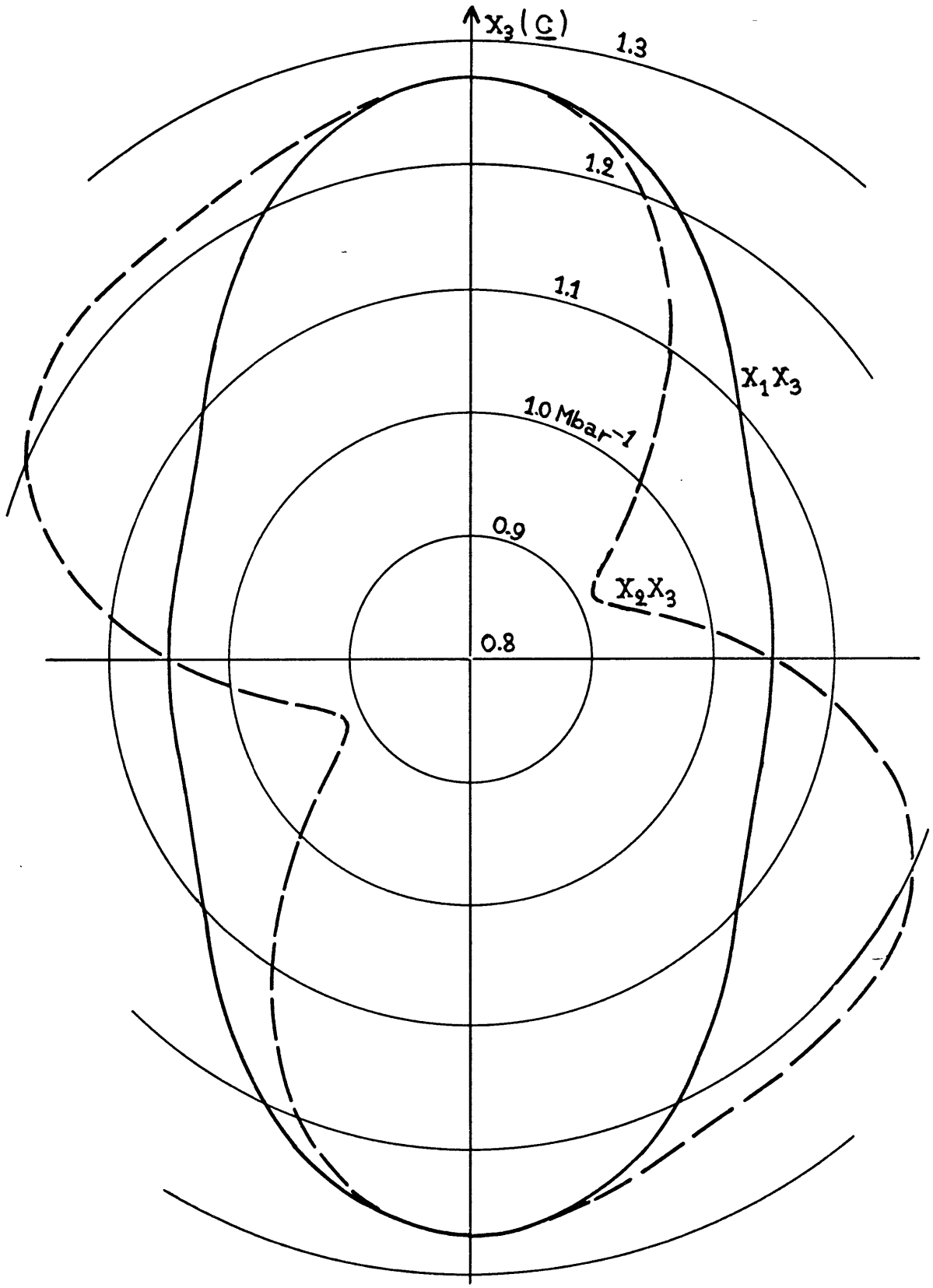

Fig. 2

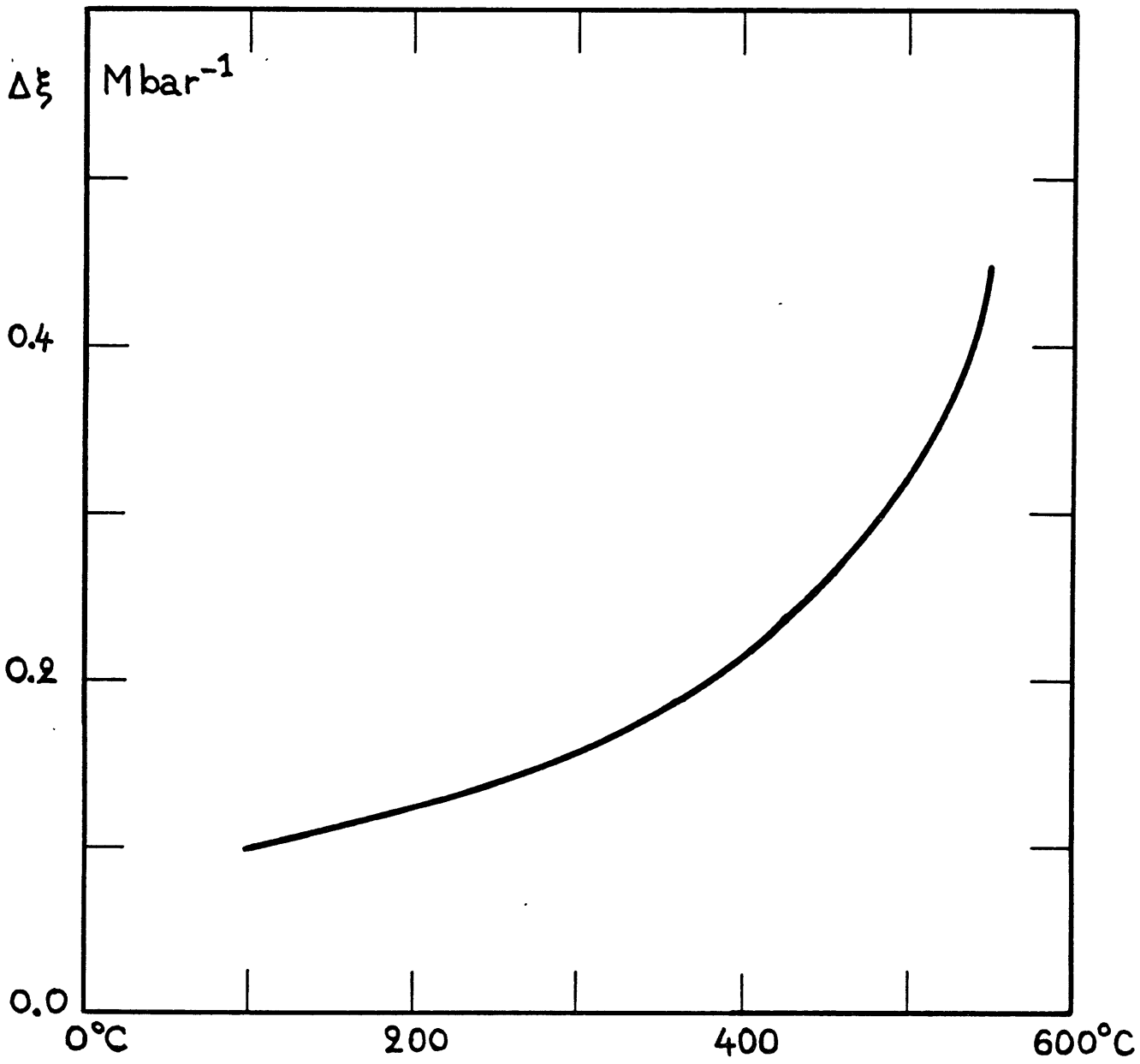

Fig. 3

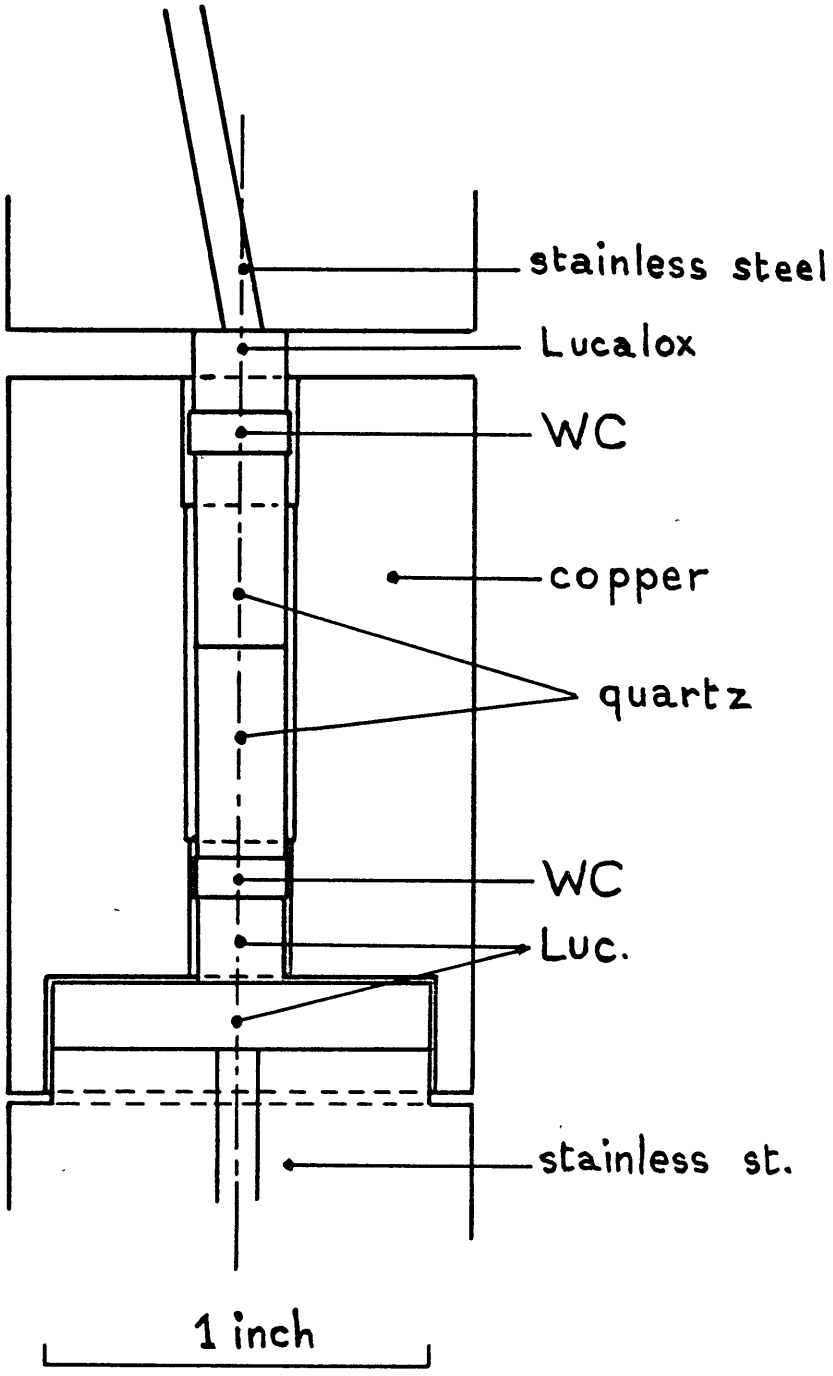
stainless steel
Lucalox
WC
copper
quartz
WC
Luc.
stainless st.
1 inch

Fig. 4

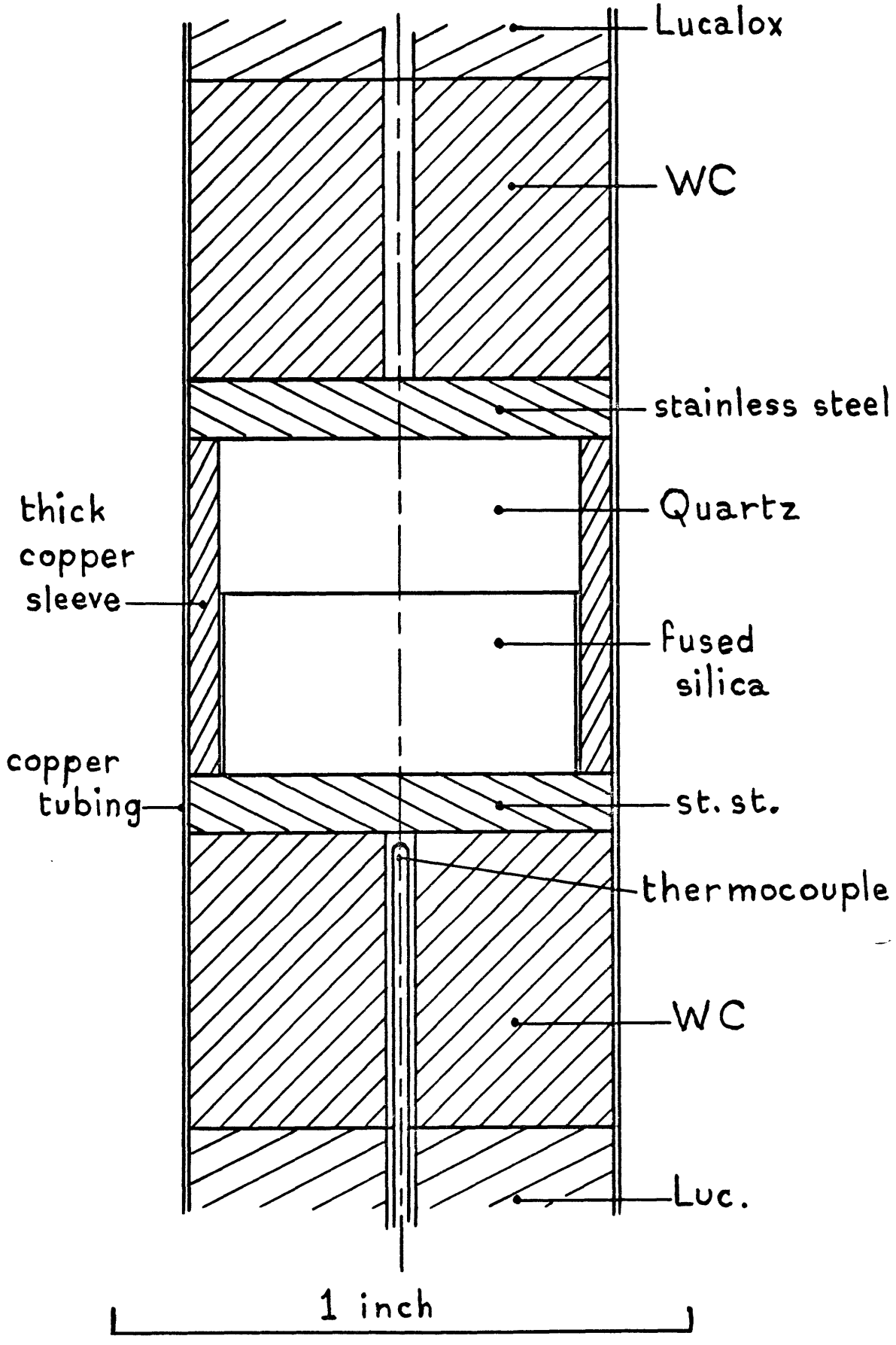
Lucalox
WC
stainless steel
Quartz
thick
copper
sleeve
fused
silica
copper
tubing
st. st.
thermocouple
WC
Luc.
1 inch

Fig. 5

CHAPTER 8

FINAL REMARKS

Any study of the equilibrium of chemical reactions or phase transformations in which stressed solids are involved belongs to the realm of 'nonhydrostatic thermodynamics'. Finding the equilibrium conditions is a relatively simple, classical problem, once the existence of a solid component of the solid is understood; the limits to the meaning of 'equilibrium' in such a case must always be kept in mind.

The sequence of steps to take in solving a problem in nonhydrostatic thermodynamics can perhaps be generalized as follows:

i) Materials studies of the solids and of the constraints on the reactions, e.g. coherency, transformation strain or characteristic vector, fluid pressures, fluid components, kinetics of nucleation of other solid phases.

ii) An elasticity study of the solid, to yield values of stresses and of strain energies.

iii) An application of classical thermodynamics which takes constraints and strain energy into account.

iv) Eventually, if equilibrium conditions are not satisfied everywhere, a study of reaction rates could follow. The elastic equilibrium could then be altered as the reaction proceeds, in which case (iii) and (iv) must be done simultaneously.

Nonhydrostatic thermodynamics have been invoked, implicitly or explicitly, in other geological or mineralogical problems than those presented in this thesis:

Metamorphic textures. Nonhydrostatic stresses have been called upon to explain many features of metamorphosed rocks besides preferred orientations:

metamorphic differentiation and banding, 'pressure solution', pressure shadows. It is not clear from the explanations of these phenomena found in standard textbooks (e.g. Turner and Verhoogen, 1960, p.583; Hyndman, 1972, pp.287-291) that their authors distinguish between nonhydrostatic stresses and pressure gradients; descriptions of the mechanisms involved are also often insufficient.

Shear melting. Ida (1970) pointed out possible applications of equilibria between stressed solids and their melts to the mechanism of deep-focus earthquakes.

Phase boundary migrations under alternating stress. Walsh (1973) analysed the effects of seismic velocity and attenuation of phase boundary migrations resulting from the passage of a stress wave. Walsh (1973, Eq. 1) took for equilibrium criterion of the boundaries, $\Delta P_1 = P_1 - P_0 = 0$ where P_1 is the stress normal to the boundary and P_0 is the equilibrium pressure at the same temperature. It was shown in Chapter 6 (Eq. 16) that this is indeed an appropriate criterion for incoherent boundaries. In many cases, however, the boundaries are likely to be coherent, particularly when the phenomenon is observed at high frequencies (Wang, 1968; Wang and Meltzer, 1973; see also Chapter 2); migration of the boundaries, and the corresponding elastic response to the stresses are expected to differ from that of incoherent boundaries.

Order-disorder and other coherent transitions in minerals. Many high- to low-temperature transitions in minerals lead to coexistence within the same solid, unbroken, framework of a phase and its antiphase. Often, like in the cases of Dauphiné twins in α-quartz, or of antiphases in $P\,2_1/\underline{c}$ clinopyroxenes, the match is stress-free: this is when the transformation from phase to antiphase is not characterized by any strain of the lattice cell. Such is not always the case, however. For example, McConnell (1965) observed alternatively strained triclinic domains within adularias and orthoclases which were macroscopically

monoclinic; in the present terminology these would be called strained anti-phases coexisting coherently. The strain energy involved should no doubt affect the temperature of such transitions, but quantitative analyses remain to be done.

It is this author's hope that the theories, arguments and examples presented in this thesis provide a sound basis for solution of these, and other, problems in nonhydrostatic thermodynamics.

> "In these criteria of equilibrium and stability, account is taken only of possible variations. It is necessary to explain in what sense this is to be understood . . . ." (Gibbs, 1906, p. 57).

REFERENCES

HYNDMAN, D.W. (1972) Petrology of Igneous and metamorphic rocks. McGraw-Hill Book Co., New-York, 533 p.

IDA, Y. (1970) Therodynamic problems related to growth of magma. J. Geophys. Res. 75, 4051 - 4062.

MCCONNELL, J.D.C. (1965) Electron optical study of effects associated with partial inversion in a silicate phase. Phil. Mag. 11, 1289 - 1301.

TURNER, F.J., and J. VERHOOGEN (1960) Igneous and metamorphic petrology, second edition. McGraw-Hill Book Co., New-York, 694 p.

WALSH, J.B. (1973) Wave velocity and attenuation in rocks undergoing polymorphic transformations. J. Geophys. Res. 78, 1253 - 1261.

WANG, C.-Y. (1968) Ultrasonic study of phase transition in calcite to 20 kilobars and 180°C . J. Geophys. Res. 73, 3937 - 3944.

WANG, C.-Y., AND/MELTZER M. (1973) Propagation of sound waves in a rock undergoing phase transformations. J. Geophys. Res. 78, 1293 - 1298.